2004

# Characterization of in-use emissions from marine engines

Sam George
*West Virginia University*

# Characterization of In-use Emissions from Marine Engines

**Sam George**

**Thesis submitted to the**
**College of Engineering and Mineral Resources**
**at West Virginia University**
**in partial fulfillment of the requirements**
**for the degree of**

**Master of Science**
**in**
**Mechanical Engineering**

**Mridul Gautam, Ph.D., Chair**
**Gregory J. Thompson, Ph.D.**
**W. Scott Wayne, Ph.D.**

**Department of Mechanical and Aerospace Engineering**

**Morgantown, West Virginia**
**2004**

**Keywords: In-use emissions, marine engines, low sulfur diesel, intake air water injection**

# ABSTRACT

## Characterization of In-use Emissions from Marine Engines

**Sam George**

Recently, exhaust emissions from marine engines have become a cause of growing concern. Emission reduction technologies applicable to marine engines need to be developed and tested so that the emission regulations can be met. A review of emission reduction technologies applicable for marine engines is presented in this study. The experimental results of onboard testing of a high-speed passenger ferry to determine the benefits of low sulfur diesel (LSD) fuel and intake air water injection are presented. Gaseous emissions of oxides of nitrogen ($NO_x$), carbon dioxide ($CO_2$), and particulate matter (PM) emissions were measured using on-board emission measurement systems developed at the Engine and Emissions Research Laboratory (EERL), West Virginia University. The $NO_x$ emissions were reduced by approximately 11%-17% with intake air water injection and, the PM emissions were reduced by approximately 38%-45% with operation on LSD fuel without a penalty in fuel consumption or work output.

# ACKNOWLEDGEMENTS

First and foremost, I would like to thank my advisor, Dr. Mridul Gautam, for the unending support, invaluable advice, and guidance provided throughout my study. He has been a good friend and advisor all along. It was a pleasure and a unique experience working with you.

I also thank Dr. Greg Thompson and Dr. Scott Wayne for being part of my advisory committee, providing me the necessary guidance and important suggestions.

Special thanks are due to Dr. Nigel Clark, Dr. Greg Thompson, Dan Carder, Ryan Barnett, and Byron Rapp for their whole-hearted cooperation during the on-site testings at Oceanside, California.

I am grateful to Wes Riddle and Dan Carder for their valuable suggestions and technical expertise provided all along my work at the EERC. I thank Dan also for spending time in going through my thesis and pointing out important corrections. I thank Tom Spencer, Richard Atkinson, Andy Pertl, and Ron for the technical help extended whenever it was required. I also thank Aaron, Dave, Glen, Tonto, Adam, Ares, Brian, Petr, and other members at EERC. The entire team at EERC was great to work with.

A big thanks to all my officemates, Guru, Mohan, Sairam, Bobby, Hemanth, Aseem, Vinay, Sasi, Ravi, and Michelangelo, for having provided great company all along my study. Special thanks are due to my roommates and friends, especially, Vinu, Ram, Ajith, Bobby, and Renee for making me feel at home in Morgantown all these years.

Last but not the least, I thank my Dad, and my brother, Saji, for their support, prayers, motivation, and being a source of inspiration all through my life. I also wish to remember and dedicate all my work to my late Mom, and my late brother, Sajan.

# TABLE OF CONTENTS

# LIST OF TABLES

# LIST OF FIGURES

# NOMENCLATURE

| | |
|---|---|
| BP | British Petroleum |
| BSFC | Brake Specific Fuel Consumption |
| $BSNO_x$ | Brake Specific Oxides of Nitrogen |
| BSPM | Brake Specific Particulate Matter |
| CARB | California Air Resources Board |
| CFR | Code of Federal Regulations |
| CFV | Critical Flow Venturi |
| CI | Compression Ignition |
| CO | Carbon monoxide |
| $CO_2$ | Carbon dioxide |
| CVS | Constant Volume Sampler |
| DPF | Diesel Particulate Filter |
| EC | Electrochemical |
| ECD | Emissions Control Diesel |
| EERL | Engine and Emissions Research Laboratory |
| EGR | Exhaust Gas Recirculation |
| EPA | Environmental Protection Agency |
| HC | Hydrocarbon |
| HEPA | High Efficiency Particulate Air |
| HFID | Heated Flame Ionization Detector |
| IMO | International Maritime Organization |
| ISO | International Organization for Standardization |

| | |
|---|---|
| LFE | Laminar Flow Element |
| LSD | Low Sulfur Diesel |
| MARAD | Maritime Administration |
| MEMS | Mobile Emissions Measurement System |
| NDIR | Non Dispersive Infrared |
| NO | Nitric Oxide |
| $NO_x$ | Oxides of Nitrogen |
| NREL | National Renewable Energy Laboratory |
| $O_2$ | Oxygen |
| PM | Particulate Matter |
| RH | Relative Humidity |
| SAE | Society of Automotive Engineers |
| SCR | Selective Catalytic Reduction |
| SOF | Soluble Organic Fraction |
| $SO_x$ | Oxides of Sulfur |
| THC | Total Hydrocarbon |
| TPM | Total Particulate Matter |
| USDOE | United States Department of Energy |
| WIS | Water Injection System |
| WVU | West Virginia University |
| $ZrO_2$ | Zirconium dioxide |

# 1 INTRODUCTION

Diesel engines are considered to be the most efficient power plants among the various types of internal combustion engines. Almost all heavy-duty trucks, urban buses, marine vessels and industrial equipment across the world are powered mostly by diesel engines; hence the exhaust emissions from diesel engines are of great concern. Diesel engines have been one of the major contributors to atmospheric pollution, which is hazardous to both human health and the environment. The emissions of oxides of nitrogen ($NO_x$) and diesel particulate matter (PM) are of particular concern.

Recent emission regulations for various categories of marine engines are a clear indication of this concern. The strict regulations on emissions from automobiles and heavy-duty on-highway diesel engines have considerably reduced the exhaust emissions from these engines, owing to development of new fuels, engine designs and various emission reduction technologies. The focus is now on curtailing emissions from non-road sources such as marine vessels, as emissions from these sources have historically not been subjected to close scrutiny. The air quality issues and increased international and domestic attention on emissions from marine sources have resulted in new regulations being promulgated.

A report from the Maritime Administration (MARAD) [1] suggests that the total volume of domestic and international marine trade is expected to more than double over the next 20 years. There is going to be a rapid growth in the high-speed ferry transportation sector owing to heavier traffic on the roads. There is an expected growth of almost 65% in the number of recreational users. The nation's ports and waterways are getting congested as a result of such growing domestic and international commerce [1].

The global objective of this project was to determine the environmental benefits of operating a hydrofoil deployed high-speed passenger ferry on low-sulfur diesel (LSD) fuel (with and without intake air water injection), compared to operating the ferry on marine diesel fuel. The study was part of United States Maritime Administration (MARAD)'s Marine Exhaust Reduction Program in partnership with other government agencies and the industry. Funding for the research program was provided by the United States Department of Energy (USDOE).

The study was conducted on-board a high-speed ferry (hydrofoil) operated by SCX Inc. between San Diego and Oceanside, California. The vessel was powered by four Detroit Diesel Corporation 12V92 engines retrofitted with an intake charge air water injection system. Exhaust emission measurements were made for LSD fuel and marine diesel fuel operations with and without the intake air water injection in both cases. The gaseous emissions of $NO_x$ and carbon dioxide ($CO_2$) were measured using the Mobile Emissions Measurement System (MEMS) [2-5] developed at the Engines and Emissions Research Laboratory (EERL), West Virginia University, for on-board emissions measurement, while a partial flow dilution tunnel [6] was used for gravimetric analysis of Particulate Matter (PM). Total Hydrocarbon (THC) emissions were not measured due to the concerns of storing compressed hydrogen needed for the Heated Flame Ionization Detector (HFID) onboard the ferry.

There is no official test protocol developed exclusively for measurement of in-use emissions from marine engines. The equipment used and the procedures followed for this study were formed from an integration of requirements included in Title 40 CFR 86, Title 40 CFR 89, Title 40 CFR 92, Title 40 CFR 94, ISO 8178, and SAE J177 [7-12]. The raw

sampling system, the experimental procedures, and the calculations employed in the collection of the data and its subsequent analysis are explained in Chapter 3 of this report.

# 2 REVIEW OF LITERATURE

## 2.1 Introduction

This chapter discusses the current emissions standards for various categories of diesel engines that are in use for marine operations, prior in-use emissions measurement studies, and potential technologies for reduction of emissions from marine engines.

The United States Environmental Protection Agency (EPA) and California Air Resources Board (CARB) are the major U.S. regulatory bodies that have set standards for emissions from the different categories of marine compression ignition and spark ignition engines operating in United States ports and waterways. The International Maritime Organization (IMO), a United Nations agency, is the international organization involved in setting out global emissions standards for marine engines in order to curtail air pollution from marine vessels.

## 2.2 Marine Emissions Regulations and Standards

Marine engines are classified into three categories based upon the displacement per cylinder as shown in Table 2-1 [13]. To promulgate emissions standards, the IMO adopted International Convention on the Prevention of Pollution from Ships, better known as MARPOL 73/78 in 1997 [14]. Annex VI to this convention contains requirements to limit the oxides of nitrogen ($NO_x$) emissions from marine diesel engines.

The Annex VI $NO_x$ limits are listed in Table 2-2 [13] and also shown in Figure 2.1 [15]. It applies to new engines greater than 175hp that are installed on vessels constructed on or after January 1, 2000, or engines, which undergo a major conversion after that date. The Annex VI will come into force and will apply retroactively with effect from January 1, 2000, once it is ratified by member states of IMO, including the United States, whose

merchant fleets constitute more than 50% of the gross tonnage of the world's merchant shipping.

**Table 2-1 Marine Engine Categories [13]**

| Category | Displacement per Cylinder (D) | Basic Engine Technology |
|---|---|---|
| 1 | D<5dm$^3$ (and power ≥ 37 kW) | Land-based nonroad diesel |
| 2 | 5dm$^3$ ≤ D < 30 dm$^3$ | Locomotive engine |
| 3 | D ≥ 30 dm$^3$ | Unique marine engine design |

**Table 2-2 MARPOL 73/78 Annex VI Emission Limits [13]**

| Engine Speed (n, rpm) | $NO_x$, g/kWh |
|---|---|
| n < 130 rpm | 17.0 |
| 130 rpm ≤ n ≤ 2000 rpm | 45 X n$^{-0.2}$ |
| n ≥ 2000 rpm | 9.8 |

The EPA, in 1999, signed the final rule entitled "Control of Emissions of Air Pollution from New CI Marine Engines at or above 37 kW" [13]. The EPA did not adopt any emission standards for Category 3 engines in this rule. Category 3 engines are very large marine diesel engines with power ratings up to 75,000 kW, which typically assist in the propulsion of large ocean-going vessels and operate on residual fuels. Residual fuels have poor ignition quality and have high ash, sulfur and nitrogen content as compared to distillate fuels. According to EPA estimates, residual fuel can increase the $NO_x$ emissions by 20%-50% and PM emissions from 750-1250% as compared to marine distillate fuel [13].

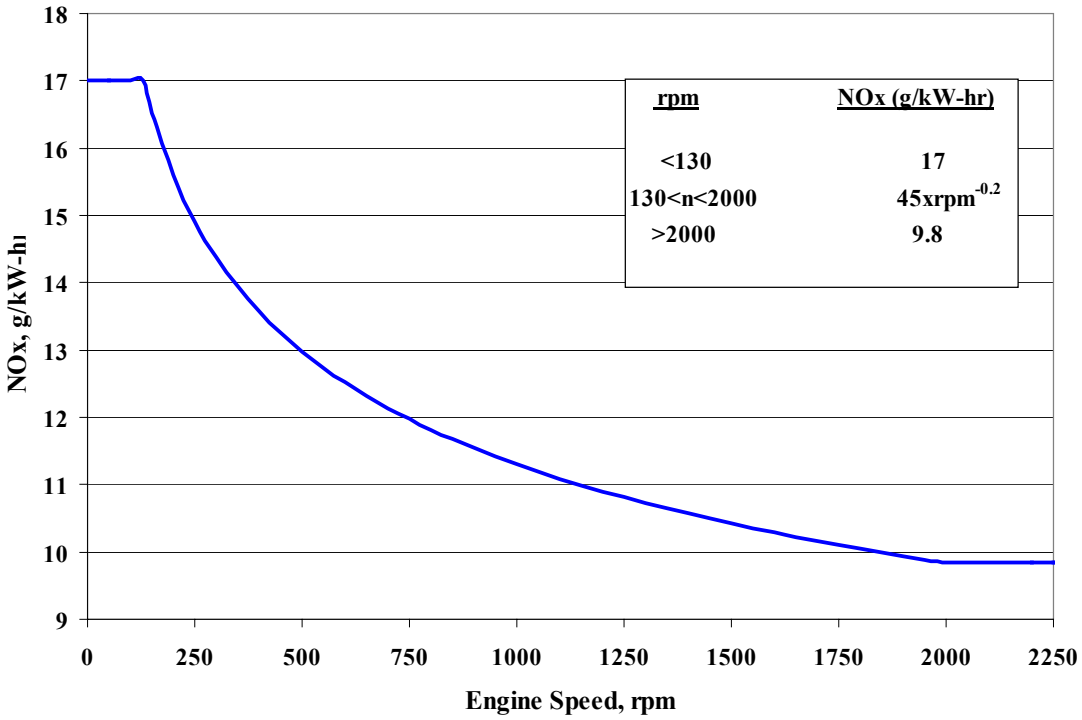


**Figure 2.1 MARPOL 73/78 Annex VI Emission limits [15]**

The use of residual fuel in Category 3 engines also limits available implementation options concerning the emission control techniques. However, the EPA proposal of May 29, 2002 [13] called for establishing Category 3 engines emission standards equivalent to the MARPOL 73/78 Annex VI limits. The rule finalizing Tier 1 emission standards for Category 3 engines was signed on January 31, 2003.

The May 29, 2002 proposal has also laid out three sets of standards for the Category 1 and 2 engines: (1) Tier 1 standards, (2) Tier 2 standards, and (3) voluntary low-emission engine standards. The Tier 1 standards are equivalent to the MARPOL 73/78 Annex VI $NO_x$ limits as listed in Table 2-2 [13] and would be applicable for new engines built in 2004 or later. These limits would be achieved by new engine technologies without the use of any exhaust aftertreatment devices. The Tier 1 standards are also applicable for Category 3

engines according to the rule signed on January 31, 2003. The Tier 2 standards would apply to engines (Category 1 and 2) built in 2007 or later. These limits would also be achieved by engine-based controls, without the use of any exhaust aftertreatment devices. The voluntary "Blue Sky Series" program permits engine manufacturers to certify their engines to comply with more stringent emission standards. This program encourages engine manufacturers to use advanced technologies such as Selective Catalytic Reduction (SCR), water-based emission control techniques, use of alternative fuels or fuel cells so as to meet the emission standards established under this program. Table 2-3 [13] and Table 2-4 [13] list the Tier 2 emission standards and the voluntary low-emission standards, respectively.

## 2.3 Prior In-use Marine Emission Measurement Studies

This section discusses few of the prior in-use emission measurements conducted on-board marine vessels. The exhaust components analyzed, the test procedures followed, and the test cycles used are mentioned in each of these studies.

### 2.3.1 US Coast Guard, 1997

The US Coast Guard conducted shipboard testing on three 82-ft. U.S. Coast Guard Cutters [16]. Each vessel was powered by two Caterpillar D3412 diesel-fueled engines. The test protocol used was based on the ISO 8178 procedure [11], with modifications based on the normal operating speed ranges for each vessel. The analyzer used was the ENERAC 2000E (Energy Efficient Systems, Inc.), which was capable of analyzing carbon monoxide (CO), nitric oxide (NO), nitrogen dioxide ($NO_2$), sulfur dioxide ($SO_2$), oxygen ($O_2$) and hydrocarbons (HC) simultaneously at discrete times. In addition, an option was available for continuous analysis of up to four components, sampling at fixed intervals. Carbon dioxide ($CO_2$) values were determined from the measured data. Air intake flow meters and

fuel flow meters were installed in order to calculate exhaust flow rate. The shaft speed and torque were determined using strain gauges epoxied onto the propeller shaft. The torque and speed were transmitted by radio frequency to a power measuring instrument (Wireless Data Corporation). The exhaust samples were taken immediately after the turbocompressor.

**Table 2-3 Tier 2 Marine Emission Standards [13]**

| **Category** | **Displacement (D)** | **CO** | **$NO_x$ + THC** | **PM** | **Effective Date** |
|---|---|---|---|---|---|
| | *$dm^3$ per cylinder* | *g/kWh* | *g/kWh* | *g/kWh* | |
| 1 | D < 0.9 & Power ≥ 37kW | 5.0 | 7.5 | 0.40 | 2005 |
| | 0.9 ≤ D < 1.2 | 5.0 | 7.2 | 0.30 | 2004 |
| | 1.2 ≤ D < 2.5 | 5.0 | 7.2 | 0.20 | 2004 |
| | 2.5 ≤ D < 5.0 | 5.0 | 7.2 | 0.20 | 2007 |
| 2 | 5.0 ≤ D < 15 | 5.0 | 7.8 | 0.27 | 2007 |
| | 15 ≤ D < 20 &Power < 3300 kW | 5.0 | 8.7 | 0.50 | 2007 |
| | 15 ≤ D < 20 & Power ≥ 3300 kW | 5.0 | 9.8 | 0.50 | 2007 |
| | 20 ≤ D < 25 | 5.0 | 9.8 | 0.50 | 2007 |
| | 25 ≤ D < 30 | 5.0 | 11.0 | 0.50 | 2007 |
| 3 | D ≥ 30 | Tier 2 standards not finalized. Tier 1 equivalent to MARPOL 73/78 Annex VI limits | | | |

In addition to the effects of shaft speed on pollutant levels, other variables examined were water depth, current, effect of towing another boat, wind direction, and sea state. The results showed that water depth had no significant effects on the pollutants. Shaft speed showed the greatest effects on the pollutants. The cold starts and

transients had higher $NO_x$ levels than at steady states. The air-fuel ratio was found to vary as a function of speed of the engines on the three boats tested.

**Table 2-4 Voluntary Low-Emission Standards [13]**

| Category | Displacement (D) | $NO_x$ + THC | PM |
|---|---|---|---|
| | *$dm^3$ per cylinder* | *g/kWh* | *g/kWh* |
| 1 | D < 0.9 & Power ≥ 37kW | 4.0 | 0.24 |
| | 0.9 ≤ D < 1.2 | 4.0 | 0.18 |
| | 1.2 ≤ D < 2.5 | 4.0 | 0.12 |
| | 2.5 ≤ D < 5.0 | 5.0 | 0.12 |
| 2 | 5.0 ≤ D < 15 | 5.0 | 0.16 |
| | 15 ≤ D < 20 &Power < 3300 kW | 5.2 | 0.30 |
| | 15 ≤ D < 20 & Power ≥ 3300 kW | 5.9 | 0.30 |
| | 20 ≤ D < 25 | 5.9 | 0.30 |
| | 25 ≤ D < 30 | 6.6 | 0.30 |

### 2.3.2 Transport Canada

#### 2.3.2.1 Field Testing of Water Injection System (WIS), 1999-2000

Transportation Development Center (TDC), Environment Canada, and BC Ferry Corporation collaborated as part of the Marine Vessel Exhaust Emissions Program and field-tested a WIS on the *Queen of New Westminster vessel* [17]. The vessel was powered by a Wartsila 9R32D diesel-fueled engine. The exhaust emissions from the #4 main engine of the vessel were tested in July 1999 and January 2000. Testing was performed with and without a continuous water injection (CWI) system manufactured by M.A. Turbo/Engine Design, Ltd. [18]. Emissions of CO, $CO_2$, $NO_x$ and particulate matter (PM) were measured

and analyzed. The test procedure was developed by Emissions Research and Measurement Division (ERMD), Environment Canada, based on the typical operation of the vessel when in normal cruise in open water. For the July 1999 tests, the analyzer used was a portable, continuous emission monitor, ECOM-AC, which measured CO, $CO_2$, $NO_x$ and $O_2$. A stainless steel particulate filter holder, vacuum pump and mass flow controllers were coupled with the analyzer to collect PM. PM was collected on pre-weighed 47mm Pallflex filters. Filters were conditioned ($40 \pm 10\%$ relative humidity and $24^oC$) prior to the tests, weighed on a Mettler AE240 balance, stored in covered Petri dishes and were then transferred to the test site on board the vessel. The filters were shipped back after the tests, conditioned for 12 to 24 hours and then weighed to determine the net mass of PM emissions. For the repeat tests performed in January 2000, an OTC MicroGas portable emission analyzer was used instead of the ECOM. The mass emissions calculations were based on the procedures outlined in ISO 8178-1:1996(E) [11].

A decrease of 10-22% in $NO_x$ emissions was noted with varying amounts of water being injected into the intake air. A linear relationship was noted between the amount of water injected and the reduction of $NO_x$ emissions. The emissions of CO and $CO_2$ were not affected with the use of WIS. The PM was reduced by an average of 19.8% with water injection. Engine horsepower was increased by approximately 1% and a corresponding decrease of approximately 1% in specific fuel consumption was found with the WIS.

#### 2.3.2.2 Engine Exhaust Emissions Evaluation of the *MV Cabot*, 2000

TDC, ERMD, Environment Canada and Oceanex collaborated on a project to characterize emissions from one of the main engines of the MV Cabot, a cargo vessel , for the purpose of design and implementation of emission control technologies [17]. The vessel

was powered by a Pielstick V-12 medium speed diesel engine. The test procedure was designed by ERMD based on the typical operation of the vessel, which was divided into four modes, i.e. leaving port, low-speed cruise, intermediate speed and higher speed. The ERMD utilized the ECOM-AC analyzer as mentioned in Section 2.3.2.1 for the measurements of CO, $CO_2$, $NO_x$ and $O_2$. PM emissions measurements were also performed as described in Section 2.3.2.1. The exhaust sampling point was immediately after the turbocharger. The mass emissions calculations were based on the procedures outlined in ISO 8178-1:1996(E) [11].

The emissions data were reported on a fuel-specific and brake-specific basis for the various cruise conditions. The calculations of exhaust emissions used approximations for both the fuel consumed by the engine and the output horsepower during the measurement periods, which were provided by the Chief Engineer of the vessel. The $NO_x$ emissions results were compared to IMO Regulations for $NO_x$ for the applicable engine size. In addition to exhaust emission measurements, the analysis also determined the nitric oxide (NO) and nitrogen dioxide ($NO_2$) components of the $NO_x$. In case of conventional internal combustion engines, the combustion of fuels results in a $NO_2/NO_x$ ratio in the exhaust stream of approximately 10% or less. The $NO_2$ results determined in this study accounted for less than 10% of the total $NO_x$ emissions. The emissions results reported for this study, though based on estimates of fuel consumption and engine horsepower, indicated that the $NO_x$ emissions exceeded the levels regulated by IMO for six of the seven different measurement points during the transit from Montreal to Trois Rivières.

### 2.3.3 Walther Engineering Services, Inc., 2001-2002

Walther Engineering Services, Inc., performed in-use emissions testing on *MV Oski*, a passenger ferry operated by Blue and Gold Fleet on San Francisco Bay, California [19]. The vessel was powered by two Detroit Diesel 12V71 naturally aspirated engines. The tests were conducted to determine emission levels using normal off-road diesel, 0.05% sulfur diesel, 20% and 100% soybean based bio-diesel fuels. All tests were conducted with and without intake air water injection. The tests were conducted on different occasions in 2001 and 2002. The exhaust was sampled in the exhaust duct at a point approximately 6ft. from the starboard engine. The analyzer used was the Enerac Model 3000 portable emissions analyzer manufactured by Energy Efficient Systems, Inc., which was capable of measuring CO, $CO_2$, $NO_x$, $O_2$, and HC. PM emissions were measured by using a flow aligned particulate probe, which was connected in-line with a quartz particulate filter and a vacuum pump drawing the sample through a stainless steel ball rotameter. For each of the tests, the engine speed was varied between a minimum and a maximum based on the range of speeds encountered in normal vessel operation. The emission results were presented in concentration format and mass production rate basis.

The off-road diesel was used as baseline. A 24% and 11% increase in $NO_x$ was found with 100% biofuel and 20% biofuel blend respectively. A 26% reduction in $NO_x$ emissions was found with intake air water injection. Water injection also reduced 100% biofuel $NO_x$ emissions by 12%. The fuel consumption was approximately the same and CO emissions were very low for all the tests. Biofuel was found to reduce the particulate emissions by about 50%. Lube oil sample analysis showed deterioration of oil total base

number (TBN) and increased wear metal. The oil samples from the generator engines, which were operated on the same fuel without water injection, were normal.

### 2.3.4 West Virginia University (WVU), 2002

WVU performed in-use emissions tests on the Hampton Road Transit Authority passenger ferryboats [20]. One of the vessels, the *James C. Echol*, was powered by two Caterpillar 3406 CNG-fueled engines, and the other, the *Elizabeth River II*, was powered by two Detroit Diesel Corporation diesel-fueled engines. The tests were conducted to determine the differences in exhaust mass emissions from the two vessel engines when operated over similar test conditions.

Gaseous emissions (CO, $CO_2$, $NO_x$, Total Hydrocarbons (THC)) and particulate matter (PM) emissions were measured and analyzed. The raw emissions sampling system was based on integration of recommendations provided by Title 40 CFR86, Title 40 CFR89, Title 40 CFR92, Title 40 CFR94, ISO 8178 and SAE J177 [7-12]. The dilution tunnel used for the measurement and analysis of PM emissions was a partial flow mini-dilution tunnel, the details of which are discussed in Section 3.7. PM was collected on 70mm Pallflex filters, that were conditioned (70$^{o}$F and 50% relative humidity) prior to the tests, weighed on Cahn C-32 microbalance, and shipped to the test site in individually labeled Petri dishes. The filters were shipped back after the tests, reconditioned, and weighed to determine the PM collected. The gas analysis bench consisted of four major analyzer components: THC analyzer (Rosemount Model 402 Heated Flame Ionization Detector (HFID) analyzer), CO and $CO_2$ analyzers (California Analytical, Inc. Model 300 Non-Dispersive Infrared (NDIR) three component analyzer), and two $NO_x$ analyzers (California Analytical, Inc. Model 400 Heated Chemiluminescent Detector (HCLD)), one of which was operated in NO only mode.

The ferryboat test cycle's steady-state points were determined based on normal ferry operation. A transient test was also performed which simulated a passenger run operating between three ports.

The in-field mass rate and brake-specific mass emissions of THC, CO, $CO_2$, $NO_x$ and PM for the two ferries were evaluated. In general, the results showed that the THC emissions from the natural gas-powered ferry were approximately 2.5 times higher than the diesel-powered ferry. The CO emissions were lower for the diesel-powered ferry, except for the 100% speed point, and $NO_x$ emissions were generally lower for the diesel-powered ferry, except at the 40% speed point. The natural gas-powered ferry had significantly lower PM emissions.

### 2.3.5 Engine, Fuel, and Emissions Engineering, Inc. (EF&EE), 2002

EF&EE performed onboard emissions measurements on three in-service diesel ferryboats operating on San Francisco Bay, namely, the *M.V. Mare Island* (propelled by two MTU 16V396 TE 74L engines), the *M.V. Peralta* (propelled by two Cummins KTTA50 engines), the *M.V. Golden Gate* (propelled by two Caterpillar 3412C engines) [21]. The tests were performed for their contractor, the San Francisco Bay Water Transit Authority, and were conducted in an in-use fashion while carrying normal service passengers on San Francisco Bay. The emissions were measured using the Ride-Along Vehicle Emissions Measurement (RAVEM) system developed by EF&EE [22]. It uses the constant volume sampler (CVS) method, with isokinetic proportional sampling of the exhaust under closed loop. The pollutants measured by RAVEM were PM, $NO_x$, CO and $CO_2$. Methane and total non-methane hydrocarbons were measured by off-board analysis of integrated samples collected in Tedlar bags using gas chromatograph. Speciated carbonyls were measured by

collecting integrated samples in di-nitro phenyl hydrazine (DNPH) cartridges, while sulfur dioxide ($SO_2$), nitrous oxide ($NO_2$), and ammonia ($NH_3$) were measured by Fourier Transform Infrared (FTIR) analysis of integrated samples.

The tests were performed in accordance with a new measurement protocol developed for this study. The test program and protocol were generally successful, but it was found that further work is needed to improve the reliability of non-methane hydrocarbon (NMHC) measurements. The results also suggested that NMHC measurements could be omitted for diesel ferries, as NMHC emissions from these vessels are generally low, and may not warrant the measurement costs involved. It was demonstrated that emissions measurements could be successfully carried out on passenger ferries while engaged in passenger service. $NO_x$ and PM emissions results from the ferryboat engines tested compared favorably with emission standards established for new engines, especially in the high-speed cruise condition, which is the dominant operating mode in typical high-speed ferry services. The results showed that use of water emulsion fuel greatly reduced PM and modestly reduced $NO_x$ emissions in high-speed cruise conditions, but increased PM emissions at idle. The results of carbonyl emissions (the most significant toxic air contaminants after diesel PM) varied considerably among the different vessels tested, but the reasons for the variation were not known.

### 2.4 Emission Reduction Technologies

There are several emission reduction technologies currently in use currently for heavy-duty diesel engines employed in the marine sector. This section discusses some of the current emission reduction technologies, namely, Water-in-fuel Emulsions, Exhaust Gas Recirculation (EGR), Intake Air Humidification, Selective Catalytic Reduction (SCR), and

Diesel Particulate Filters (DPF). Water-in-fuel Emulsions are considered to be the most cost-effective method for $NO_x$ reduction. EGR is also effective for both $NO_x$ and PM reduction. Demonstrations of SCR have shown reductions of up to 90% in $NO_x$ emissions. SCR is considered as the most effective available technology for elimination of $NO_x$, but its major setback is the huge capital, maintenance costs, and system complexity that are involved. Of those identified, the most inexpensive technology for $NO_x$ reduction is the intake air water injection system (WIS). The test engine in this study was retrofitted with such an intake air water injection system.

The percentage $NO_x$ reduction afforded by the water injection technique is less than that provided by other technologies, but the major advantages of low capital investment and the ease of installation are very appealing. Use of low-sulfur diesel fuel, which is also easily implemented, helps reduce $SO_x$ emissions and also PM emissions. The effect of using low sulfur diesel fuel on exhaust emissions is also reported in this study.

### 2.4.1 Water Aided Emission Reduction Technologies

Introduction of water into the combustion chamber reduces peak combustion temperatures; hence, reducing $NO_x$ emissions primarily. Water may be introduced into the combustion chamber with either fuel (water-in-fuel emulsions) or air (intake air water injection), discussed in Sections 2.4.1.1 and 2.4.1.3, respectively, or directly into the combustion chamber (in-cylinder water injection), discussed in Section 0.

#### 2.4.1.1 Water-in-Fuel Emulsions

Water-in-Fuel emulsions are prepared by mixing water in the form of fine droplets into the diesel phase. This is shown schematically in Figure 2.2. Although similar in make

up, fuel-in-water emulsions are not used, as there is a chance of water contacting the cylinder liner surface. This would lead to corrosion and other engine related problems [23].

Water-in-fuel emulsions introduce water directly into the area of combustion, as it is part of the fuel spray; hence reducing the peak combustion temperatures, thereby reducing $NO_x$ emissions. Fuel emulsions also result in enhanced fuel spray atomization, a result of increased momentum of the vaporized emulsion jet. This results in improved mixing of air and fuel in the cylinder resulting in better combustion, which in turn reduces the PM emissions [23]. The presence of water droplets in the fuel spray results in an increase in ignition delay. The increased ignition delay and the improved mixing of the air and fuel mixture result in increased premixed combustion [24, 25]. This in turn results in higher heat release rates and increased combustion pressures. However, offsetting this is the fact that peak combustion temperatures are lowered, due to the presence of water; hence, the reduction in $NO_x$ emissions. Certain studies have cited increases in PM emissions with the use of water-in-fuel emulsions [26]. The problem with a fuel emulsion is that it consists of two immiscible liquids having different densities and other fluid properties; hence, it does not stay stable for a long period of time. It should also be noted that the brake-specific emissions may not show significant reductions for the same amount of fuel consumed in the case of fuel emulsions, since, water displaces some of the fuel resulting in lesser power output.

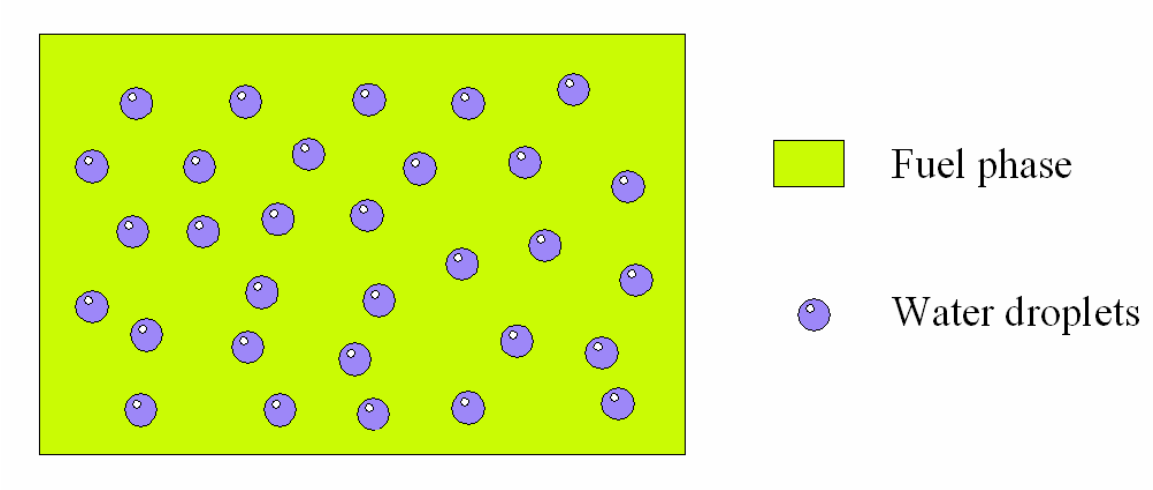


**Figure 2.2 Water-in-Fuel Emulsion [23]**

Emulsions are classified into two categories on the basis of stability and the manner in which they are prepared, namely, unstabilized emulsions and stabilized emulsions [23].

*2.4.1.1.1 Unstabilized Emulsions*

Unstabilized emulsions are prepared on-board the vehicle and fed into the fuel system [23]. The fuel and water are stored aboard in two separate tanks and the emulsion is prepared immediately before the fuel injection process. These emulsions tend to be more stable in cases of heavier fuels, as the difference in densities of the two phases is lesser; hence, the separation of water takes more time.

*2.4.1.1.2 Stabilized Emulsions*

Stabilized emulsions are prepared off-board the vessels and are stored in the form of emulsions aboard the vessels [23]. These emulsions are prepared by the mixing of water droplets in the fuel phase with the addition of certain chemicals to keep the emulsion stable without any separation for long periods.

The major drawback of fuel emulsions is that modifications in the fuel system need to be done to incorporate this technology. The setup is even more complex in the case of

unstabilized emulsions. For instance, for the same engine performance, the fuel injection system would have to feed more fuel emulsion compared to regular fuel in order to achieve similar performance. Since the capacity of the injection system is limited, the engine has to be either derated or both the water content in the fuel emulsion and maximum achievable $NO_x$ reduction must be kept at less than 20% (there is a 1% reduction in $NO_x$ for every 1% of fuel quantity in the emulsion [27]). In order to obtain the maximum $NO_x$ reduction at rated condition and full load, the injection system must be modified for longer injection duration provided the fuel pump has sufficient capacity and the camshaft has sufficient strength to complement this [28]. Once, the injection system design has been changed for operation with fuel emulsions, it would result in higher fuel consumption if the engine were to be operated on regular fuel [27].

Another important drawback of fuel emulsions is that the maximum temperature in the fuel system should be below the boiling point of water or else it may be destroyed by the evaporation of water droplets in the fuel phase [23].

#### 2.4.1.2 In-cylinder Water Injection

This technique involves direct injection of water into the combustion chamber. Water is supplied through a water injection nozzle, which may be either a separate injector or part of a combined water-fuel injector. Such a technique provides for independent control of water injection time, rate and quantity. To be effective, in-cylinder injection must be directed into the flame area at the time of formation of emissions. Since, most of the $NO_x$ is formed in the initial part of the combustion process when the combustion chamber experiences peak temperatures, the water needs to be injected during this period. Injection of water towards the latter part of combustion has resulted in poor $NO_x$ reductions and

increased fuel consumption [27]. In-cylinder water injection techniques appear to have minimal effect on PM emissions. Published studies have reported very little or no reductions in engine-out PM emissions [23].

Stratified water-fuel injection is another technique of in-cylinder water injection. In this method, the injector sprays fuel, water and then fuel in a sequence. This technique combined with EGR has shown 60-75% $NO_x$ reduction together with reductions in PM emissions [29].

Wartsila, a Finland-based manufacturer of marine diesel engines, has developed a direct water injection system [30], that has been reported to reduce $NO_x$ emissions by 50-60% for engines running on marine diesel fuel at an injected water-fuel ratio of 0.4 - 0.7(28-41% water in the water-fuel mix)[30]. The main components of the Wartsila system are shown in Figure 2.3.

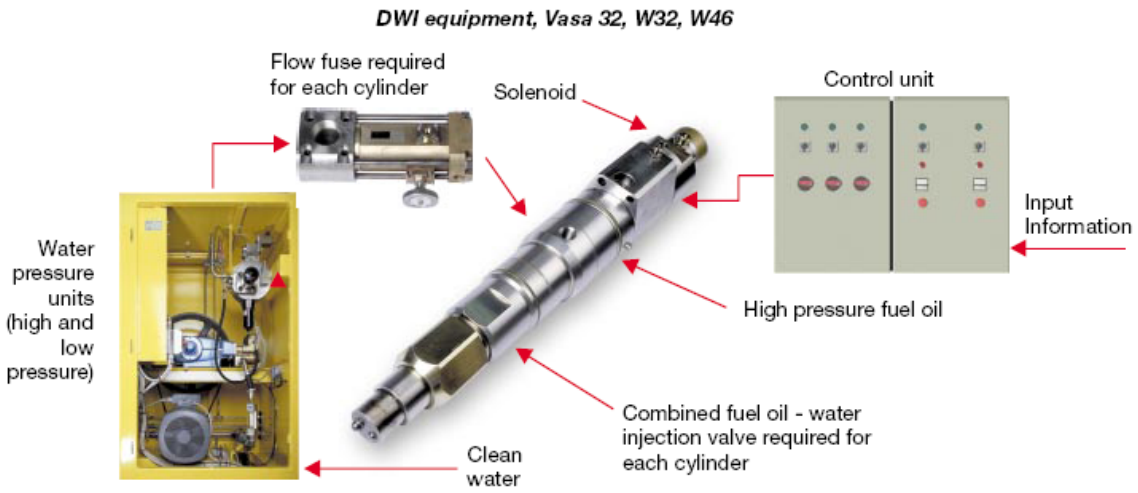


**Figure 2.3 Wartsila Water Injection System [30]**

The direct water injection system consists of a combined injection valve and nozzle, as shown in Figure 2.4, which allows injection of water and fuel into the cylinder.

**Figure 2.4 Combined Nozzle for Injecting Fuel and Water [30]**

The water injection takes place before the fuel injection so as to make the combustion space cooler for lower $NO_x$ emissions. The water injection also stops before fuel injection so that the ignition and combustion processes are not disturbed [30].

#### 2.4.1.3 Intake Air Water Injection

In this method water is sprayed into the intake air stream increasing its humidity. The effect in emissions as a result of intake air water injection is discussed later in this report. As discussed earlier in this chapter, this technique is the simplest method of water injection in terms of installation and maintenance costs. Some studies have reported this method as being the most cost beneficial method of $NO_x$ reduction in marine engines [31]. Earlier studies report that $NO_x$ reductions as a result of this method is very low compared to other methods [27, 32]. The chances of water droplets reaching the cylinder without proper vaporization and affecting the engine lube oil film are higher in this technique. Fumigation of water vapor instead of spraying liquid water is considered to minimize this problem. Figure 2.5 shows the reduction of $NO_x$ as a result of the increase in humidity of intake air in a study conducted by Ishida and Chen [33].

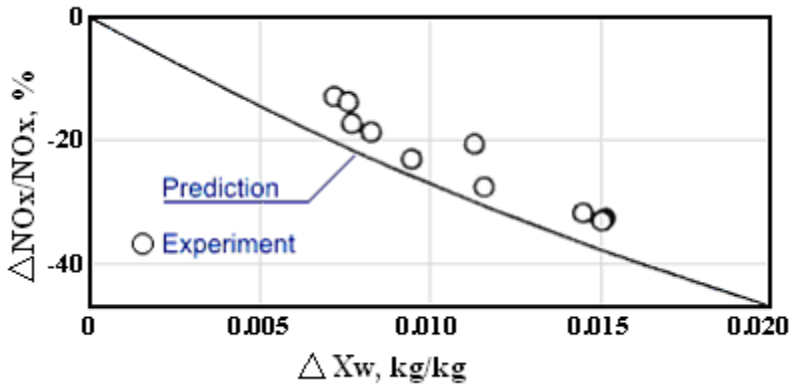


**Figure 2.5 $NO_x$ Reductions Due to Increase in Intake Air Humidity [33]**

Mellor [34] has reported the use of steam as a method of water injection into the intake air. This would help overcome the corrosion problems associated with spraying of water droplets into the intake air, which affects the lube oil.

### 2.4.2 Ultra-low Sulfur Diesel Fuels

The use of ultra-low sulfur diesel fuels is a highly effective enabling technology that will allow for notable reductions in engine emissions. Emissions Control Diesel (ECD) features less than 10ppm (wt.) sulfur content, less than 10% aromatics by volume and a cetane number of 60. Laboratory tests have reported that ECD reduces the engine-out emissions of $NO_x$ by 5% and PM emissions by 15% [35]. This study discusses the comparison of engine-out emissions for an engine operating on ordinary marine diesel and a low sulfur diesel.

The lower sulfur content results in an increase in the mole fraction of hydrocarbons in the fuel; hence, provides superior flame propagation properties and better heat content for the fuel. This helps in achieving slightly higher energy levels for the same mass of low sulfur fuel burned. Likewise, lower brake-specific fuel consumption is obtained for low sulfur diesel as compared to regular marine diesel fuel. The comparison of brake-specific

emissions and fuel consumption for the engine operating on low sulfur diesel and marine diesel is discussed later in this report.

The primary source of acidity formation in the engine oil is the fuel sulfur content. Hence, the use of low sulfur diesel also helps reduce engine wear. Additionally, low sulfur diesel enables the use of catalyzed exhaust after-treatment systems, which would otherwise be difficult owing to excessively high sulfate formation and catalyst poisoning.

### 2.4.3 Selective Catalytic Reduction (SCR)

Selective catalytic reduction (SCR) of $NO_x$ using ammonia or urea as reagent has been used in stationary diesel engine applications for a long time. SCR involves the injection of ammonia or urea into the exhaust gas stream before it is passed over a Platinum, Vanadium or Zeolite catalyst.

SCR helps in achieving the maximum reductions in $NO_x$ emissions as compared to other methods. Tests of an SCR-equipped engine have shown reductions in $NO_x$ emissions of about 80%-85% depending on engine design, application, and test method [36]. In addition to reductions in $NO_x$, SCR has also demonstrated reductions in hydrocarbon (HC) emissions and particulate matter (PM) emissions. Further, reduction in PM emissions is obtained by using SCR in combination with Diesel Particulate Filters (DPF) [37, 38].

The ammonia reduces any NO present according to the reaction,

$$6NO + 4NH_3 = 5N_2 + 6H_2O$$

Since oxygen is always present however, some $NO_2$ is formed through the reaction

$$4NO + 4NH_3 + O_2 = 4N_2 + 6H_2O$$

This too can be reduced by ammonia through the reaction,

$$2NO_2 + 4NH_3 + O_2 = 3N_2 + 6H_2O$$

The catalysts are used to promote the above reduction reactions and are usually titanium and vanadium oxides formed as honeycomb-shaped metal or ceramic plates and operated at temperatures of 370-425°C (700-800°F) for best catalytic efficiency. The ammonia is typically injected downstream from the combustion chamber and upstream of the catalyst grid.

The SCR unit requires a minimum exhaust gas temperature to be maintained, which depends upon the catalyst type. These temperatures are achieved primarily at engine loads greater than 30% of the rated capacity. In marine operations, such as those encountered in this study, engines are operated at approximately 80-90% load most of the time; hence, the SCR method could be an effective method of reducing $NO_x$ emissions. SCR is not yet widely accepted in the marine industry due to the following reasons: sulfur content in typical marine diesel is very high, the installation and maintenance costs are high, space constraints, and the additional weight of the units. Most marine engines operate on ordinary marine diesel fuel, which has very high sulfur content, which is not compatible with SCR. The reagents used in SCR method, commonly urea or ammonia require large storage tanks, which would need considerable space, another problem associated with the SCR method. The weight of retrofitting an SCR unit on an existing vessel, such as a passenger ferry, would demand an inherent reduction in passenger capacity (payload) as a result of the additional weight and space requirements of the SCR module.

### 2.4.4 Exhaust Gas Recirculation (EGR)

Exhaust gas recirculation (EGR) has been in use for a long time on both spark ignited and compression ignited engines, mainly in light-duty applications, as an effective means of $NO_x$ reduction. EGR works on the principle of recirculating a portion of the

exhaust gas stream into the engine intake air. The carbon dioxide ($CO_2$) in the recycled portion has a higher heat capacity than nitrogen ($N_2$) and oxygen ($O_2$) present in the intake air. Hence, $CO_2$ absorbs more energy during combustion and reduces the peak combustion temperatures. This results in a reduction in $NO_x$ formation. EGR has been considered to be inapplicable in case of marine diesel engines using heavy fuel oils, as the high sulfur concentrations and other abrasive particles may result in excessive engine wear and contamination [31]. However, EGR in combination with fuel emulsions and stratified fuel-water injection systems have been shown to yield up to 60%-75% $NO_x$ reductions [29, 37].

### 2.4.5 Diesel Particulate Filters (DPF)

Diesel Particulate Filters (DPF) are devices that physically trap the particulate matter (PM) emissions and prevent them from being emitted into the atmosphere. A catalyzed DPF with a high filtration efficiency is one the most efficient technologies for the reduction of PM emissions from heavy-duty diesel engines.

The DPF operation is based on the separation of solid particles from the exhaust gas stream by deposition on a collecting surface. The collected particles are removed from the filter surface in a continuous manner or periodically by the process of thermal regeneration. Detailed description regarding filtration mechanisms, filtration materials, and thermal regeneration can be found in literature [39, 40]. DPF in combination with EGR and SCR is of particular interest in recent times [38, 41], due to the high efficiency of these combinations in reducing $NO_x$ and PM emissions simultaneously.

# 3 EXPERIMENTAL EQUIPMENT AND PROCEDURES

## 3.1 Introduction

This chapter discusses the experimental equipment and procedures employed in this study. The tests for this study were conducted on the Pacific Ocean aboard a high-speed ferry (hydrofoil) operated between Oceanside and San Diego, California by SCX Inc. The validation tests for the PM Cart (Partial-flow dilution tunnel) and the MEMS (Mobile Emissions Measurement System), the major measurement systems used for particulate and gaseous emissions analysis, respectively, were conducted at the WVU Engines and Emissions Research Laboratory (EERL) prior to the onboard tests. The experimental setup and procedures are detailed in three different sections, namely, the PM Cart, MEMS, and the WVU Engines and Emissions Research Laboratory. A schematic of the experimental test setup onboard the ferry is shown in Figure 3.1. The first few sections in this chapter provide details regarding the test vessel, engine, fuels and the test matrix. The partial-flow dilution tunnel (dilution tunnel) is in compliance with ISO 8178-1:1996(E) Section16-Determination of the Particulates [11]. The exhaust sampling train and analysis systems at the WVU Engine Dynamometer Laboratory are in compliance with requirements of 40CFR Part 86, Subpart N-Emission Regulations for Heavy-Duty Diesel Engines and the Gaseous and Particulate Exhaust Test Procedures [7], and the ISO 8178-1:1996(E)[11].

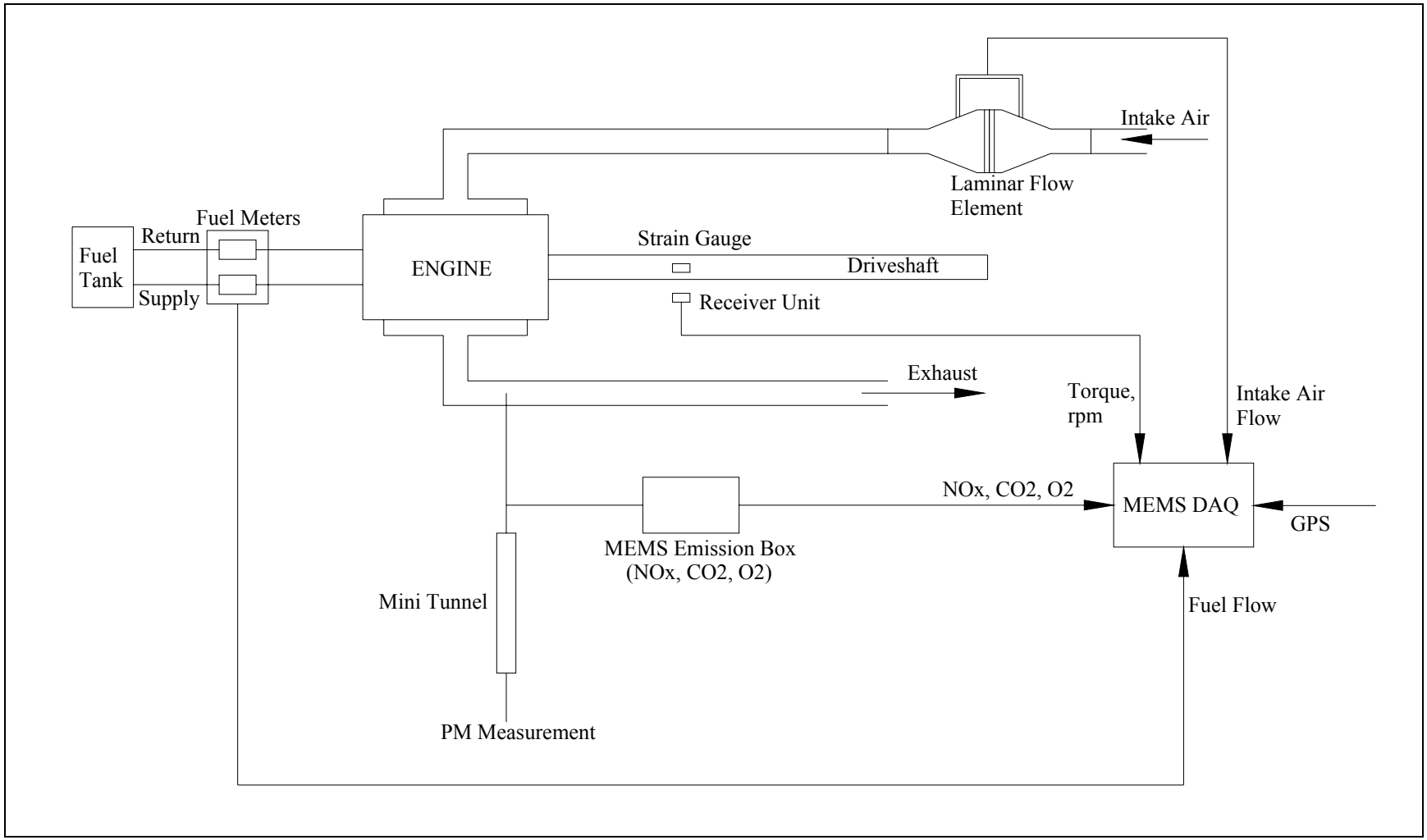


**Figure 3.1 Schematic of Test Setup Aboard the Ferry**

## 3.2 Test Vessel and Test Engine Specifications

This section describes the test vessel and test engine specifications. These details are also available in the final data report submitted to the National Renewable Energy Laboratory (NREL) [42].

### 3.2.1 Test Vessel

The test vessel was a high-speed hydrofoil-incorporated passenger ferryboat operating between Oceanside and San Diego, California. It had a capacity of 150 passengers and made a single round trip service during weekdays. The retractable hydrofoil when deployed lifts the hull of the boat out of the water, thus reducing the effects of the waves on the vessel, thus reducing the power required to sustain high speed operation. Figure 3.2 shows the test vessel with the hydrofoil deployed. The vessel was approximately 80 feet in length and was powered by four Detroit Diesel Corporation 12V92 compression ignition engines.


**Figure 3.2 Test Vessel, The Wave (SCX Inc. Ferryboat)**

### 3.2.2 Test Engine Specifications

The vessel was powered by four engines as mentioned in the previous section, two located on the starboard side, and two on the port side of the vessel. The two engines on each side were positioned in a staggered manner so that the drive shafts of the fore engines ran alongside the aft engines. The drive shafts from engines on each side were connected to a gearbox, the output from which was used to drive a water jet propulsion system. The forward starboard side engine was used to obtain data for the study. Figure 3.3 shows the test engine. Figure 3.4 shows the engine pair on the starboard side. The drive shaft of the fore engine can be seen alongside the aft engine; hence, the staggered arrangement. All four engines have wet exhausts, that is, water is injected into the exhaust gas stream downstream of the turbocharger to reduce the exhaust temperature prior to being discharged under water.

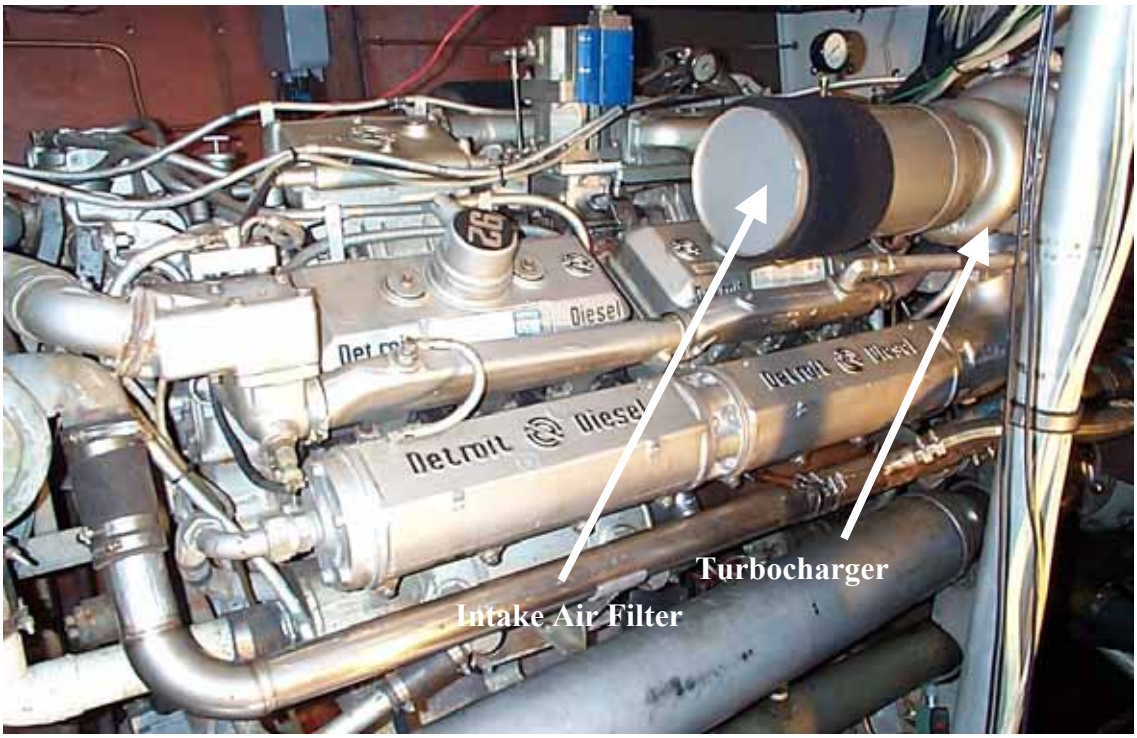


**Figure 3.3 Test Engine, Starboard Side Fore Engine**

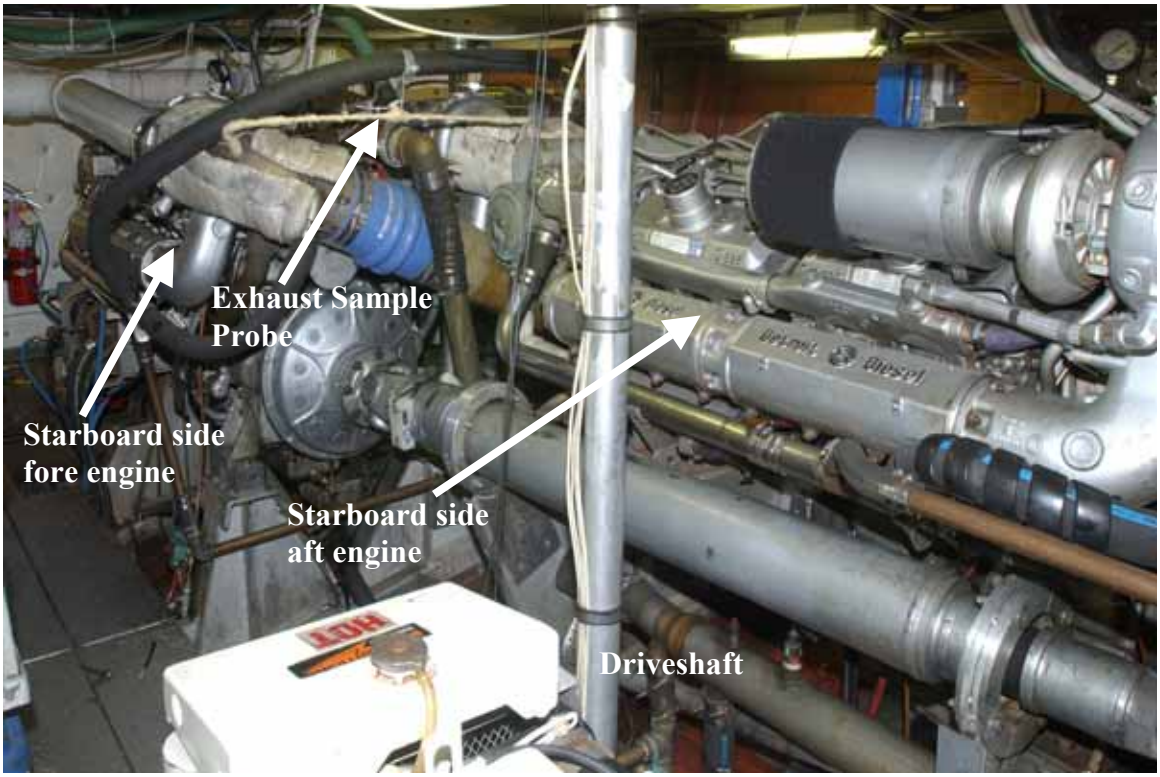


**Figure 3.4 Engine Pair on the Starboard Side**

Each engine utilized dual turbochargers, one on each side of the engine. The turbocharger outlets lead into superchargers and then into the intake manifold. The engine specifications are given in Table 3-1.

### 3.3 Water Injection System (WIS)

The water injection system supplied and installed by M.A.Turbo/Engine, Ltd. [18] injected water into the intake air stream between the turbocharger outlet and the supercharger inlet. A simple schematic of the WIS is shown in Figure 3.5. The major components of the system are the pump, pressure regulator, solenoid valve, pressure sensor, and the water injection nozzle. The operation of the water injection system was driven by the intake manifold pressure signal. It was deactivated if the manifold pressure was below a

certain value. For this reason, water injection data is not available for the idle and docking modes.

**Table 3-1 Test Engine Specifications**

| | |
|---|---|
| Engine Manufacturer | Detroit Diesel Corporation |
| Engine Model | 12V92 |
| Model Year | 1981 |
| Engine I.D. | 12VF002734.5.0.2A83804 |
| Displacement | 18.1 liters |
| Power Rating | 805 kW @ 2300 rpm |
| Configuration | 12 cylinder Vee |
| Bore (m) x Stroke (m) | 0.12 m x 0.13 m |
| Induction | Turbocharger with Blower |
| Fuel Type | Diesel |
| Engine Strokes per Cycle | Two |
| Injection | Mechanical |

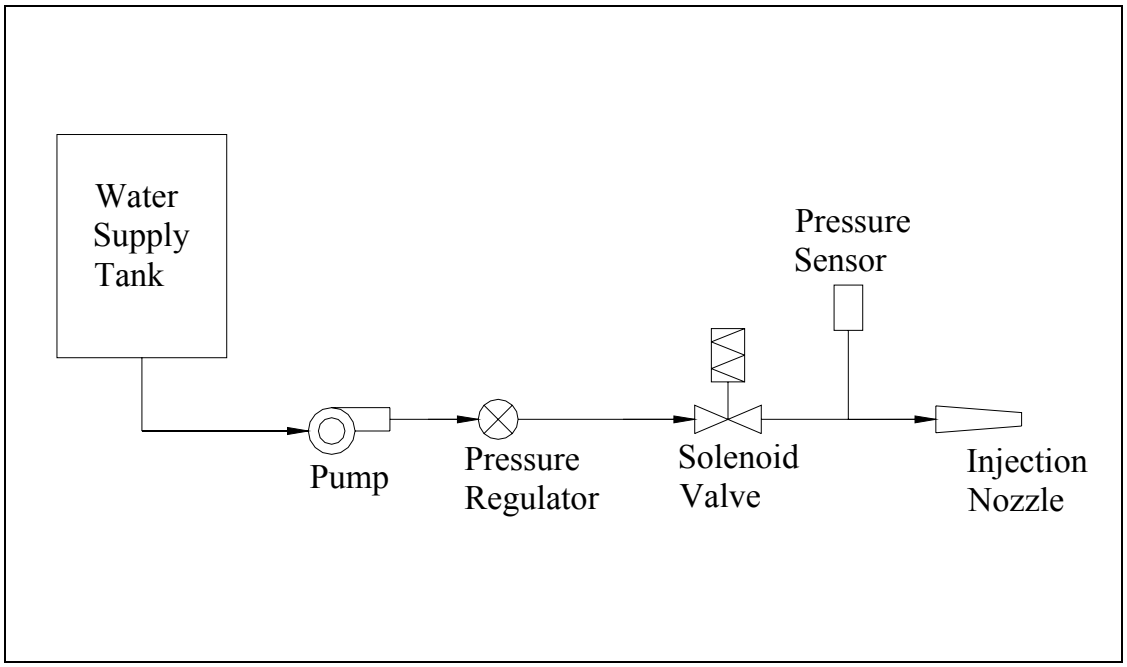


**Figure 3.5 Water Injection System (WIS) Schematic**

### 3.4 Test Fuels

All four engines are operated on conventional marine fuel during normal operation. The test fuels in this study were the conventional marine fuel and a low sulfur fuel supplied by BP, BP ECD®. The fuel analysis report as shown in Table A-1 indicates that the sulfur content for the collected in field BP ECD® fuel sample was approximately 320 ppm, whereas ECD fuels typically have sulfur content as low as 15 ppm (fuel analysis report for a typical ECD fuel is shown in Table A- 2). Hence, it is suspected that the BP ECD® may have been contaminated in this study, and for this reason it is referred to as Low Sulfur Diesel (LSD) in the later sections of this report. The fuel analysis report shows that the marine fuel sample had a sulfur content of approximately 3940 ppm. The fuel was stored in two separate 800-gallon tanks. The two tanks were reportedly completely separated from each other. The return lines and the sight gauges for the tanks are shown in Figure 3.6.

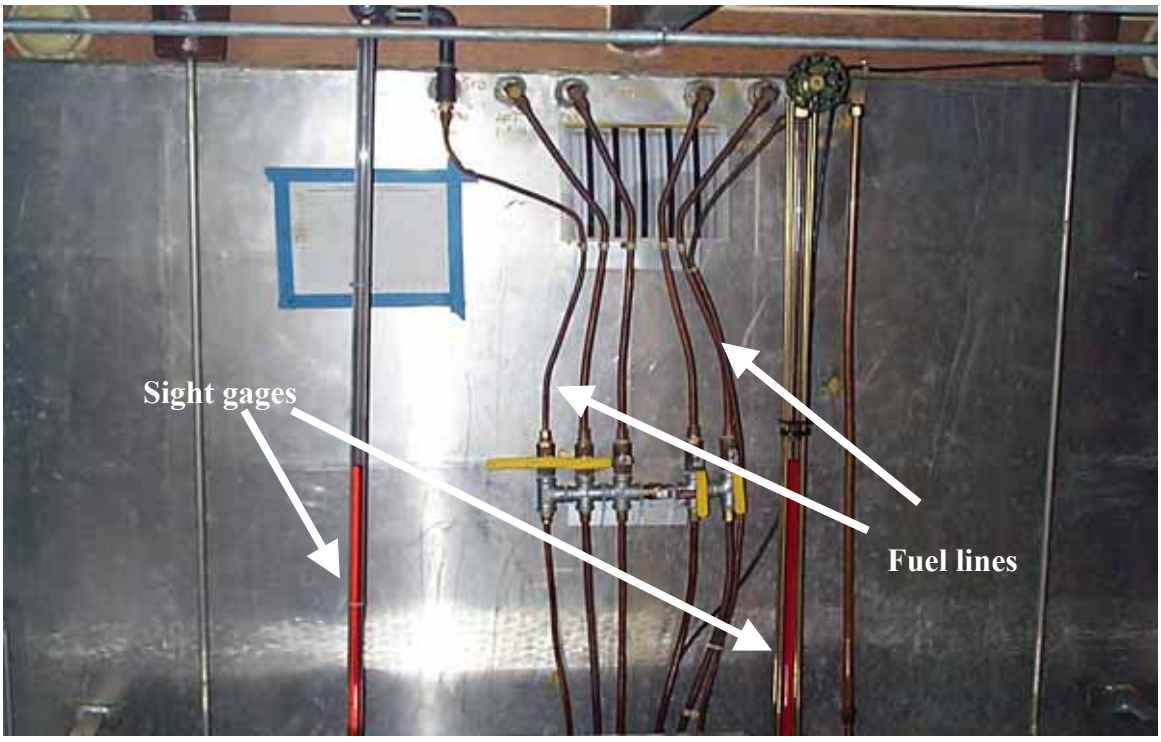


**Figure 3.6 Fuel Return Lines and Sight Gauges for the Fuel Tanks**

### 3.5 Test Matrix

The engine was operated on four different configurations while the necessary data required for the determination of brake-specific emissions of $NO_x$, $CO_2$, $O_2$ and particulate matter were recorded for each of the four configurations at four different steady state points, namely, idle (650 rpm), 1900 rpm, 2000 rpm and 2100 rpm. The four different configurations were obtained by operating the engine on conventional marine fuel and a low sulfur diesel fuel as mentioned in the previous section. For each of the two fuels, the engine was operated with and without intake air water injection system (WIS). The test matrix is as shown in Table 3-2. The data for the 1900 rpm steady-state point with the engine operating on LSD fuel with WIS could not be taken because the torque measurement device failed during this mode. With limited time available on the second day of testing, data was also recorded for a dockside mode, also referred to as the harbor mode throughout this document. The data logging for this mode began as soon as the vessel entered the marina from the ocean, and ended when the vessel reached the dock. Similarly, data was also taken from the time the vessel left the dock until it entered the ocean.

**Table 3-2 Test Matrix**

| | | WIS | | | | NWIS | | | |
|---|---|---|---|---|---|---|---|---|---|
| Low Sulfur Diesel | Speed (rpm) | 2100 | 2000 | 1900 | 650 (Idle) | 2100 | 2000 | 1900 | 650 (Idle) |
| | Runs | 2 | 3 | 0 | 0 | 2 | 2 | 1 | 2 |
| Marine Diesel | Speed (rpm) | 2100 | 2000 | 1900 | 650 (Idle) | 2100 | 2000 | 1900 | 650 (Idle) |
| | Runs | 6 | 2 | 2 | 0 | 5 | 2 | 2 | 2 |

While WIS in Table 3-2 denotes 'Water Injection System', NWIS denotes 'No Water Injection System'. The harbor mode is not shown in the test matrix, as it was not part

of the initial test plan. The data for the idle modes with WIS is not available because the WIS was activated only at high manifold pressures.

### 3.6 Important Parameters Recorded

This section lists the important parameters that were recorded for the calculation of brake-specific gaseous and particulate matter emissions.

#### 3.6.1 Parameters Recorded by the PM Cart (Partial-flow dilution tunnel)

The following is the list of major parameters that were recorded by the data acquisition system of the PM Cart. These values were used for the calculation of brake-specific particulate emissions:

- Total flow through the mini-tunnel, $V_t$
- Dilution air flow, $V_d$
- Dilution Ratio, D.R.

The PM mass collected on the fluorocarbon coated glass micro fiber filter (T60A20) was measured using a Cahn C-32 microbalance, details of which are provided in Section 3.7. The mass of particulate mass collected, $M_f$, is a sum of the particulate mass collected on the primary and secondary filters. The background mass, $M_{bf}$, is the particulate mass collected during the background test and is used for background correction. $M_f$ and $M_{bf}$ are used along with the other recorded parameters to calculate the brake-specific particulate emissions using the equations outlined in Section 3.10.1.2.

#### 3.6.2 Parameters Recorded by the MEMS (Mobile Emissions Measurement System)

The following is the list of important parameters recorded by the data acquisition system of the MEMS, which were used for the calculation of brake-specific gaseous emissions and brake-specific fuel consumption:

- Torque
- Concentration of $NO_x$
- Concentration of $CO_2$
- Concentration of $O_2$
- Differential pressure across the Laminar Flow Element (LFE)
- Absolute pressure at the LFE
- Fuel flow (both in the supply and return lines)

### 3.7 PM Cart (Partial-flow dilution tunnel)

A portable partial-flow dilution tunnel (mini-tunnel) was used for gravimetric analysis of PM emissions. The mini-tunnel was of a partial-flow design [6], where a known amount of raw exhaust gas sample was routed into the tunnel via a heated line and was mixed with metered HEPA-filtered, and temperature- and humidity-conditioned dilution air in order to achieve desired dilution ratios. The dilution ratio was controlled via a computer program using inputs from two mass flow controllers (flow based dilution ratio control) or time-aligned raw and dilute $CO_2$ concentrations obtained using a two-channel $CO_2$ analyzer ($CO_2$ based dilution ratio control). The dilution air flow rate and the total diluted exhaust flow rate (sum of raw exhaust sample flow rate and dilution air flow rate) through the mini-tunnel were controlled with Sierra mass flow controllers. In case of $CO_2$ based dilution ratio control, raw and dilute $CO_2$ measurements were used as inputs to a closed loop control system to obtain the desired dilution ratio. $CO_2$ based dilution ratio control was used for all the tests conducted on the ferry engine. In the case of the validation tests conducted in the laboratory, some of the tests were conducted using flow-based dilution ratio control, while others were conducted using $CO_2$-based dilution ratio control.

The PM cart contains all the components necessary for exhaust, sampling, and sample conditioning. Figure 3.7 shows the PM Cart mounted aboard the ferry during actual tests. A schematic of the cart is shown in Figure 3.8.

The dilution tunnel was approximately 0.05m (2") in diameter and 0.61m (24") in length and was constructed of stainless steel to prevent corrosion. The mini-tunnel design was in compliance with the requirements of ISO 8178-1:1996(E) 16.1.1[11].

The dilution air was provided to the tunnel by a rotary-vane pump. The dilution air was pumped through a HEPA-filter, and then passed through a heat exchanger and a chiller to regulate temperature and humidity. Temperature was maintained as close to ambient temperature prior to entering the mass flow controller.

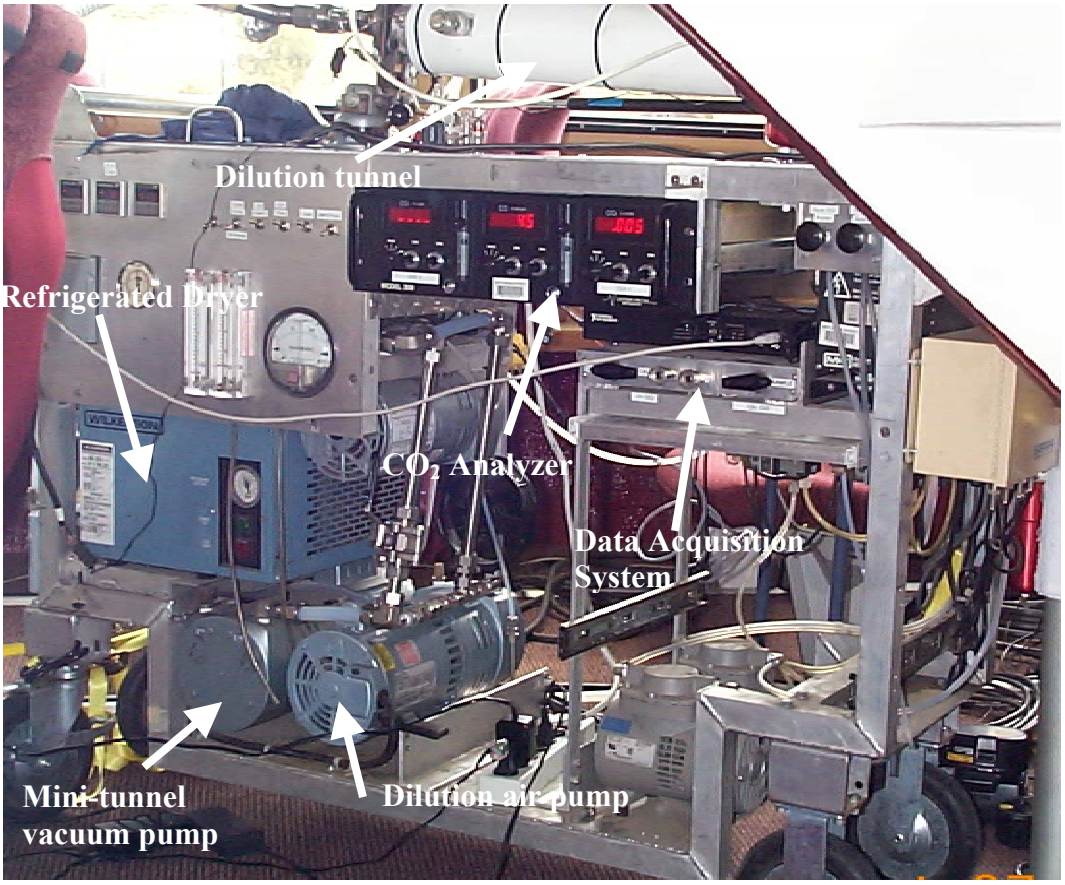


**Figure 3.7 The PM Cart Aboard the Ferry During the Tests**

The raw exhaust gas sample entered the tunnel along its centerline and passed through a mixing orifice plate that was close-coupled to the divergent tunnel entrance. The orifice plate created turbulence in the flow path that promoted thorough mixing. The tunnel flow rates were maintained sufficiently high in order to obtain the fully developed, blunt-shaped turbulent flow profile that reduced the sensitivity of sample probe placement. A second rotary-vane pump drew the entire tunnel flow stream across a stainless steel filter holder which contained two Pallflex 70mm diameter Model T60A20 fluorocarbon coated glass micro fiber filters. The diluted exhaust flow across the filters was metered through a mass flow controller. The diluted sample stream was maintained at temperatures below 125$^{o}$F, measured at the stainless steel filter holder inlet.

A mass flow controller downstream of the filter controlled the total flow rate through the tunnel. A 3-way ball valve was fitted between the tunnel exit and the stainless steel filter holder so as to bypass the tunnel flow stream for the time during which PM data was not being taken. This provided for stabilized system parameters prior to PM collection. Two Sierra mass flow controllers provided flow rate control of the total flow and dilution air flow based on computer voltage outputs determined from the raw and dilute $CO_2$ concentrations. The mass flow controllers were routinely recalibrated by the manufacturer and were additionally checked in-house against Merriam Instruments laminar flow elements. The dilution ratio was continuously controlled and maintained at the target value using the dilute and raw $CO_2$ concentration measurements in the dilution tunnel. Exhaust sample flow rate into the tunnel was inferred from this dilution ratio along with the total mass flow rate measured using the mass flow controller.

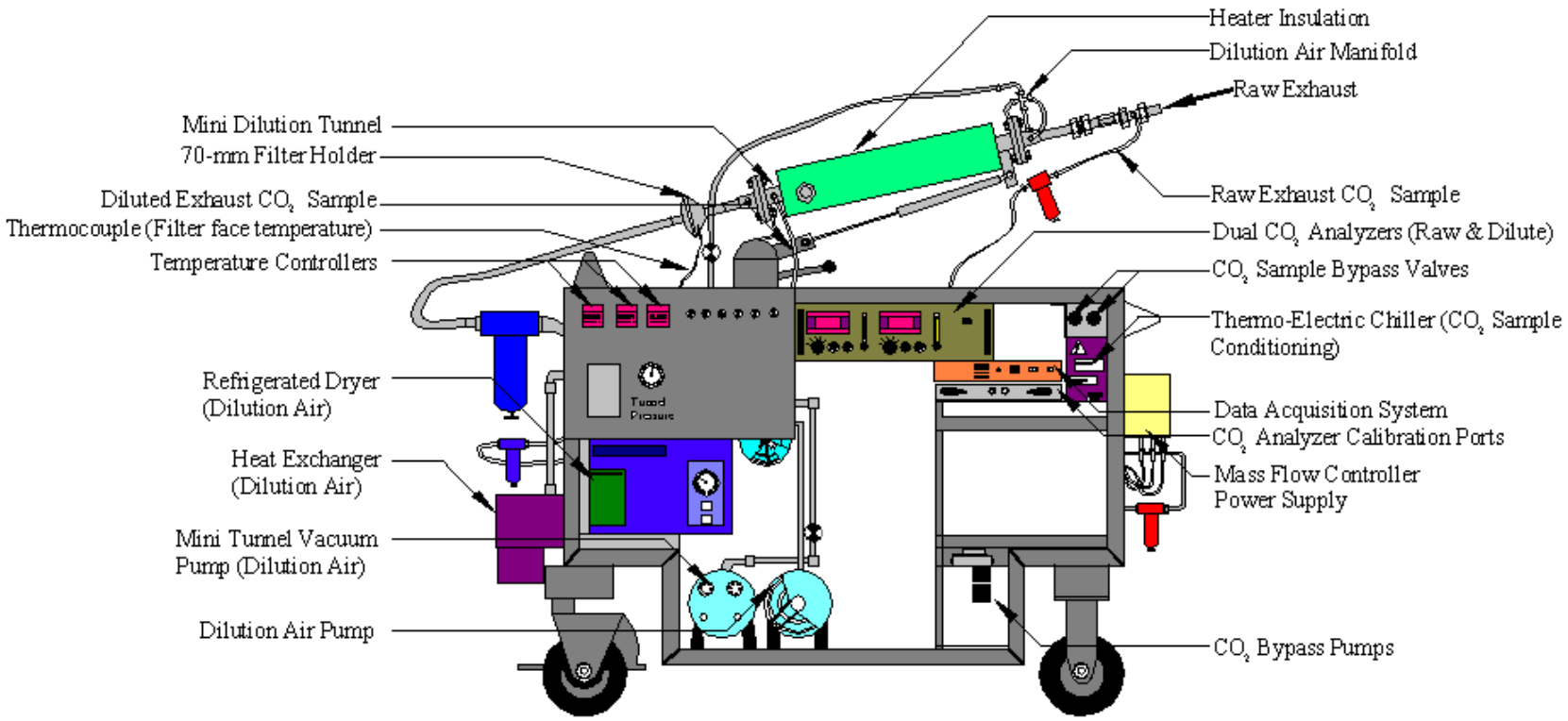


**Figure 3.8 Schematic of the Partial-flow Dilution Tunnel (PM Cart)**

The PM samples were collected on filters during each mode of engine testing. The PM collected on filters consisted primarily of elemental carbon as well as sulfates, soluble organic fraction (SOF), engine wear metal, and bound water. The sample filters were conditioned in an environmentally controlled chamber to 70$^{o}$F and 50% relative humidity, in compliance with requirements of 40 CFR Parts 86 and 89 [7, 8], and weighed before and after sample collection using a Cahn C-32 microbalance, a 40 CFR Part 86 compliant microbalance. The filters used in all the tests were pre-weighed in the weighing room at the WVU Engine and Emissions Research Laboratory (EERL), and were shipped to the test site in labeled petri dishes placed in individually sealed padded envelopes. Filters with the collected particulate matter were shipped back from the field to the WVU EERL after tests were completed. Test filters were post-weighed after being conditioned in an environmentally controlled chamber, which was maintained at 70$^{o}$F and 50% relative humidity, in compliance with requirements of 40 CFR Parts 86 and 89 [7, 8]. Filters were not conditioned immediately before or after the tests as set forth in 40 CFR Parts 86 and 89 [7, 8], but were conditioned prior to pre weighing before the test dates, and prior to post weighing the in-field tests, because the filters had to be shipped back and forth. An additional set of filters was also shipped along with filters that were to be used for testing. This set of filters was conditioned, pre-weighed and shipped to and from the test site in a similar manner, but were kept unused. This was done in order to determine the effects of shipping and handling of the filters and also to determine the effects of not conditioning the filters immediately before and after the tests. The detailed results from gravimetric analysis are discussed in Section 4.1.1.2. The results showed that the effects of shipping and

handling and the effects of not conditioning the filters immediately before and after the tests were small enough to be neglected.

### 3.8 MEMS (Mobile Emissions Measurement System)

One of the five in-use emissions measurement systems developed at the WVU Engines and Emissions Research Laboratory (EERL) was used for conducting tests on-board the ferry at Oceanside, California. The system was capable of recording $NO_x$, $CO_2$, $O_2$, torque, fuel flow and intake airflow as mentioned earlier in Section 3.5.2. Several other engine parameters were also recorded. Figure 3.9 shows the MEMS data acquisition box and the MEMS emissions box, which housed the emissions sampling and conditioning systems, as well as gas sensors.

**Figure 3.9 MEMS Data Acquisition Box (Left) and MEMS Emissions Box (Right)**

The system used for on-board testing was compared with the WVU Engine Laboratory data during tests conducted on a Detroit Diesel Series 60 engine in the engine test cell at WVU EERL, prior to being shipped to the test site. The facility at WVU EERL

is detailed in Section 3.9 and the results of the validation tests are discussed in Section 4.8. The following sections give a brief description of the MEMS. Several published reports [2-5] give more detailed description of the MEMS.

### 3.8.1 Gaseous Emissions Sampling and Conditioning System

The gaseous sampling system operated under principles consistent with engine certification testing procedures as defined in 40 CFR Part 89, 40 CFR Part 92, 40 CFR Part 94 and ISO 8178-2:1996(E) [8-11], wherever applicable. A schematic of the gaseous emissions sampling system is shown in Figure 3.10. The sample was maintained above its dew point temperature along the entire sampling system, and materials were used such that they did not react with the raw exhaust gas sample. The sampling system consisted of the raw exhaust sample probe, heated sample line, heated filter assembly, a $NO_x$ converter, diaphragm pump, gas sensors, flow control devices and sample moisture control system.

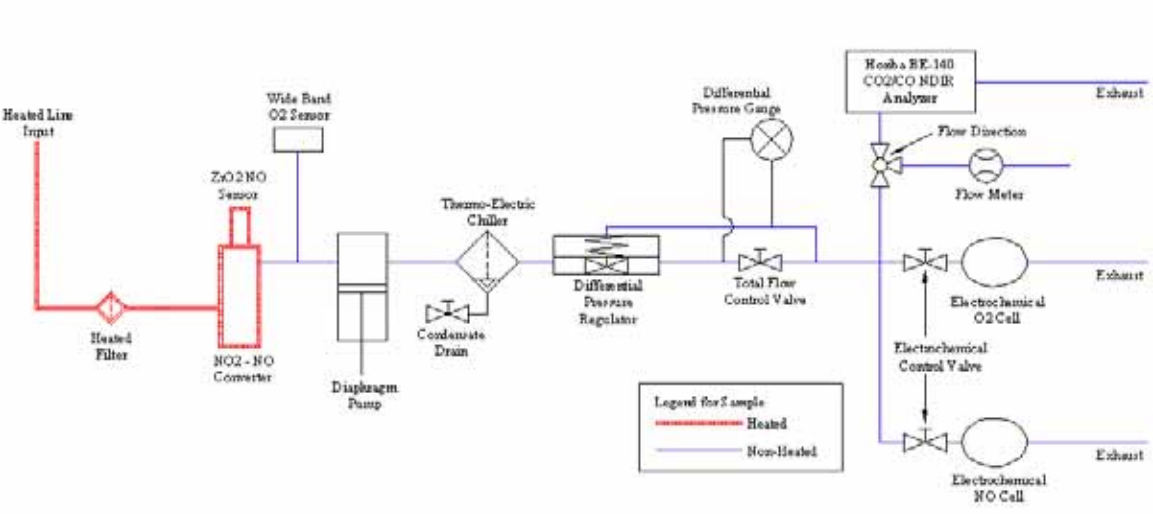


**Figure 3.10 Schematic of the MEMS Sampling System**

#### 3.8.1.1 Exhaust Sample Probe and Heated Sampling Line

The sample probe used was a multi-hole stainless steel probe mounted in the raw exhaust stack immediately downstream of the turbocharger outlet. The probe design was in compliance with guidelines in 40 CFR Part 89, Subpart E [8] and the ISO 8178-1:1996(E) [11]. Figure 3.11 shows the exhaust sample probe that was installed in an elbow downstream of the turbocharger of the test engine. The raw exhaust was sampled from each side of engine (downstream of both turbochargers on the engine) before the location where water is injected into the exhaust stream. It was insured that equal amounts were sampled from each exhaust stream so that the integrated sample was representative of the total exhaust flow. The sampling probes were insulated as shown in Figure 3.11. The heated sample line (the green line in Figure 3.11) fed the sample to both the gaseous emissions measurement system and the particulate sampling system. The sample line was electrically heated and maintained at $375^{o} \pm 10^{o}$F, in compliance with 40 CFR Part 86, Subpart N [7], using electronic temperature controllers. This temperature ensured that the higher molecular weight hydrocarbons did not condense in the lines even though the hydrocarbon emissions were not measured in this study, yet this condensation would affect PM formation (adsorption).

#### 3.8.1.2 $NO_x$ Converter

A $NO_2$ to NO converter [43] downstream of the heated filter was incorporated with the MEXA 120 Zirconium Oxide $NO_x$ sensor, which is briefly described in Section 3.8.1.5.1. The converter ensured an accurate measurement of oxides of nitrogen ($NO_x$) components (mainly, nitric oxide (NO) and nitrogen dioxide ($NO_2$)) in the exhaust stream.

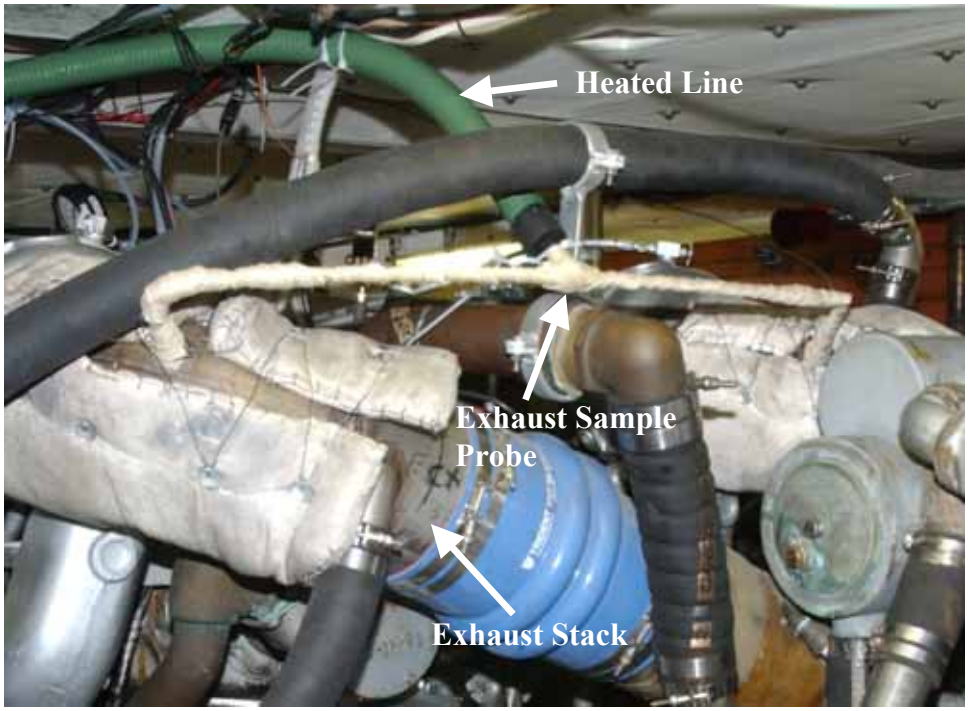


**Figure 3.11 Exhaust Sampling Probes and the Heated Line**

.

### 3.8.1.3 Diaphragm Pump

An Air Dimensions Inc. Micro DiaVac ® unheated sample pump located downstream of the wide-band $O_2$ sensor directed the exhaust sample to the rest of the sampling system. The pump required 115 volts and 1.9 amperes of current.

### 3.8.1.4 Temperature Controllers

An Omega CN 616 temperature controller was used to measure, monitor and maintain the heated sample line temperature at 375$^{o}$F, heated filter temperature at 300$^{o}$F, $NO_x$ converter temperature at 400$^{o}$F, chiller surface temperature at 45$^{o}$F, internal enclosure temperature to under 100$^{o}$F.

### 3.8.1.5 Oxides of Nitrogen ($NO_x$) Analyzers

Two sensors were used for $NO_x$ concentration measurements in the MEMS sampling system, namely, an Electrochemical (EC) cell and a Zirconium Oxide ($ZrO_2$)

sensor. The EC cell, serving as a redundant $NO_x$ measurement, was utilized primarily as a QA/QC device in the event of $ZrO_2$ failure.

*3.8.1.5.1 Horiba MEXA 120 $NO_x$ Analyzer*

A Horiba $ZrO_2$-based MEXA $NO_x$ sensor was used for $NO_x$ measurements. It was capable of concentration measurements from 0 ppm to 5000 ppm $NO_x$. The sensor consisted of two chambers. The first chamber included a $ZrO_2$ electrolyte coated with Platinum which acted as catalyst for the removal of $O_2$ from the sample. The sample then entered the second chamber, which dissociated the NO molecules into $N_2$ and $O_2$. The $O_2$ produced from this dissociation was further pumped out by a $ZrO_2$ electrolyte and the current required to do so was used to infer NO concentration in the sample.

*3.8.1.5.2 EC $NO_x$ Analyzer*

The EC cell operates on the Fick's law of diffusion. The EC cell in the MEMS sampling system was manufactured by City Technology, U.K., and marketed by Sensors Inc. The EC $NO_x$ cell had a range of 0 ppm to 5000 ppm. The cell was placed downstream of the $NO_x$ converter catalyst in order to provide total $NO_x$ measurements. It consisted of two electrodes separated by an electrolyte, one of which was porous so as to allow the gas sample to pass through after diffusing through a membrane. The voltage drop induced as a result of the current flowing across a resistor connected between the electrodes is proportional to the concentration of the total $NO_x$, the diffusion of which is controlled by a membrane between the electrodes.

**3.8.1.6 $CO_2$ Analyzer**

A Horiba Model BE-140 Non-Dispersive Infra Red (NDIR) gas analyzer was used for $CO_2$ concentration measurements. NDIR analyzers use the principle of selective

absorption, in that the infrared energy of a particular wavelength, specific to a certain gas, will be absorbed by that gas. Infrared energy of other wavelengths is transmitted by that gas just as the absorbed wavelength is transmitted by other gases. The changes in energy measured by a detection scheme downstream of the sample cell is then used to infer constituent gas concentrations.

#### 3.8.1.7 $O_2$ Analyzer

Two sensors were used for $O_2$ concentration measurements in the MEMS sampling system, namely, an Electrochemical (EC) cell and a Wide-band Oxygen sensor. The EC cell was installed as a QA/QC device in the event of the wide-band analyzer failure.

##### *3.8.1.7.1 Wide Band $O_2$ Analyzer*

A Honda (part # 36531-P07-003) wide-band oxygen sensor was used to detect the $O_2$ content in the exhaust stream; hence, obtain a measure of the air-fuel ratio. These sensors incorporate a reference cell coupled to a pump cell and a small diffusion chamber. The exhaust sample passes through the diffusion gap into the pump cell. The reference cell produces a voltage above or below a reference voltage signal, which corresponds to the stoichiometric air-fuel ratio. This voltage in turn produces a pump current the direction of which depends on whether the exhaust is rich or lean. When the free oxygen or free fuel has been neutralized, the feedback voltage signal becomes equal to the reference voltage signal. The pump current required to produce this equilibrium is a measure of the Lambda or Air-Fuel Ratio. The electronics required to operate the sensor convert the pump current to an output voltage, which is correlated with $O_2$ concentration.

*3.8.1.7.2 EC $O_2$ Analyzer*

EC cells operate on the Fick's law of diffusion. The EC $O_2$ cell in the MEMS sampling system was manufactured by City Technology, U.K., and marketed by Sensors Inc. as Model ClassR-22ASEN $O_2$ cell, with a range of 0% to 100%. The working principle is similar to that of the EC $NO_x$ discussed in Section 3.8.1.5.2. It consisted of two electrodes separated by an electrolyte, one of which is porous so as to allow the gas sample to pass through after diffusing through a membrane. The voltage drop induced as a result of the current flowing across a resistor connected between the electrodes is proportional to the concentration of the total $O_2$, the diffusion of which is controlled by a membrane between the electrodes.

### 3.8.2 Fuel Flow Measurement

Fuel flow rate was recorded on a continuous basis using two Micro Motion CMF025 Coriolis flow meters with RFT9739D4SUA transmitters. One unit measured the fuel flow rate in the supply line, while the other measured that in the return line. The data was recorded continuously by the data acquisition system of MEMS. Figure 3.12 shows the flow meters installed in the fuel lines during the tests. Figure 3.13 shows the RF9739 transmitters placed on the main deck during the tests.

### 3.8.3 Intake and Exhaust Flow Measurements

A Meriam Laminar Flow Element (LFE) was used to measure the intake air flow rate. Differential pressure was measured using a Validyne Model P55D pressure transducer. Absolute pressure was measured using an Omega Model PX213 pressure transducer. Figure 3.14 shows the LFE and the box that housed the pressure transducers. The LFE temperature was recorded using a thermocouple.

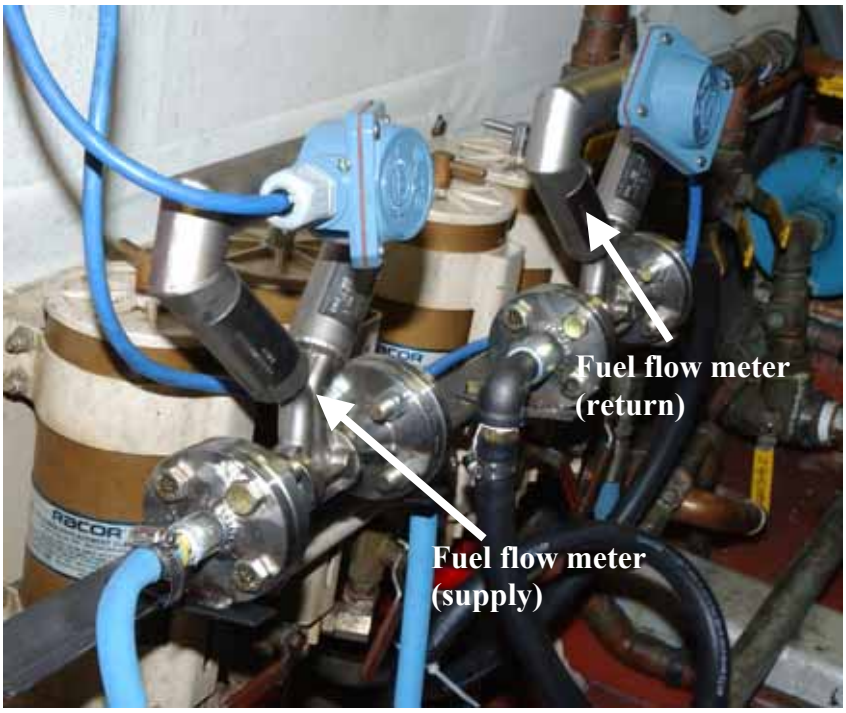


**Figure 3.12 Fuel Flow Meters Installed in the Fuel Lines**

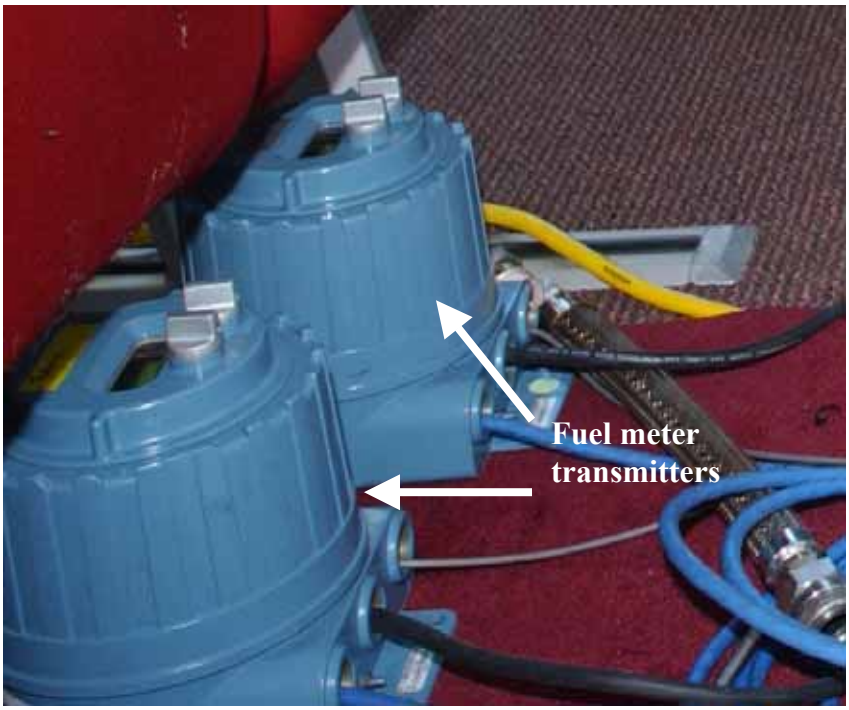


**Figure 3.13 Transmitters for the Fuel Flow Meters**

The absolute pressure, differential pressure, and the LFE temperature were recorded continuously by the MEMS data acquisition box. The transducers were calibrated at WVU EERL prior to in-field tests and calibrations were then checked at the test-site before testing commenced.

The exhaust flow rate was determined by summing the intake air flow rate, measured by the LFE, and the fuel flow rate, measured by the fuel flow meters. The fuel flow rate was also determined using the carbon balance method by using the $CO_2$ concentrations in the exhaust stream.

### 3.8.4 Torque Measurement

Engine shaft torque was measured using an Advanced Telemetrics International Model 2025B-S transmitter and receiver. The device was also meant to measure the shaft speed, but the speed sensor was damaged beyond repair during the tests; hence, speed was recorded manually from the tachometer on board the ferry. The magnetic speed sensor was attached to the engine frame, and the mating sensor was fixed on the engine drive shaft in the radio frequency (RF) housing. It was determined that the fiberglass haul of the ferry distorted during high speed operation, which resulted in a relative movement of the magnetic pickup and RF housing, and caused the two to come into contact and resulted in breakage of the sensor. The transmitter was mounted on the drive shaft as shown in Figure 3.15. It transmitted a radio frequency signal, which was picked up by an integrated receiver, and sent to the MEMS data acquisition system. The strain gage load cell for torque measurement was also mounted on the drive shaft, and was calibrated using a shaft locking system and calibration torque arm with known weights. Figure 3.15 and Figure 3.16 shows the load cell and the calibration arm with weights, respectively. Figure 3.15 shows the shaft

in the locked position, which was done by using an arm that was bolted to the drive flange on one end and the other end rested on the hull of the vessel.

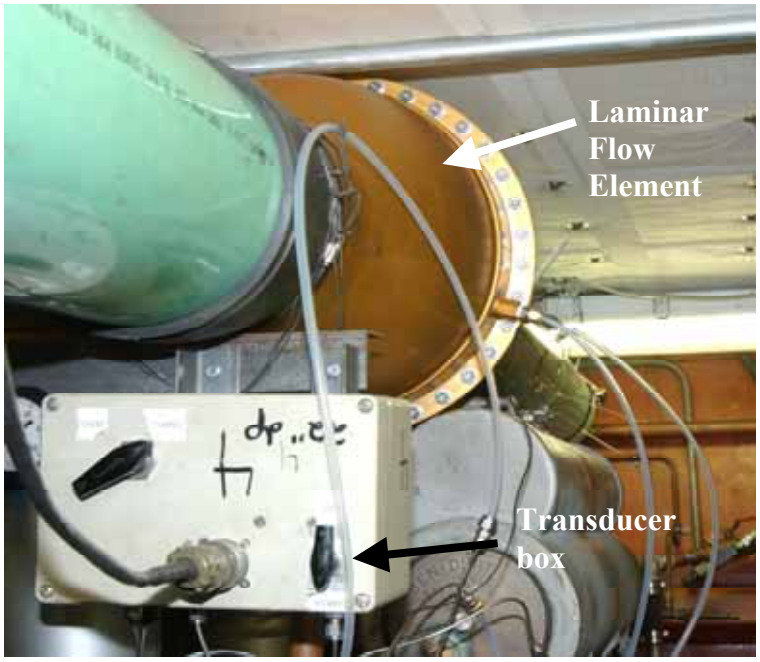


**Figure 3.14 Laminar Flow Element (LFE) in the Intake Air Stream, and the Transducer Box**

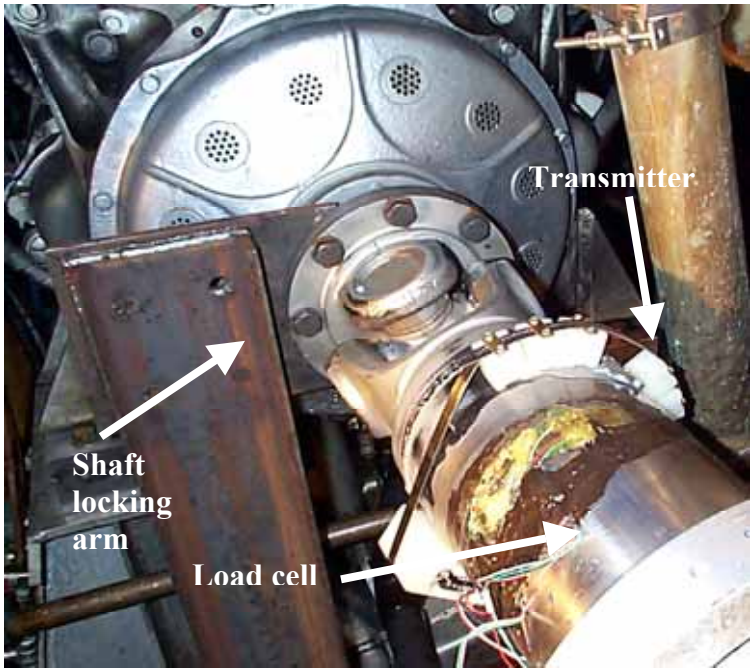


**Figure 3.15 Driveshaft in the Locked Position and with the Load Cell Mounted**

At the rear end of the shaft, another arm was bolted to the drive flange and this was held horizontally so that known weights could be placed for the calibration of the load cell, as shown in Figure 3.16. The response of the load cell for various known weights was then recorded.

### 3.9 Engine Dynamometer Laboratory

Prior to shipping the MEMS and the PM Cart to the test site in California, extensive qualification tests were conducted at the WVU Engines and Emissions Laboratory (EERL). This section describes the engine test cell facility at the WVU EERL. Figure 3.17 shows a layout of the Engine Dynamometer Laboratory. The exhaust sampling train is based on Title 40 CFR Part 86 [7], the Subpart N-Emission Regulations for Heavy-Duty Diesel Engines and the Gaseous and Particulate Exhaust Test Procedures.

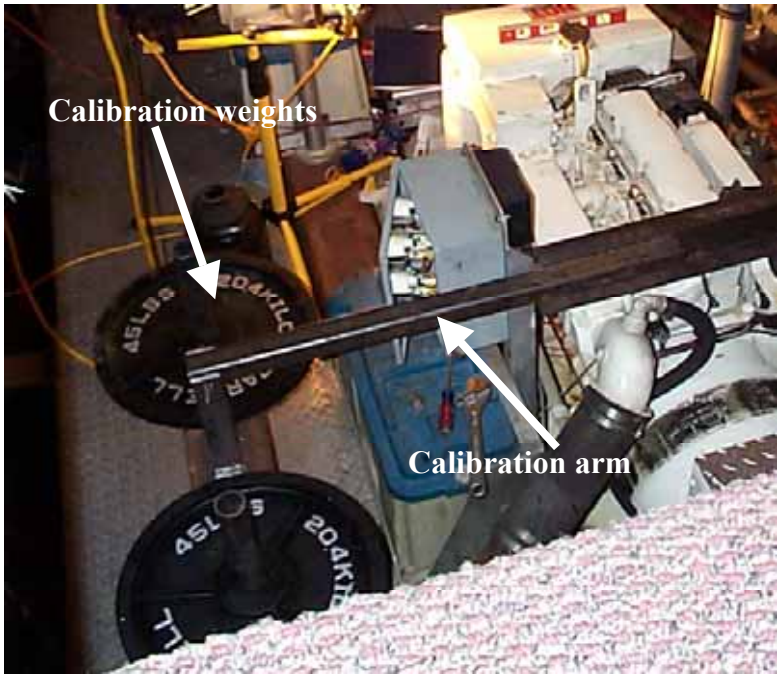


**Figure 3.16 Calibration Arm with Known Weights During the Calibration**

### 3.9.1 Engine

An electronically controlled, turbo-charged, six-cylinder in-line Detroit Diesel Corporation Series 60 on-highway engine was used to generate exhaust for the validation tests of the partial-flow dilution tunnel and the MEMS prior to the on-board tests. These tests were conducted to study the amount of variation in the particulate matter data measured using the partial-flow dilution tunnel, and the gaseous emissions data measured using the MEMS compared to that measured using the full-flow dilution tunnel and the laboratory analyzers. Table 3-3 lists the specifications of the engine.

### 3.9.2 Operating Conditions

The engine was operated at rated speed and 100% load (Rated 100) condition for most of the validation tests conducted at the WVU Engines and Emissions Laboratory. The engine was also operated over two multi-mode steady state tests. The seven steady state modes that were selected from the ISO 8 Mode Test Cycle (ISO 8178 Parts 1-4, 1996 [11]) are listed in Table 3-4. ISO 8178 Part 4, 1996 [11] states the concepts that were considered to achieve the objectives for the development of this cycle. Steady-state test evaluation was used since majority of vessel operation is predominantly steady state. The modes that constitute the ISO cycle were sub-sets of a universal test cycle. The universal test cycle consisted of 11-modes, of which the rated and intermediate speed modes at 25% load, and the intermediate speed mode and 10% load are not included in the ISO 8-mode cycle.

**Table 3-3 Engine Specifications (DDC Series60)**

| | |
|---|---|
| Engine Manufacturer | Detroit Diesel Corporation |
| Engine Model | Series 60 |
| Model Year | 1992 |
| Displacement | 12.7 liters |
| Power Rating (hp) | 261 kW @ 1800 rpm |
| Configuration | Inline-6 |
| Bore (m) x Stroke (m) | 0.13 m x 0.16 m |
| Induction | Turbocharged |
| Fuel Type | Diesel |
| Engine Strokes per Cycle | Four |
| Injection | Electronically Controlled |

### 3.9.3 Dynamometer/Dynamometer Control

A General Electric DYC-243 DC dynamometer was used to apply the steady loads to the engine. The dynamometer was capable of absorbing power up to a maximum of 550 hp, and 500 hp while motoring. A load cell attached to the stator measured the load applied to the engine. The dynamometer speed was digitally reported by the dynamometer control system.

**Table 3-4 ISO 8 Mode Test Cycle**

| Mode Number | Engine Speed | Observed Torque | Modes Selected |
|---|---|---|---|
| 1 | Rated | 100 | √ |
| 2 | Rated | 75 | √ |
| 3 | Rated | 50 | √ |
| 4 | Rated | 10 | √ |
| 5 | Intermediate | 100 | √ |
| 6 | Intermediate | 75 | √ |
| 7 | Intermediate | 50 | √ |
| 8 | Idle | 0 | |

### 3.9.4 Particulate Matter Sampling and Handling

The particulate matter from the dilute exhaust drawn into the heated line was collected on primary and secondary Pallflex T60A20, 70 mm (2.76 inches) fluorocarbon coated glass micro fiber filters. According to Title 40 CFR Part 86 [7], filters were conditioned for at least one hour and no more than 80 hours at a 50% relative humidity (RH) and 70°F environmental chamber both before and after the tests. The filters used for this research were conditioned for at least 6 hours for both pre- and post-test weighings. Sulfuric acid in the diesel exhaust contains bound water. Wall and Hoekman [44] suggested that at 50% RH, 1.3 grams of water is present for every gram of sulfuric acid. They further showed a linear relationship between bound water and sulfuric acid up to 60% RH. The amount of bound water increases rapidly beyond 60% RH. Therefore, humidity control of the environmental chamber provides for improved accuracy for gravimetric analysis of PM. Continuity was maintained by having two reference filters in the environmental chamber at all times. These filters were not used for testing, but served as a quality control check for humidity control within the chamber. The reference filters were weighed before and after a test along with the test filters. The measured sample weights were either used or discarded based on the variations in reference filter weights in accordance with the Title 40 CFR Part 86 [7] specifications. The particulate filters, reference and sample, were stored in glass petri dishes, while conditioning in the environmental chamber. These dishes were covered but not sealed to prevent dust from accumulating on the filters while allowing humidity exchange to take place. Ferguson [45] stated that the glass petri dishes should be used instead of plastic petri dishes because the static electric charge carried by the plastic petri dishes could result in the loss of particulate matter from the filter.

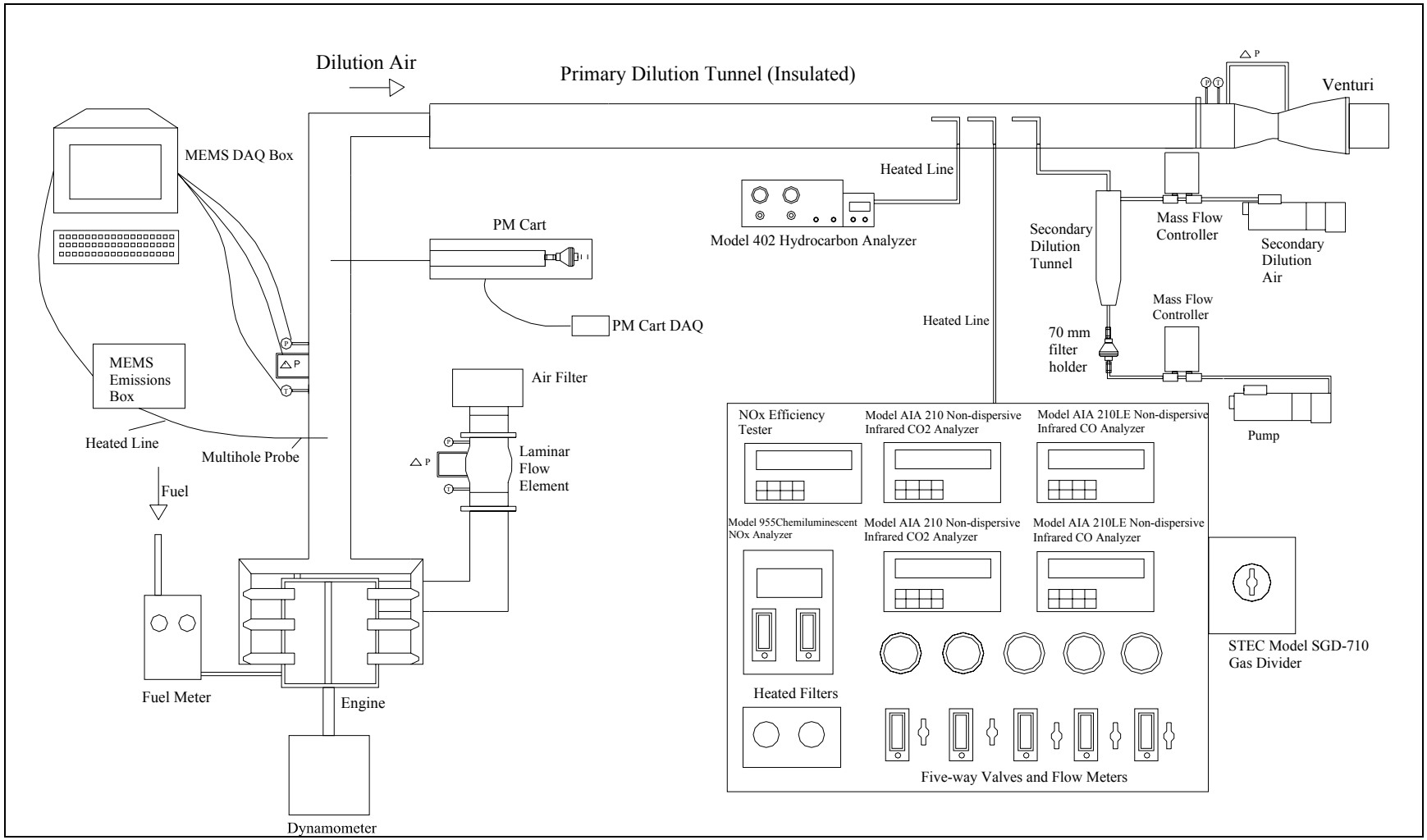


**Figure 3.17 Laboratory Equipment Layout at WVU, EERL**

Since the dilution air was not effectively filtered before entering the primary or the secondary dilution tunnels, and also to determine tunnel shedding, background samples were taken. The procedure required placing a weighed and conditioned filter in the primary position of the filter holder and pulling a metered sample of the ambient air across the filter. Post conditioning and weighing of the filter resulted in a background and tunnel-shed contribution that could be subtracted from the sample filter net weight data.

Total particulate matter (TPM) was determined by weighing the filters before and after each test after conditioning. A Cahn 32 microbalance was used for weighing the filters. The microbalance had a remote weighing chamber that was placed inside the environmental chamber on a vibration isolation table, while the electronic unit was left outside of the chamber. The balance had three weighing ranges, namely, 25 mg (sensitivity of 0.1 μg), 250 mg (sensitivity of 1 μg), and 1250 mg (sensitivity of 10 μg). The 250 mg weighing range was used for this study.

### 3.9.5 Dilution Tunnel

The purpose of the dilution tunnel is two fold: to dilute an engine's raw exhaust gas with fresh ambient air so as to simulate the emission of exhaust in real world conditions, and to lower the dew point temperature to prevent water condensation. Water condensation would cause the loss of certain gaseous components (for example, $NO_2$) and hence, compromise the exhaust emissions results. Water condensation affects certain instruments, such as the non-dispersive infrared analyzers and the particulate matter measurements would also be affected. In some instances, the dilution air may be conditioned before it is mixed with the exhaust, through filtration systems (to remove particulate matter from the air) and

humidity and temperature control. An alternative to this is to measure the level of background PM and subtract it from the value obtained from the exhaust sample.

In a study about laboratory variability in exhaust measurements [46] it was found that in each of the engine laboratories studied, there were a variety of dilution tunnel designs. Differences included tunnel diameter, tunnel length, method of mixing, flow rate, and the length from point of exhaust injection to the sampling zone. The dilution tunnel used in the WVU laboratory was of a double dilution type. The dilution tunnel was eighteen inches in diameter and had a total length of twenty feet. The dilution tunnel used an eight inch orifice placed three feet from the beginning of the tunnel. The orifice insured that the dilute exhaust mixture was thoroughly mixed by the time it reached the sampling zone; ten diameters downstream, so that the gaseous and particulate probes sampled a representative sample.

### 3.9.6 Critical Flow Venturi

In compliance with Title 40 CFR Part 86 [2], Subpart N, a constant volume sampler (CVS) was used to draw the diluted exhaust through the dilution tunnel. The CVS system operated based on the theory of critical flow nozzles [47], wherein a critical flow venturi (CFV) is placed upstream of a blower and diluted exhaust mixture is pulled at a constant mass flow rate through the sonic venture. Under such choked flow conditions through a critical flow venturi, the flow rate is controlled by the diameter of the throat and the upstream flow conditions. The CFV-CVS system used for this research had four critical venturis installed in line with a 55.9 kW (75 hp) centrifugal blower. The constant volume sampling system had four different venturis, three of which had a design flowrate of 28.3 $m^3$/min. (1000 scfm) and the fourth had a design flowrate of 11.3 $m^3$/min. (400 scfm). A

maximum tunnel flowrate of 85 $m^3$/min. (3000 scfm) could be achieved by using this system.

The critical flow venturi allowed for the measurement of the mass flow rate of diluted exhaust by monitoring the upstream absolute pressure, P, with a Viatran absolute pressure transducer (Model No 1042 AC3AAA20), and temperature, T, with a 3-wire resistive temperature device (Tayco Model No. 68-3839). The mass flow rate was then calculated as follows:

$$Q = \frac{K_V \times P}{\sqrt{T}}$$

where,

Q = flow rate in standard cubic feet per minute at standard conditions of 20°C, 101.3 kPa (68°F, 29.92 in Hg).
$K_v$ = calibration coefficient,
P = absolute pressure at venturi inlet, kPa
T = absolute temperature at venturi inlet, °K

The venturis were calibrated with the use of a subsonic flow venturi traceable to NIST [48].

### 3.9.7 Fuel Flow Metering

A Max Flow Media 710 Series fuel measurement system performed the fuel flow rate measurements. A transfer pump directs fuel from the storage tank, through a filter, and into a vapor eliminator maintained at 30 psi (206.8 kPa). The fuel then enters a Model 214 piston-displacement flow meter, before which, excess fuel is routed back to the storage tank via a pressure regulator and through an internal heat exchanger. The internal heat exchanger uses the by-pass supply fuel to cool the engine return fuel. The metered fuel then passes into a level controlled tank, where it is mixed with the engine

return fuel, which has been cooled by the internal heat exchanger. The tank level is controlled so that the amount of metered fuel recorded during a particular test would be the quantity of fuel consumed by the engine during that test. The outlet of the tank is connected to a secondary fuel pump, which ensures further increase in injection pressure, so as to minimize the requirements of the engine's original equipment fuel pump. The fuel then passes through a bubble detector, which controls a solenoid valve that connects the to-engine and from-engine fuel lines. Removal of air and fuel vapors in the fuel supply line ensures superior engine performance and prevents flow meter inaccuracies. After the fuel passes the purge solenoid, it passes through an external heat exchanger, where the temperature is controlled via a Fuji Model No. 223-1806 temperature controller.

### 3.9.8 Intake Air Flow Measurement

A Meriam Instruments Model 50MC2-6 Laminar Flow Element (LFE), 6 in. (15.2 cm ) I.D.-1000 cfm (28.3 $m^3$/min), was used for the purpose of measuring intake air flow rate during the validation tests. A LFE comprises a series of small capillary tubes aligned parallel to the direction of airflow. The purpose of the capillary matrix is to convert the turbulent flow in the intake line into a laminar flow. As the air passes through these capillaries, a pressure drop is created due to friction of the air. Meriam Instruments supply a calibration equation and coefficients that are unique to each LFE, which are determined with a flow meter that is traceable to NIST standards. The absolute temperature and pressure of the intake flow, and the differential pressure across the LFE are the only parameters needed for intake volume flow calculation.

The equation used for this calculation is,

$$\dot{V}_{actual} = \left\{ B \times (\Delta P) + C \times (\Delta P)^2 \right\} \times \frac{\mu_{std}}{\mu_{flow}}$$

where,

| | | |
|---|---|---|
| $\dot{V}_{actual}$ | = | volume flow rate of intake air through the LFE, |
| B | = | coefficient supplied by Meriam Instruments, |
| C | = | coefficient supplied by Meriam Instruments, |
| $\Delta P$ | = | differential pressure across the LFE, |
| $\mu_{std}$ | = | standard kinematic viscosity of air, |
| $\mu_{flow}$ | = | actual flow kinematic viscosity. |

The viscosity variations are calculated using the following correction factors,

$$CorrectionFactor = \left( \frac{529.67}{459.67 + T} \right) \times \left( \frac{181.87}{\mu_g} \right)$$

where,

T = absolute temperature of the intake air ($^{o}$F), and

$$\mu_g = \frac{14.58 + \left( \frac{459.67 + T}{1.8} \right)^{1.5}}{110.4 + \left( \frac{459.67 + T}{1.8} \right)}$$

Differential pressure across the LFE was measured with an Omega Model PX653-10DSV (0-10”WC) differential pressure transducer, while absolute pressure was determined with a Viatran Model1042ACA (0-15psi) pressure transducer. The absolute temperature of the intake air measured upstream of the LFE was recorded with a Resistive Temperature Device (RTD).

### 3.9.9 Secondary Dilution Tunnel and Particulate Sampling

The process of measuring the PM emissions from diesel engines consists of conveying the exhaust to a dilution tunnel (single or double) in which the exhaust is diluted

with air and cooled to a temperature not exceeding 51.7°C (125°F), obtaining a representative sample of the particulate matter in the dilute sample by filtration, and then determining the mass collected on the filter or filters [46]. The WVU facility used the double dilution method for particulate matter sampling. The double dilution method sampled a proportional sample of diluted exhaust (first stage of dilution) from the primary tunnel and diluted it further in the secondary dilution tunnel (second stage of dilution). The sample then passed through two, a primary and a secondary, Pallflex 70 mm (2.76 inches) fluorocarbon coated micro fiber glass filters, T60A20, which collected the particulate matter.

The particulate sampling system [45] was designed to perform in accordance with the 40 CFR Part 86 [2]. The secondary dilution tunnel was required to maintain the double diluted exhaust stream at a temperature of 51.7°C (125°F) or less immediately before the primary particulate filter in the secondary dilution tunnel. Particulate Matter (PM) collected from a dilution tunnel is influenced by the conditions at which the tunnel is operated, most significant being the temperature and dilution ratio [49].

The exhaust sample was drawn through a 1.3 cm (0.5 inches) diameter transfer tube located at the sampling zone in the primary dilution tunnel. The inlet faced upstream and was approximately 17.8 cm (7 inches) in length. The total PM sample flow and the secondary dilution air flow through the secondary tunnel was controlled by two Sierra 740-L-1 series mass flow controllers and two Gast series 1023-101Q-583X rotary vane pumps. The total flow ranged from 0 lpm to 170 lpm (0 scfm to 6 scfm) while secondary dilution air flow ranged from 0 lpm to 85 lpm (0 scfm to 3 scfm). During testing, flow through the secondary dilution tunnel varied in proportion to the flow through the primary dilution

tunnel. The mass flow controllers were calibrated using a Meriam Instruments laminar flow element (LFE) Model No. 50MW20, rated at 0 $m^3$/min to 6.52 $m^3$/min (0 scfm to 23 scfm).

The secondary dilution tunnel was 7.62 cm (3.0 inches) in diameter and 76.2 cm (30 inches) long. This provided sufficient time for the exhaust sample to be mixed with the dilution air and to reach temperatures less than 51.7°C (125°F). A stainless steel filter holder with the primary and secondary filters was connected at the end of the secondary dilution tunnel. The filter holder was constructed of stainless steel to prevent reactions with the corrosive exhaust sample and was designed to allow easy access to the filters.

### 3.9.10 Gas Analysis System

A gas analysis bench was used to measure the concentration of gaseous components in a diluted exhaust gas stream from the heavy-duty diesel engine. The gas analysis bench consisted of four major components: $CO_2$ analyzer, CO analyzer, $NO_x$ analyzer, and a HC analyzer. The gaseous samples were taken 10 diameters downstream of the mixing zone in the primary dilution tunnel to allow for development of a fully-developed turbulent duct flow profile, which made probe placement outside the boundary layer region less critical. Four heated stainless steel probes were inserted into the dilution tunnel at the sampling zone at a depth of approximately six inches. These probes were connected to heated lines, which transferred the gaseous samples to their respective analyzers. The hydrocarbon line and probe were kept at a wall temperature of 191°C ± 6°C (375°F ±10°F) to prevent the higher-molecular weight hydrocarbons from condensing out on the walls and other surfaces in the sampling stream. The other system probes and lines were kept at 113°C ± 6°C (235°F±10°F) at the wall, in order to prevent water condensation, which would have affected the measurements by the analyzers.

#### 3.9.10.1 Hydrocarbon Analyzer

The hydrocarbon analyzer used for the study was a Rosemount Analytical Model 402 heated flame ionization detector (HFID), which operated on the following principle. The sensor is a burner where a regulated flow of sample gas flows through a flame produced by regulated flows of air and a pre-mixed hydrogen/helium fuel gas. Polarized electrodes then collect the ions that are produced causing current to flow through the associated electronic measuring circuitry. The current flow is proportional to the rate at which carbon atoms enter the burner [50, 51].

#### 3.9.10.2 $CO/CO_2$ Analyzer

CO and $CO_2$ measurements were made using Horiba Model AIA–210LE and Horiba Model AIA-210 Non-Dispersive Infrared (NDIR) analyzers, respectively. NDIR analyzers use the exhaust gas species being measured to detect itself by the principle of selective absorption, in which the infrared energy of a particular wavelength, specific to a certain gas, will be absorbed by that gas. Infrared energy of other wavelengths will be transmitted by that gas, just as the absorbed wavelength will be transmitted by other gases.

#### 3.9.10.3 $NO_x$ Analyzer

The $NO/NO_x$ analyzer used was a Rosemount Model 955 Chemiluminescent Analyzer. The analyzer was capable of determining the concentration of either NO or NO + $NO_2$ which together is called $NO_x$. For the determination of NO, the sample NO was quantitatively converted into $NO_2$ by gas-phase oxidation with molecular ozone, which was generated inside the analyzer by an ozone generator that was supplied by external bottled air supply. When this reaction takes place, approximately 10% of the $NO_2$ molecules are elevated to an electronically excited state followed by immediate reversion to the non-

excited state accompanied by a photon emission. The instrument response is proportional to the total NO in the converted sample. The operation for $NO_x$ is identical to that of NO except that the gas sample stream is first passed through a converter, which converts the $NO_2$ into NO. In this case, the instrument response is proportional to the NO present in the original sample plus the NO produced by the dissociation of $NO_2$.

#### 3.9.10.4 Bag Sampling

Although continuous samples were taken of the regulated exhaust gases, bag samples of dilute exhaust and dilution (background concentration) air were also taken. These samples were collected in separate 80-liter Tedlar bags. Once the test was completed, the bag samples were introduced into the gas analyzers so that their respective concentrations would be measured. At the conclusion of the test, the bags were evacuated so that they could be re-used during the next test.

The background bag samples of ambient air concentrations were used to correct the dilute exhaust bag sample and the continuous sample readings. The dilute bag samples served only as a quality control/quality assurance check that provided comparison with the results obtained from the continuous sample.

### 3.9.11 Instrumentation Control and Data Acquisition

The software used in the study was already developed and installed in the Stationary Laboratory [52] at West Virginia University. The program utilized an RTI-815F data acquisition board and a rack mounted signal conditioning board comprised of a number of Analog Devices 3B series conditioning modules. The data acquisition programs acquired the raw data in the form of ADC codes and another program [53] converted the raw data into proper engineering units and then wrote the final data to a file.

### 3.10 Calculation of Emissions

This section describes the basic equations that were used for the calculation of the results for brake-specific gaseous and particulate emissions from the measured concentrations. The equations used for the calculation are an integration of recommendations prescribed in Title 40 CFR 86, Title 40 CFR 89, Title 40 CFR 92, Title 40 CFR 94, ISO 8178, and SAE J177 [6-12] wherever applicable.

#### 3.10.1 Calculation of In-use Brake-specific Data

The brake-specific gaseous emissions, particulate emissions, and fuel consumption were calculated from the data recorded by the Mobile Emissions Measurement System (MEMS) and the Mini-tunnel.

The mass flow rates of $NO_x$, $CO_2$, $O_2$ were calculated using the corresponding concentrations measured, fuel mass flow rate and the concentration of $CO_2$ as described in Title 40 CFR 92 [9].

##### 3.10.1.1 Calculation of Brake-specific Gaseous Emissions

The mass flow rate of the exhaust constituents can be expressed as,

$$\dot{M}_X = C_X * Vol * \frac{MW_X}{V_M} \qquad \textbf{Equation 3-1}$$

where,

$\dot{M}_X$ = Mass flow rate (g/hr) of exhaust component X (e.g., $NO_x$),

$C_X$ = Concentration (ppm or % volume) of the exhaust component X,

$Vol$ = Total exhaust flow rate ($ft^3$/hr),

$MW_X$ = Molecular weight (g/mole) of exhaust component X,

$V_M$ = Volume of one mole of gas ($ft^3$/mole) at standard conditions.

The total exhaust flow rate (on a dry basis), *DVol*, neglecting carbon monoxide and hydrocarbons can be expressed as,

$$DVol = \frac{V_M * \dot{M}_F}{(12.011 + 1.008 * \alpha) * C_{CO_2,D}} \qquad \textbf{Equation 3-2}$$

where,

$\dot{M}_F$ = Fuel mass flow rate (g/hr),

$\alpha$ = Atomic hydrogen/carbon ratio of the fuel,

$CO_{2,D}$ = $CO_2$ concentration in exhaust, percent (dry).

The mass flow rate of each exhaust component can be expressed on a wet basis, using the equations above as,

$$\dot{M}_X = \frac{C_{X,W} * \dot{M}_F * MW_X}{(12.011 + 1.008 * \alpha) * C_{CO_2,W}} \qquad \textbf{Equation 3-3}$$

where,

$C_{X,W}$ = Concentration (ppm or % volume) of the exhaust component X (wet),

$CO_{2,W}$ = $CO_2$ concentration in exhaust, percent (wet).

Similarly the mass flow rate of each exhaust component can be expressed on a dry basis as,

$$\dot{M}_X = \frac{C_{X,D} * \dot{M}_F * MW_X}{(12.011 + 1.008 * \alpha) * C_{CO_2,D}} \qquad \textbf{Equation 3-4}$$

where,

$C_{X,D}$ = Concentration (ppm or % volume) of the exhaust component X (dry).

The relation between dry and wet concentrations is given as,

$$C_{X,D} = K_w * C_{X,W} \qquad \textbf{Equation 3-5}$$

where,

$K_W$ = Wet to dry conversion factor and can be written as,

$$K_w = \frac{WVol}{DVol} = 1 + D_{H_2O} \qquad \textbf{Equation 3-6}$$

where,

$WVol$ = Total exhaust flow rate ($ft^3$/hr) on a wet basis,

$D_{H_2O}$ = Volume of water in exhaust/dry volume of exhaust.

A precise calculation of the conversion factor can be done by iteration. An alternate calculation involves approximation and, neglecting carbon monoxide, can be given as,

$$D_{H_2O} = \frac{\alpha * C_{CO_2,D}}{2} + Y * DVol_{Ratio} \qquad \textbf{Equation 3-7}$$

where,

$Y$ = Water volume concentration in intake air, volume fraction (dry),

$$DVol_{Ratio} = \frac{DVol_{Air}}{DVol} = 1 - \left( C_{CO_2,D} * \frac{\alpha}{4} \right) \qquad \textbf{Equation 3-8}$$

where,

$DVol_{Air}$ = Air intake flow rate ($ft^3$/hr) on a dry basis.

In this study the carbon dioxide ($CO_2$) was measured dry, while oxides of nitrogen ($NO_x$) and oxygen ($O_2$) were measured wet. The redundant measurements of $NO_x$ and $O_2$ made by the electrochemical cells were measured dry.

The molecular weight of $CO_2$ was taken as 44.01 and that for $NO_x$ was taken as 46.008, per CFR requirements. The mass flow rate of $NO_x$ was corrected for ambient temperature and humidity based on the procedure outlined in Title 40 CFR 89 [8].

The brake-specific emissions of each exhaust component is given as,

$$BS_X = \frac{\dot{M}_X}{P} \qquad \textbf{Equation 3-9}$$

where,

$BS_X$ = Brake-specific emissions of exhaust component X (g/bhp-hr).

The power, $P$ was calculated from the measured shaft speed and torque and is given as,

$$P = \frac{T * N}{5252} \qquad \textbf{Equation 3-10}$$

where,

$T$ = Shaft torque (lb-ft),

$N$ = Shaft speed (rpm).

**3.10.1.2 Calculation of Brake-specific Particulate Matter Emissions**

The equations used for particulate matter (PM) mass flow rate calculations is in accordance with the calculation procedures included in ISO 8178:1996(E) [11]. The brake-specific PM emission is given as,

$$BS_{PM} = \frac{\left[ M_f - \left( M_{bf} * \frac{V_t}{V_{bf}} \right) \right]}{V_t} * D.R. * \frac{V_e}{W} \qquad \textbf{Equation 3-11}$$

where,

$BS_{PM}$ = Brake-specific PM emissions (g/bhp-hr),

$M_f$ = Mass of PM collected on the filters,

$M_{bf}$ = Mass of background PM collected,

$V_t$ = $V_d$ + $V_s$,

= Total flow (standard liters) through the mini-tunnel,

$V_d$ = Dilution air flow (standard liters),

$V_s$ = Raw exhaust sample flow (standard liters),

$V_{bf}$ = Total background flow (standard liters) through the mini-tunnel,

*D.R.* = Dilution ratio,

$V_e$ = Total engine exhaust flow (standard liters),

$W$ = Work done (bhp-hr).

A schematic illustrating the total mini-tunnel flow, dilution air flow and raw exhaust sample flow is shown in Figure 3.18.

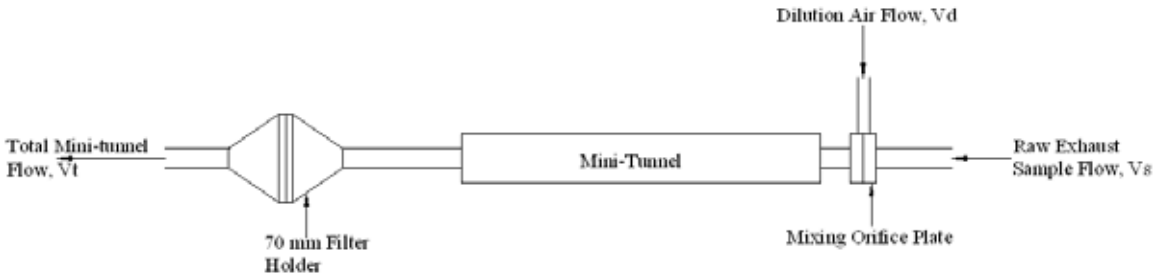


**Figure 3.18 Schematic of the Mini-tunnel Flow Details**

The total flow, $V_t$, through the mini-tunnel was determined by integrating the total flow measurements recorded by the data acquisition system of the mini-tunnel. $V_{bf}$ was also determined in a similar manner by performing a background run for 20 minutes. The background run was done by unhooking the sample line from the exhaust stack and allowing the mini-tunnel to draw ambient air on the first day of tests and engine room air on

the second day. There was not a significant difference in the background PM collected between the two days. The total engine exhaust flow, $V_e$, was obtained from the MEMS data. The exhaust flow rate is given as,

$$\dot{V}_e = \rho * \dot{M}_e \qquad \textbf{Equation 3-12}$$

where,

$\dot{V}_e$ = Standardized exhaust flow rate (scfm),

$\rho$ = Density of engine exhaust gases (g/ft$^3$),

$\dot{M}_e$ = Mass flow rate of exhaust gases (g/min).

The mass flow rate of the engine exhaust can be given as,

$$\dot{M}_e = \dot{M}_a + \dot{M}_f \qquad \textbf{Equation 3-13}$$

where,

$\dot{M}_a$ = Mass flow rate of intake air (g/min),

$\dot{M}_f$ = Mass flow rate of fuel (g/min).

The measurements of fuel flow rate and intake air flow rate are mentioned in Section 3.8.2 and Section 3.8.3 respectively.

### 3.10.2 Calculation of Brake-specific Emissions from Brake-Specific Fuel Consumption Data

The brake-specific emissions were also calculated using the brake-specific fuel consumption data that was obtained from the fuel flow measurements, the results of which are discussed in Section 4.2. The calculation of brake-specific emissions from BSFC data

avoids the need for speed and torque measurements, as well as fuel flow measurements. However, this method necessitates that BSFC data be obtained from the engine manufacturer. In an attempt to illustrate this approach, BSFC data obtained from the fuel measurements and torque measurements recorded by the MEMS are used in these calculations, since the BSFC data from the manufacturer was not available for the test engine.

The brake-specific fuel consumption is given as,

$$BSFC = \frac{\dot{M}_F}{P} \qquad \textbf{Equation 3-14}$$

The mass of fuel consumed is given by,

$$M = \frac{G_s}{R_2} \qquad \textbf{Equation 3-15}$$

where,

$M$ = Mass of fuel consumed (g),

$G_s$ = Grams of carbon measured,

$R_2$ = Grams of carbon in fuel.

Neglecting the hydrocarbon mass and carbon monoxide mass, the grams of carbon (C) measured can be expressed as,

$$G_s = 0.273 * M_{CO_2} \qquad \textbf{Equation 3-16}$$

where,

$M_{CO_2}$ = Mass of $CO_2$ measured (g).

$R_2$ can be expressed as,

$$R_2 = \frac{12.011}{12.011 + (1.008 * \alpha)} \qquad \text{Equation 3-17}$$

The work done, $W$ (bhp-hr), for a particular mode was then obtained using the BSFC for that particular mode and the mass of fuel consumed during that particular mode as,

$$W = \frac{M}{BSFC} \qquad \textbf{Equation 3-18}$$

The brake-specific emissions were then calculated using the bhp-hr calculated above and the mass of exhaust constituent measured during that particular mode as,

$$BS_X = \frac{M_X}{W} \qquad \textbf{Equation 3-19}$$

The values of brake-specific emissions of $NO_x$, $CO_2$ and PM calculated by the above procedure were compared with the values obtained using the in-use method.

### 3.10.3 Calculation of Brake-Specific Emissions for the CFV-CVS

This section describes the basic equations that were used for the calculation of the results for brake-specific gaseous and particulate emissions from the measured concentrations for the CFV-CVS. The equations used for the calculation are based on the procedures laid out in Title 40 CFR 86, Subpart N [6].

#### 3.10.3.1 Calculation of Brake-specific Gaseous Emissions

The mass of each pollutant per test phase for bag measurements and continuously heated sampling system measurements can be expressed as,

$$M_X = C_X * V_{mix} * Density_X \qquad \textbf{Equation 3-20}$$

where,

$M_X$ = Mass (grams) of exhaust component X (e.g., $NO_x$),

$C_X$ = Concentration (ppm or % volume) of the exhaust component X,

$V_{mix}$ = Total dilute exhaust volume per test phase ($ft^3$),

$Density_X$ = Density ($g/ ft^3$) of exhaust component X.

The concentration of the exhaust component X is given as,

$$C_X = C_{Xe} - C_{Xd}(1 - (1/DF)) \qquad \textbf{Equation 3-21}$$

where,

$C_{Xe}$ = Concentration (ppm or % volume) of X in the dilute exhaust sample,

$C_{Xd}$ = Concentration (ppm or % volume) of X in the dilution air,

$DF$ = Dilution Factor.

The dilution factor (DF) is given as,

$$DF = \frac{13.4}{\left[CO_{2e} + (HC_e + CO_e) * 10^{-4}\right]} \qquad \textbf{Equation 3-22}$$

where, $CO_{2e}$, $HC_e$ and $CO_e$ are the concentrations of $CO_2$ (% vol.), HC (ppm) and CO (ppm) in the dilute exhaust sample.

The brake-specific emissions are calculated using equation 3.19.

### 3.10.3.2 Calculation of Brake-specific Particulate Matter Emissions

The mass of particulate for a particular test phase is given as,

$$P_{MASS} = (V_{mix} + V_{SF}) \times \left[\frac{P_F}{V_{SF}} - \left(\frac{P_{BF}}{V_{BF}} \times \left[1 - (1/DF)\right]\right)\right] \qquad \textbf{Equation 3-23}$$

where,

$P_{MASS}$ = Mass (grams) of particulate emitted by the engine per test phase,

$V_{SF}$ = Total volume ($ft^3$) of sample removed from the primary dilution tunnel,

$P_F$ = Mass (grams) of particulate collected on the filters per test phase,

$P_{BF}$ = Net weight of particulate on the background particulate filter,

$V_{BF}$ = Actual volume ($ft^3$) of primary dilution air sampled by background sampler.

The brake-specific particulate matter emissions is given as,

$$BSPM = \frac{P_{MASS}}{W} \qquad \textbf{Equation 3-24}$$

# 4 RESULTS AND DISCUSSIONS

The objective of this study was to determine the environmental benefits of operating a hydrofoil-deployed, high-speed passenger ferry using low sulfur diesel fuel (with and without intake air water injection), as compared to operation using conventional marine diesel fuel. The study was conducted onboard a high-speed ferry (hydrofoil) operated by SCX Inc. between San Diego and Oceanside, California. A partial flow dilution tunnel was used for collecting particulate matter for gravimetric analysis, while brake-specific emissions of $NO_x$ and $CO_2$ were measured using the Mobile Emissions Measurement System (MEMS), developed by the Engines and Emissions Research Laboratory (EERL) at West Virginia University.

The ferry was powered by four Detroit Diesel Corporation 12V92 engines, which were retrofitted with charge air water injection systems. The test engine was the starboard side, fore engine. The engine was tested on four steady-state modes, which included an idle mode. The modes were determined based on the regular operation of the ferry between San Diego and Oceanside, California. The four steady-state modes used in this study included a 2100 rpm mode, 2000 rpm mode, 1900 rpm mode, and an idle mode. The first three modes were run for each of the following four engine, fuel, and water injection system (WIS) configurations:

1) with WIS / Low Sulfur Diesel (LSD) fuel,
2) without WIS / Low Sulfur Diesel (LSD) fuel,
3) with WIS / Marine Diesel fuel,
4) without WIS / Marine Diesel fuel,

With little extra time available on the second day of tests, the engine was operated on an additional mode, referred to as Harbor Mode. For this test, the engine was fueled with marine diesel. Harbor Mode began as the vessel entered the harbor from the ocean and ended after the vessel had docked. This was called the Harbor-In mode. Likewise, the Harbor-Out mode started when the vessel left the docks and ended when it entered the ocean. The Harbor Mode and the idle mode were performed without the water injection system, because the system was designed to operate only when the intake manifold pressure was above a threshold value, which was achieved only for the other three modes. Data was recorded for the idle mode tests using both LSD fuel and marine diesel fuel, whereas Harbor Mode data was recorded only for tests using the marine diesel fuel. Brake-specific mass emissions of $NO_x$ and PM (g/bhp-hr) are presented for each mode and configuration.

## 4.1 On-board Test Results

This section discusses the results of on-board testing conducted aboard the high-speed ferry (hydrofoil). Brake-specific $NO_x$ and $CO_2$ emissions, brake-specific particulate matter emissions, brake-specific fuel consumption, and output power are reported in this section. Emissions reduction as a result of the engine retrofit (with WIS) and emissions reduction due to the low sulfur fuel (LSD fuel) are also discussed in this section.

### 4.1.1 Regulated Gaseous Emissions and Particulate Matter

#### 4.1.1.1 Oxides of Nitrogen

Table 4-1and Figure 4.1illustrate the average brake-specific $NO_x$ emissions for the various steady-state modes at which the engine was tested. Results for the individual runs are shown in Figure B-1. A reduction of 10%-17% was observed in the average brake-specific $NO_x$ ($BSNO_x$) emissions with the WIS as compared to operation without the WIS

for all engine operation modes with low sulfur diesel (LSD) fuel and marine diesel fuel. This reduction is attributed to the decrease in peak combustion temperatures as a result of water injection in the charge air. The highest decrease in $BSNO_x$ emissions was observed at 1900 rpm with the engine operating on marine diesel fuel with the WIS. There was a decrease of approximately 17% in the $BSNO_x$ emissions at this mode when the engine was operating on marine diesel with the WIS. However, the $BSNO_x$ emissions could not be measured at 1900 rpm with LSD fuel and WIS, due to failure of torque measurement. Hence, any change in $BSNO_x$ emissions at this mode relative to the engine operation at the same conditions without WIS is not known. Intuition would suggest that the decrease in $BSNO_x$ emissions would have been highest at this condition, because reductions in $BSNO_x$ emissions were higher for the lower engine speeds with LSD fuel. This could be attributed to the uniform amount of water injected into the intake air, irrespective of the engine speed, which would mean lower combustion temperatures at lower engine speeds; hence, the higher reductions in $BSNO_x$ at lower speeds. The $BSNO_x$ emissions decreased by approximately 12% when the engine was operating at 2100 rpm on LSD fuel and WIS, as compared to operation at the same conditions without WIS. The corresponding decrease in $BSNO_x$ emissions was approximately 10% when the engine was operating on marine diesel fuel. There was a decrease of approximately 14% in the $BSNO_x$ emissions at 2000 rpm with the engine operating on LSD fuel with WIS, as compared to engine operation at the same conditions without WIS. The corresponding decrease in $BSNO_x$ emissions was approximately 13% when the engine was operating on marine diesel fuel. The $BSNO_x$ emissions during the harbor mode were 18.4 g/bhp-hr.

**Table 4-1 Average $BSNO_x$ Emissions (g/bhp-hr) for Steady State Modes and Different Configurations**

| | Brake-specific $NO_x$ emissions (g/bhp-hr) | | | |
|---|---|---|---|---|
| Mode | LSD/ Without WIS | LSD/ With WIS | Marine Diesel/ Without WIS | Marine Diesel/ With WIS |
| 2100 rpm | 6.72 | 5.92 | 7.14 | 6.43 |
| 2000 rpm | 6.50 | 5.61 | 6.50 | 5.69 |
| 1900 rpm | 5.97 | ------- | 5.91 | 4.93 |

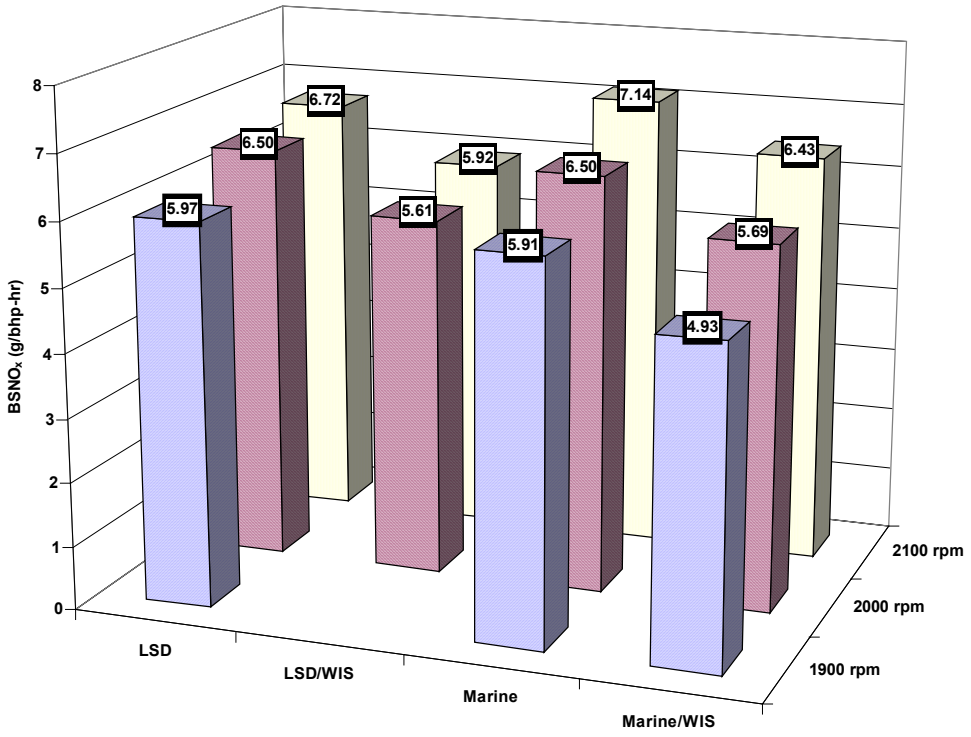


**Figure 4.1 Average Brake-specific $NO_x$ ($BSNO_x$) Emissions for Various Modes and Configurations**

#### 4.1.1.2 Total Particulate Matter

Table 4-2 and Figure 4.2 illustrate the average brake-specific PM emissions for the various steady-state modes at which the engine was tested. Results for the individual runs

are shown in Figure B-2. There was no significant difference in the brake-specific particulate matter (BSPM) emissions with WIS, relative to engine operation without WIS, at any of the test modes with either low sulfur diesel (LSD) fuel or marine diesel fuel. However, the difference in BSPM emissions was significant when operation with marine diesel was compared to operation with LSD. BSPM emissions decreased approximately 40%-45% when operating on LSD fuel as compared to operation on Marine Diesel fuel at identical conditions. The difference in emissions resulting from the use of different fuels is discussed later in this chapter. BSPM emissions were almost the same (difference of approximately 3%) with and without WIS at 2100 rpm with the engine operating on LSD fuel. Similar results were observed with the engine operating on marine diesel fuel (difference of less than 1%). The difference in BSPM emissions was approximately 4% for engine operations on LSD fuel, with and without WIS at 2000 rpm. The highest decrease in BSPM emissions (approximately 7%) was observed with WIS at 2000 rpm with the engine operating on marine diesel fuel, as compared to the same engine operation without WIS. There was a decrease of approximately 5% in BSPM emissions for the engine with WIS at 1900 rpm operating on marine diesel fuel, as compared to the same engine operation without WIS. The BSPM emissions during the harbor mode was 0.16g/bhp-hr.

### 4.1.2 Fuel Consumption

Table 4-3 and Figure 4.3 illustrate the average brake-specific fuel consumption for the various steady-state modes over which the engine was tested. Results for the individual runs are shown in Figure B-3. The brake-specific fuel consumption (BSFC) was almost identical for all test modes and engine configurations. These results show that there was no

measurable fuel penalty associated with the engine being retrofitted with the intake air water injection system.

**Table 4-2 Average BSPM Emissions (g/bhp-hr) for Steady State Modes and Different Configurations**

| | Brake-specific PM emissions (g/bhp-hr) | | | |
|---|---|---|---|---|
| Mode | LSD/ Without WIS | LSD/ With WIS | Marine Diesel/ Without WIS | Marine Diesel/ With WIS |
| 2100 rpm | 0.10 | 0.10 | 0.17 | 0.17 |
| 2000 rpm | 0.12 | 0.11 | 0.19 | 0.19 |
| 1900 rpm | 0.17 | ------- | 0.26 | 0.25 |

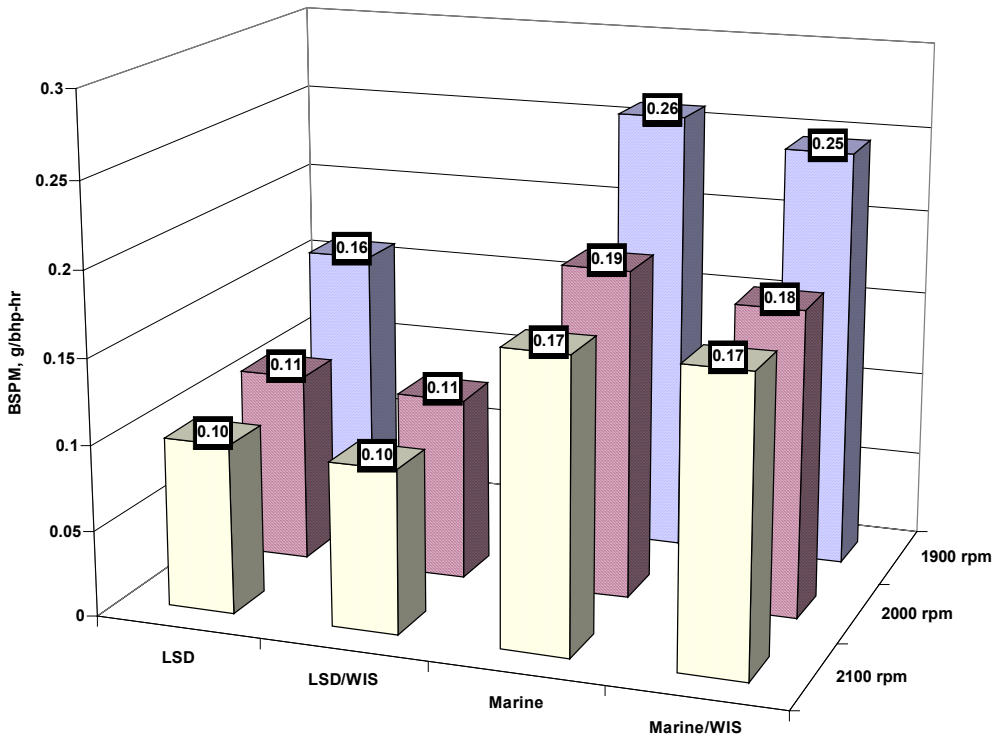


**Figure 4.2 Average Brake-specific Particulate Matter (BSPM) Emissions for Various Modes and Configurations**

**Table 4-3 Average BSFC (g/bhp-hr) for Steady State Modes and Different Configurations**

| | Brake-specific fuel consumption (g/bhp-hr) | | | |
|---|---|---|---|---|
| Mode | LSD/ Without WIS | LSD/ With WIS | Marine Diesel/ Without WIS | Marine Diesel/ With WIS |
| 2100 rpm | 183 | 183 | 185 | 186 |
| 2000 rpm | 182 | 182 | 182 | 182 |
| 1900 rpm | 184 | -------- | 184 | 183 |

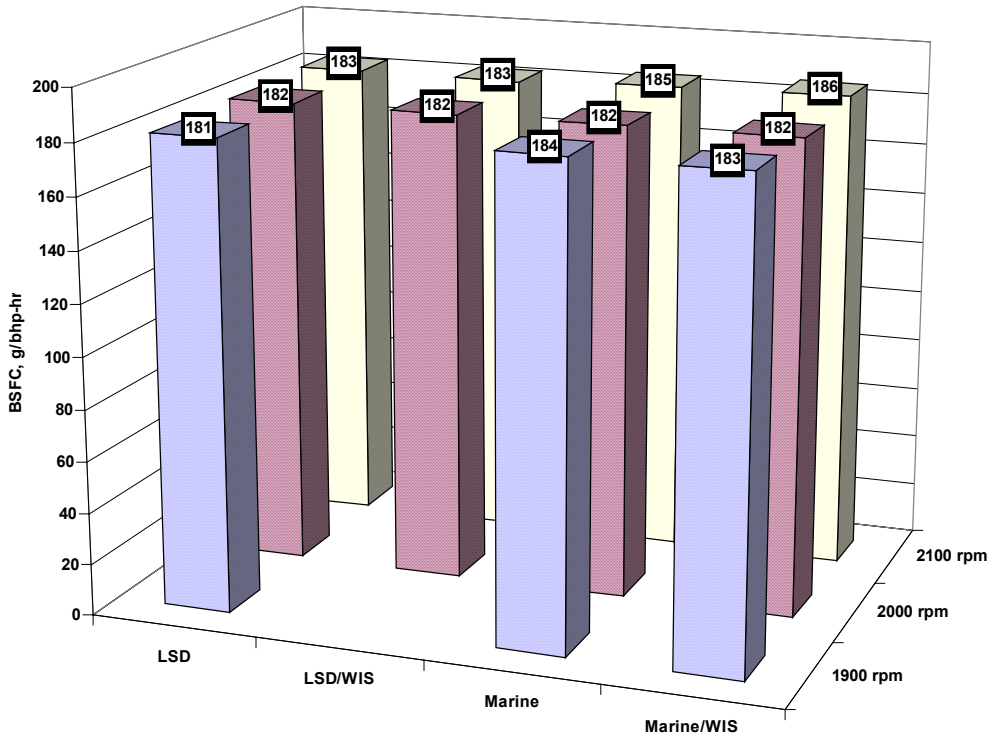


**Figure 4.3 Average Brake-specific Fuel Consumption (BSFC) Emissions for Various Modes and Configurations**

### 4.1.3 Output Power

Table 4-4 and Figure 4.4 illustrate the average output power (hp) for the various steady-state modes at which the engine was tested. Results for the individual runs are shown

in Figure B-4. The power output for a given mode did not change significantly with or without the engine retrofit (WIS). There was no notable difference in the output power for a given engine operating condition with the different test fuels used (low sulfur diesel fuel or marine diesel fuel), or with or without the WIS.

**Table 4-4 Average Output Power (hp) for Steady State Modes and Different Configurations**

| | Output Power (hp) | | | |
|---|---|---|---|---|
| Mode | LSD/ Without WIS | LSD/ With WIS | Marine Diesel/ Without WIS | Marine Diesel/ With WIS |
| 2100 rpm | 854 | 852 | 857 | 858 |
| 2000 rpm | 731 | 738 | 731 | 731 |
| 1900 rpm | 620 | -------- | 619 | 621 |

### 4.1.4 Percentage Reductions in Emissions due to Intake Air Water Injection

Table 4-5 and Figure 4.5 illustrate the percentage reductions in average brake-specific emissions, average brake-specific fuel consumption, and average power output due to the WIS for the various steady-state modes at which the engine was tested. The values given in Table 4-5 are averages of the different runs for each of the modes and configurations. Intake air water injection reduced the brake-specific $NO_x$ ($BSNO_x$) emissions considerably for all modes and configurations. However, the effected reductions in brake-specific particulate matter (BSPM) emissions, brake-specific fuel consumption (BSFC), and power output were less significant. The results are discussed in Sections 4.1.1, 4.1.2 and 4.1.3.

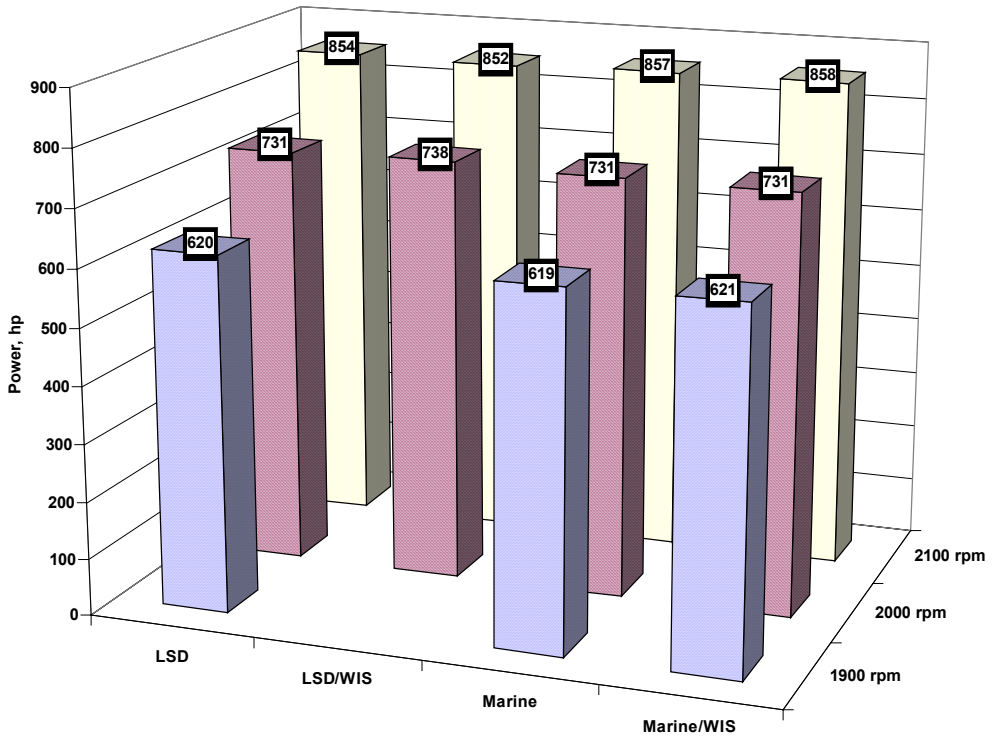


**Figure 4.4 Average Power Output for Various Modes and Configurations**

**Table 4-5 Percentage Reductions in Brake-specific Emissions, Brake-specific Fuel Consumption and Output Power with WIS Relative to those without WIS**

| | Reductions (%) | | | |
|---|---|---|---|---|
| Mode | $BSNO_x$ | BSPM | BSFC | Power |
| 2100 rpm/LSD | 11.8 | 3.5 | 0.2 | 0.3 |
| 2100 rpm/Marine | 9.9 | -0.6 | -0.5 | -0.1 |
| 2000 rpm/LSD | 13.7 | 4.1 | 0.0 | -0.8 |
| 2000 rpm/Marine | 12.4 | 6.9 | 0.1 | 0.1 |
| 1900 rpm/LSD | ----- | ----- | ----- | ----- |
| 1900 rpm/Marine | 16.6 | 5.4 | 0.2 | -0.3 |

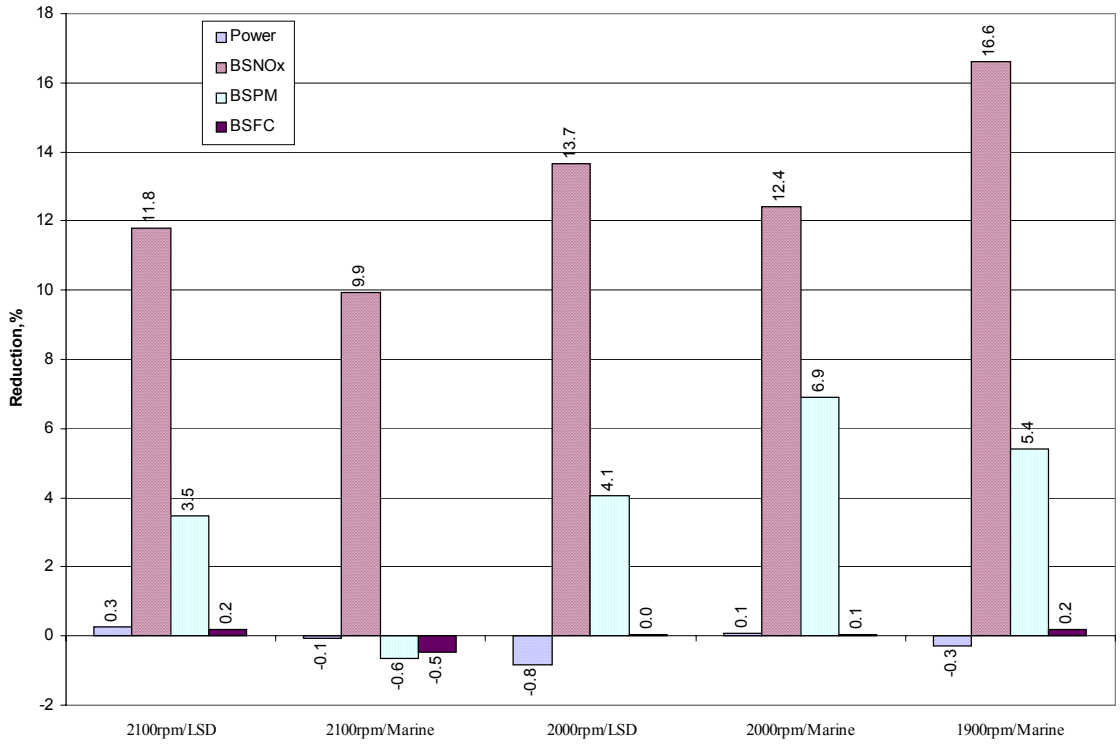


**Figure 4.5 Percentage Reductions in Brake-specific Emissions, Brake-specific Fuel Consumption and Output Power with WIS Compared to without WIS**

### 4.1.5 Percentage Reductions in Emissions due to Low Sulfur Diesel (LSD) fuel

Table 4-6 and Figure 4.6 illustrate the percentage reductions in average brake-specific emissions, average brake-specific fuel consumption, and average power output due to the use of LSD fuel compared to the use of conventional marine diesel fuel for the various steady-state modes at which the engine was tested. The values given in Table 4-6 are average of the different runs for each of the modes and configurations (WIS denotes water injection system). Operating the engine on LSD fuel resulted in significant reductions in brake-specific particulate matter (BSPM) emissions for all modes and configurations, as compared to reductions in brake-specific $NO_x$ ($BSNO_x$) emissions, brake-specific fuel consumption (BSFC), and improvements in power output. Results are discussed in Sections 4.1.1, 4.1.2, and 4.1.3.

**Table 4-6 Percentage Reductions in Brake-specific Emissions, Brake-specific Fuel Consumption and Output Power due to LSD Fuel Compared to Marine Diesel Fuel**

| | Reductions (%) | | | |
|---|---|---|---|---|
| Mode | $BSNO_x$ | BSPM | BSFC | Power |
| 2100 rpm | 6.0 | 41.8 | 0.9 | 0.3 |
| 2100 rpm/WIS | 7.5 | 44.2 | 1.4 | 0.6 |
| 2000 rpm | 0.9 | 42.0 | 1.4 | -1.1 |
| 2000 rpm/WIS | 2.8 | 40.2 | 0.3 | -1.2 |
| 1900 rpm | -0.5 | 38.4 | 1.6 | -0.1 |
| 1900 rpm/WIS | ----- | ----- | ----- | ----- |

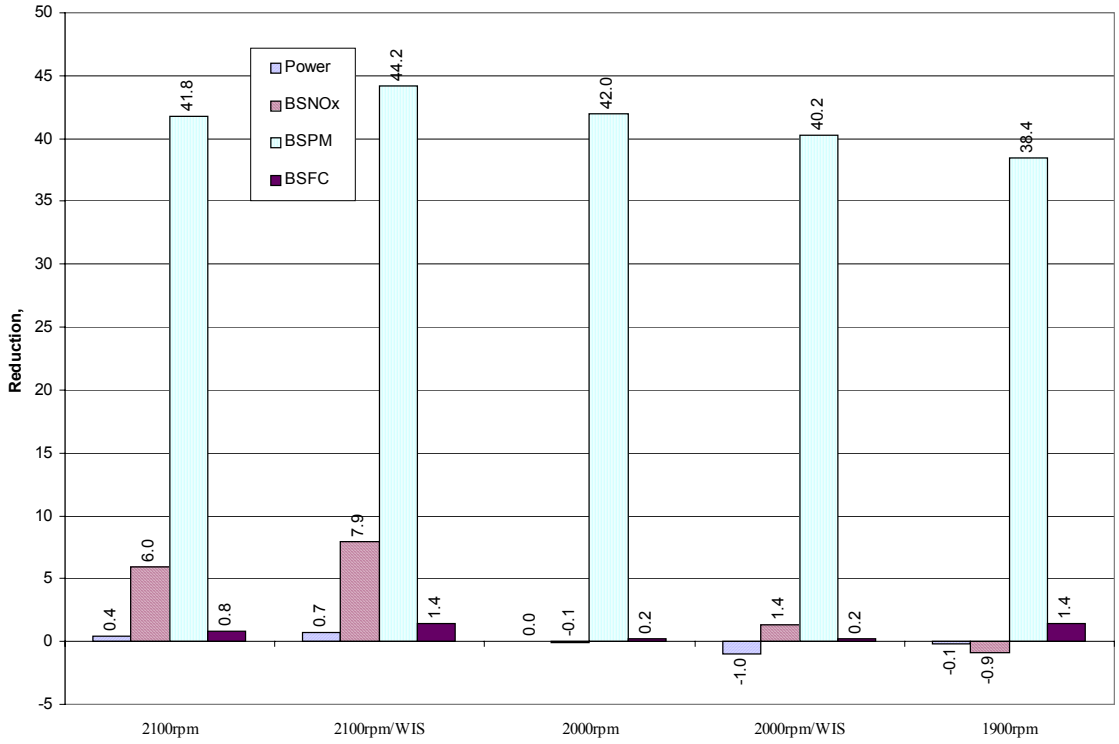


**Figure 4.6 Percentage Reductions in Brake-specific Emissions, Brake-specific Fuel Consumption and Output Power Due to LSD Fuel Compared to Marine Diesel Fuel**

### 4.1.6 Emissions Reduction due to the Combined Effect of Intake Air Water Injection and Low Sulfur Diesel (LSD) fuel

The combined effect of the intake air water injection and the use of LSD fuel resulted in considerable reductions in the brake-specific $NO_x$ and brake-specific particulate matter emissions, without significant fuel penalty or a reduction in power output. Results are available only for the 2100 rpm and 2000 rpm modes, as illustrated in Table 4-7 and Figure 4.7. As mentioned in Section 4.1.1.1 no measurements could be made for the 1900 rpm mode with WIS and LSD fuel. The reductions in $BSNO_x$ emissions were approximately 17% and 14% for the 2100 rpm and 2000 rpm modes, respectively. The corresponding reductions in BSPM emissions were approximately 44% for both the modes.

**Table 4-7 Percentage Reductions in Brake-specific Emissions, Brake-specific Fuel Consumption and Output Power with WIS and LSD Fuel Compared to that without WIS and Marine Diesel Fuel**

| | Reductions (%) | | | |
|---|---|---|---|---|
| Mode | $BSNO_x$ | BSPM | BSFC | Power |
| 2100 rpm | 17.1 | 43.8 | 1.0 | 0.6 |
| 2000 rpm | 13.6 | 44.4 | 0.2 | -0.9 |

## 4.2 Brake-specific Emissions Calculated from Brake-specific Fuel Consumption (BSFC) data (Carbon Balance Method)

This section discusses the brake-specific emissions calculated from the brake-specific fuel consumption (BSFC) data. The procedure for calculation of brake-specific emissions from BSFC data by the Carbon balance method is explained in Section 3.10.2. Values of $BSNO_x$ and BSPM that were calculated using BSFC data (referred to as C-

balance in Figure 4.8, Figure 4.9, Figure 4.10, Figure B-9, and Figure B-10) were compared with those calculated using the MEMS data acquisition system, which uses the raw emissions data, combined with the speed and torque data to obtain the brake-specific emissions (referred to as In-use in Figure 4.8, Figure 4.9, Figure 4.10, Figure B-9, and Figure B-10). Results show that there is a difference of approximately 7% in the brake-specific emissions obtained from BSFC data with those obtained from the MEMS. Figure 4.8 and Figure 4.9 show the comparison of $BSNO_x$ emissions and BSPM emissions obtained from BSFC data with those obtained from in-use calculations. The data points in the figures represent the different test configurations. Figure B-9 and Figure B-10, found in the appendices, show the same in the form of bar charts.

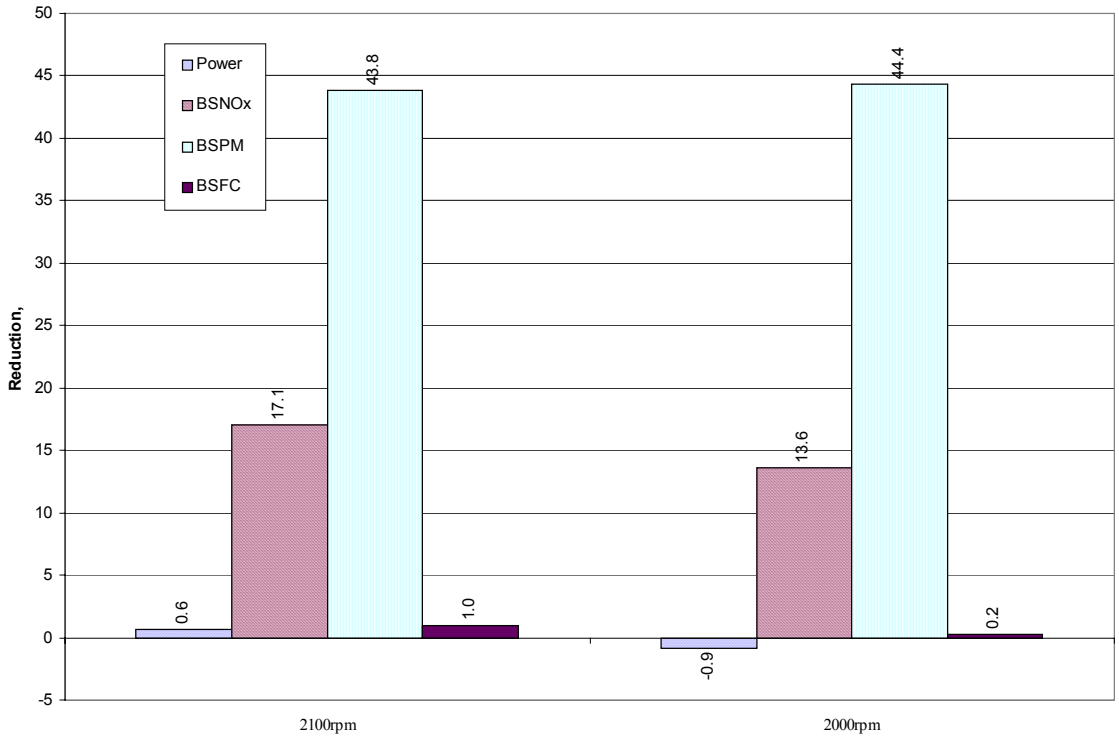


**Figure 4.7 Percentage Reductions in Brake-specific Emissions, Brake-specific Fuel Consumption and Output Power with WIS and LSD Fuel Compared to that without WIS and Marine Diesel Fuel**

The brake-specific emissions calculations from BSFC data obviate the need for speed, torque and fuel flow measurements in the field. The fuel consumed can be obtained from the $CO_2$ measured in the exhaust stream. The mass of fuel consumed along with the BSFC data gives the integrated work output for a particular mode; hence, the brake-specific emissions can be obtained. However, the BSFC data needs to be accurate and reflect the engine's performance at the time of emissions testing. Engine degradation due to injector and fuel system problems could result in significant errors. It should be noted that the BSFC data for the test engine under consideration was not obtained from the manufacturer, but was calculated from the fuel flow, torque and speed data that was measured during the tests for this study. Figure 4.10 shows the percentage difference in the brake-specific emissions data obtained from BSFC data and that obtained from in-use calculations. Results show that the method of determining brake-specific emissions from BSFC data could be used for in-use emissions calculations.

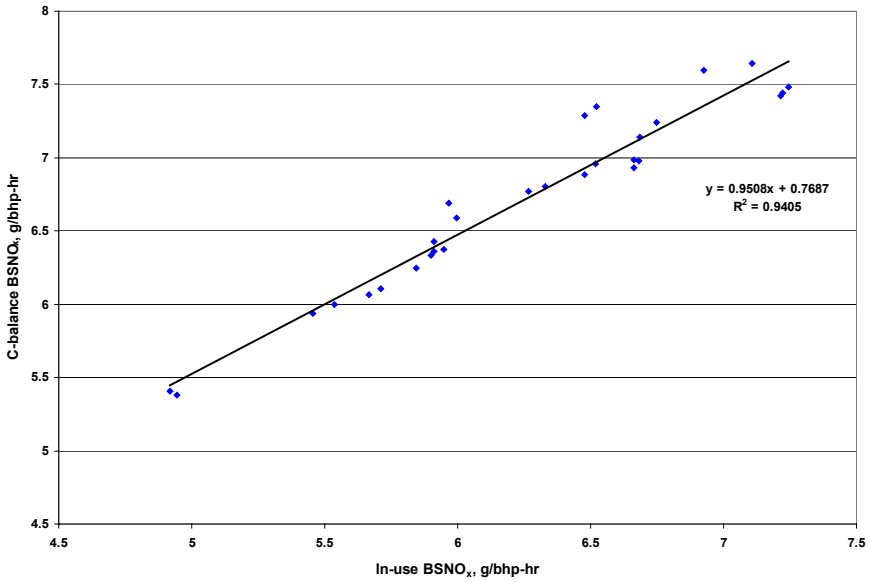


**Figure 4.8 Comparison of $BSNO_x$ emissions Obtained from Carbon (C) Balance Method with that Obtained from In-use Calculations**

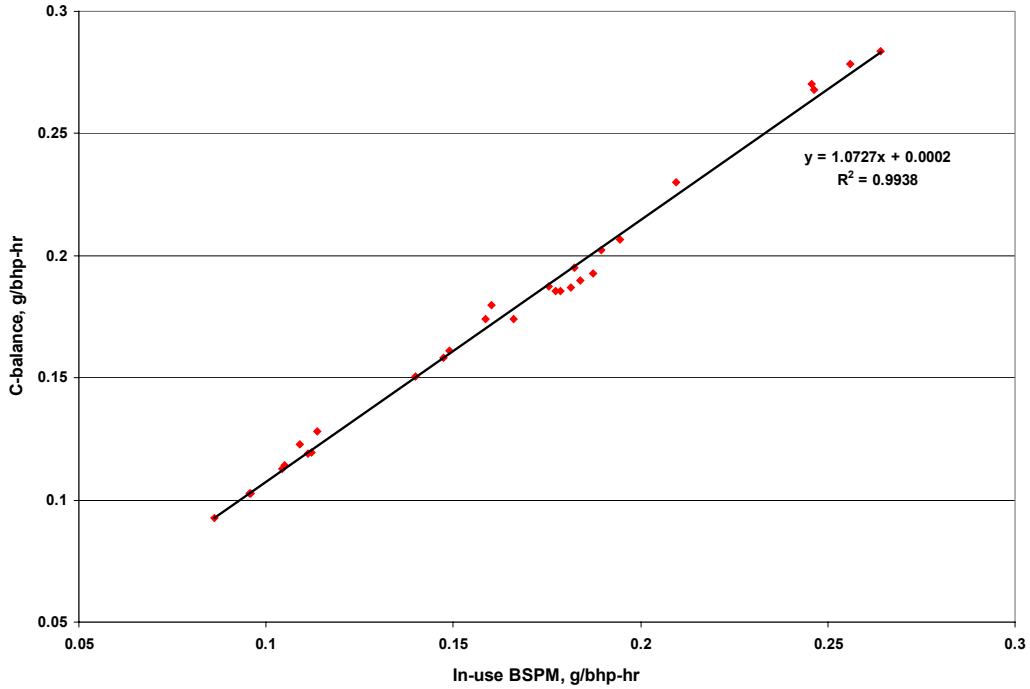


**Figure 4.9 Comparison of BSPM Emissions Obtained from C Balance Method With that Obtained from In-use Calculations**

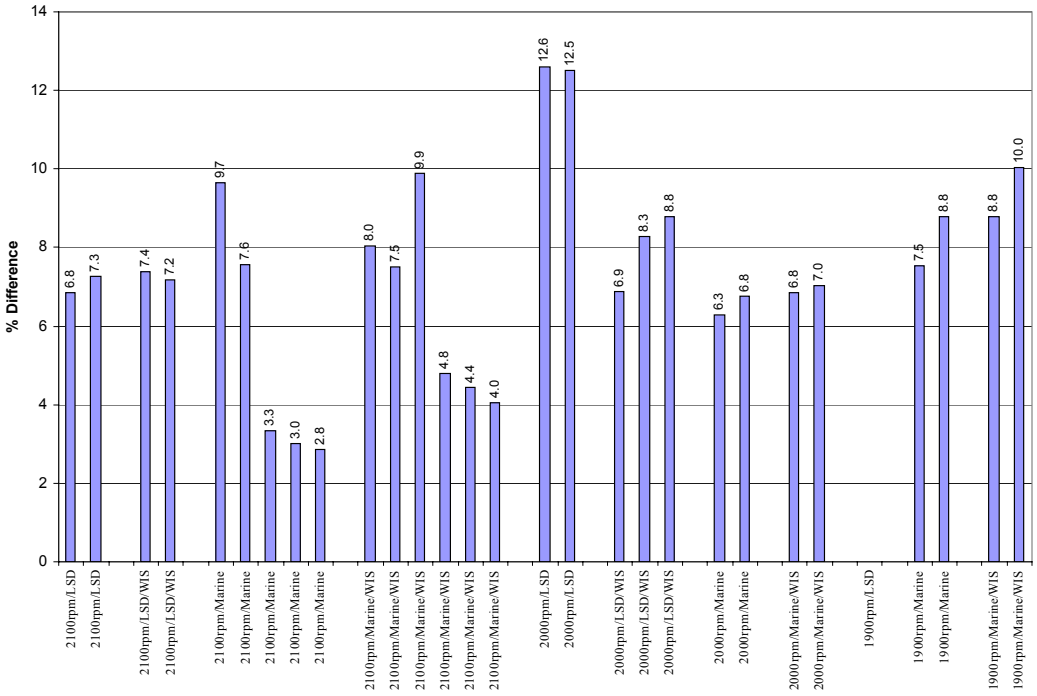


**Figure 4.10 Percentage Difference in Brake-specific Emissions Obtained from C Balance Method with that Obtained from In-use Calculations**

## 4.3 Comparison of Fuel Consumption Measurements

This section discusses the results of a comparison of fuel consumption obtained from the carbon balance method with that obtained from the fuel flow meters. The calculation of mass of fuel consumed by carbon balance method is described in Section 3.10.2. Figure 4.11 shows the comparison of the fuel consumption measurements for the various modes and engine configurations. The data points in the figure represent the different test configurations. Figure B-11, in the appendix, shows the same in the form of bar charts. Figure 4.12 shows the percentage difference between the two methods for the different modes and configurations. The results show that the carbon balance method gives accurate results of fuel consumption. This suggests that the installation of fuel flow meters for in-use emissions measurements could be avoided without significant penalty in data accuracy.

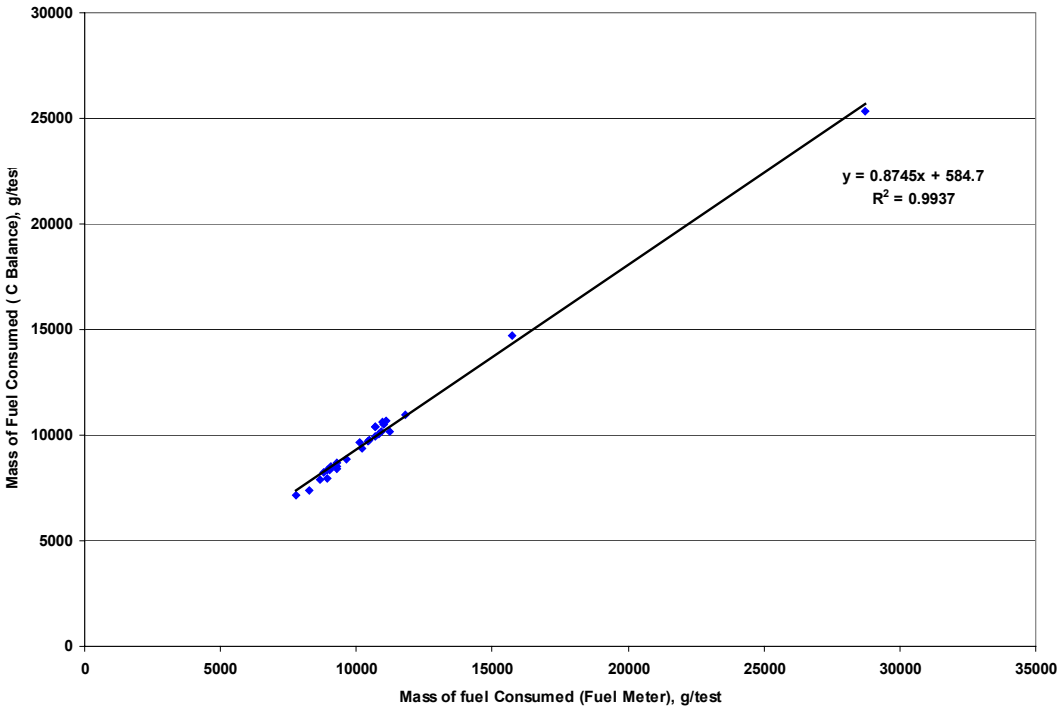


**Figure 4.11 Comparison of Calculated Fuel Consumptions (Fuel Meter vs. Carbon Balance)**

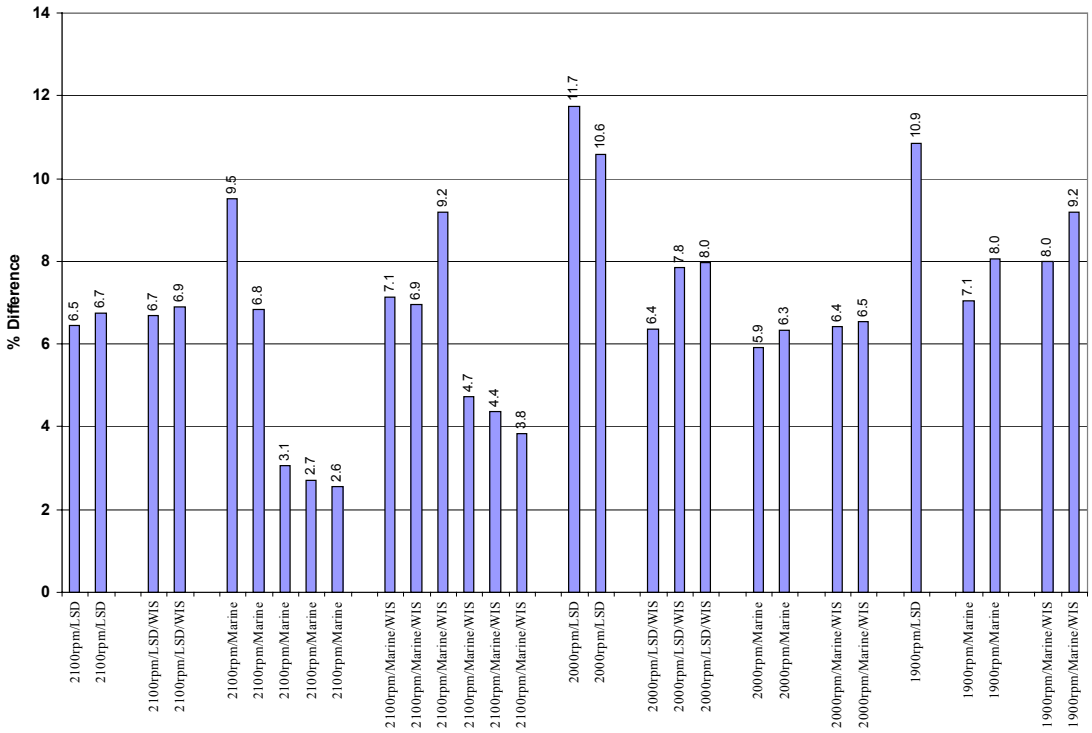


**Figure 4.12 Percentage Difference in Fuel Consumption Measurements (Fuel Meter vs. Carbon Balance)**

## 4.4 Comparison of $BSNO_x$ Emissions with Corresponding Annex VI [14] Limits

The brake-specific $NO_x$ ($BSNO_x$) emission results obtained from different configurations for the three modes, namely, 2100 rpm, 2000 rpm and 1900 rpm were compared with the IMO Annex VI [14] $NO_x$ limits, given in Table 2-2. Table 4-8 gives the average $BSNO_x$ values for various modes and configurations and corresponding IMO $NO_x$ limits. Figure 4.13 shows the measured $BSNO_x$ values superimposed on the IMO $NO_x$ limit curve.

**Table 4-8 Comparison of Measured $BSNO_x$ versus IMO $NO_x$ Limits**

| Mode | Engine RPM | $NO_x$ (g/kW-hr) | IMO $NO_x$ Limit (g/kW-hr) |
|---|---|---|---|
| 2100/LSD | 2100 | 9.01 | 9.8 |
| 2100/LSD/WIS | 2100 | 7.94 | 9.8 |
| 2100/Marine | 2100 | 9.57 | 9.8 |
| 2100/Marine/WIS | 2100 | 8.62 | 9.8 |
| 2000/LSD | 2000 | 8.72 | 9.8 |
| 2000/LSD/WIS | 2000 | 7.52 | 9.8 |
| 2000/Marine | 2000 | 8.72 | 9.8 |
| 2000/Marine/WIS | 2000 | 7.63 | 9.8 |
| 1900/LSD | 1900 | 8.00 | 9.94 |
| 1900/LSD/WIS | 1900 | ------- | 9.94 |
| 1900/Marine | 1900 | 7.93 | 9.94 |
| 1900/Marine/WIS | 1900 | 6.61 | 9.94 |

Figure 4.13 shows that the $BSNO_x$ emissions for all the modes tested were below the $BSNO_x$ limits set forth by the IMO Annex VI [14], which is also equivalent to the Tier 1 $NO_x$ standards set for Category 1 and 2 engines. The measured $BSNO_x$ values are represented by diamonds in the figure. It should be noted that the values of $BSNO_x$ obtained are for fixed speed and load conditions, whereas the IMO $NO_x$ limit curve is based on a weighted average over several speed and load conditions.

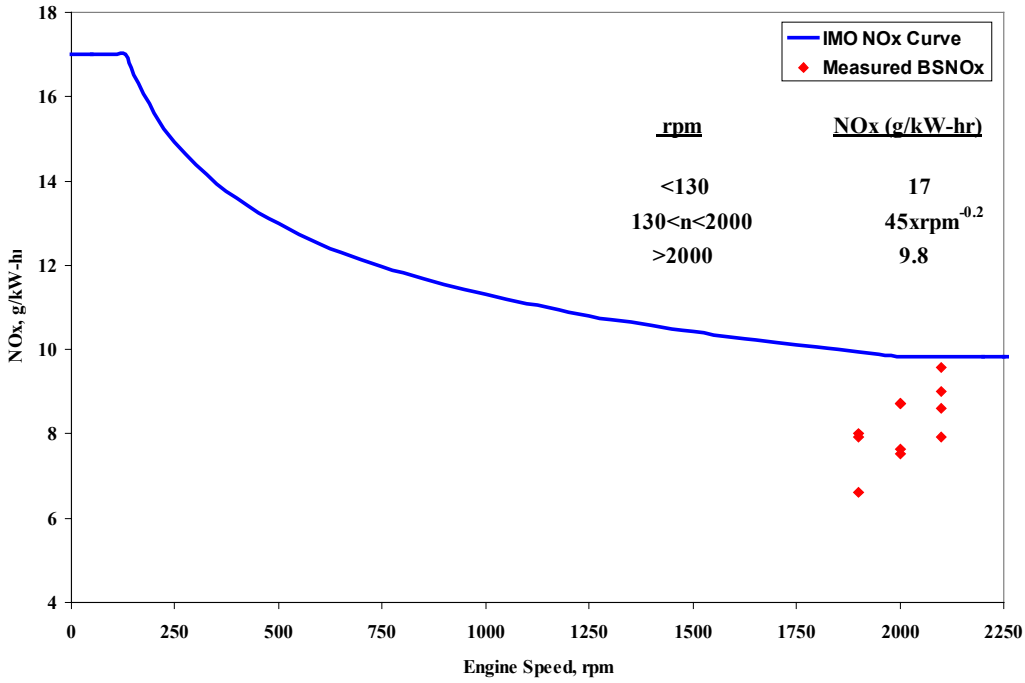


**Figure 4.13 $BSNO_x$ Values for Various Modes versus IMO $NO_x$ Limit Curve**

## 4.5 Comparison of Entire Test Duration Data versus 60 Seconds Data

The calculations for gaseous emissions were based on procedures presented in Title 40 CFR 92 [9], wherein, it suggests that the data from the last 60 seconds of each test phase be used for reporting of results. In this report, the data for the entire test phase has been averaged for all the steady-state tests conducted. The time traces of the loads in each test were checked for any major variations. The time trace of torque in case of the 2100rpm/LSD configuration is as shown in Figure 4.14. The maximum and minimum variations from average torque for the entire data set are 3% and 8%, respectively, and similar results were observed in all the tests. In all the cases, the load was found to remain approximately stable during the entire data collection period. In the final report submitted to the National Renewable Energy Laboratory (NREL) [42], the results presented are obtained from averaging the last 60 seconds of data for each test phase.

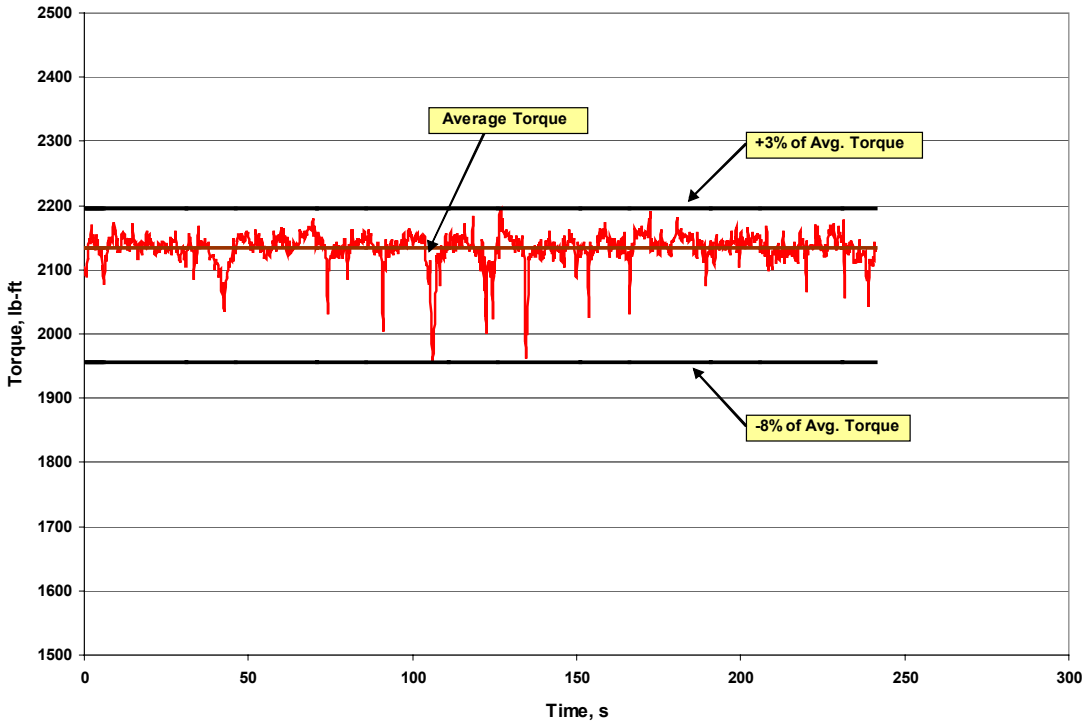


**Figure 4.14 Time Trace of Torque for the 2100rpm/LSD Configuration**

Average data from the last 60s of mode operation was compared with the emission results obtained by averaging the data from the entire test mode. Figure 4.15 and Figure 4.16 shows the comparison of brake-specific $NO_x$ emissions and percentage difference in brake-specific $NO_x$ emissions, respectively, for the two cases (ETD in Figure 4.15 represents Entire Test Duration). The data points in the figures represent the different test configurations. Figure B-14, found in the appendix, shows the same in the form of bar chart. Figure 4.16 shows that the percentage difference is approximately 0.5% in most of the steady state tests. The data records for the steady-state tests were started after an initial stabilization period; hence, the differences are neglible whether the entire test data is averaged or simply the last 60 seconds, provided there are no major variations in load during the entire data collection period. However, for the purpose of standardization of test procedures it would be appropriate to average the last 60 seconds data or the best 60 seconds

data (for tests where any major variations in load occur during the last 60 seconds period) from the entire data collection period.

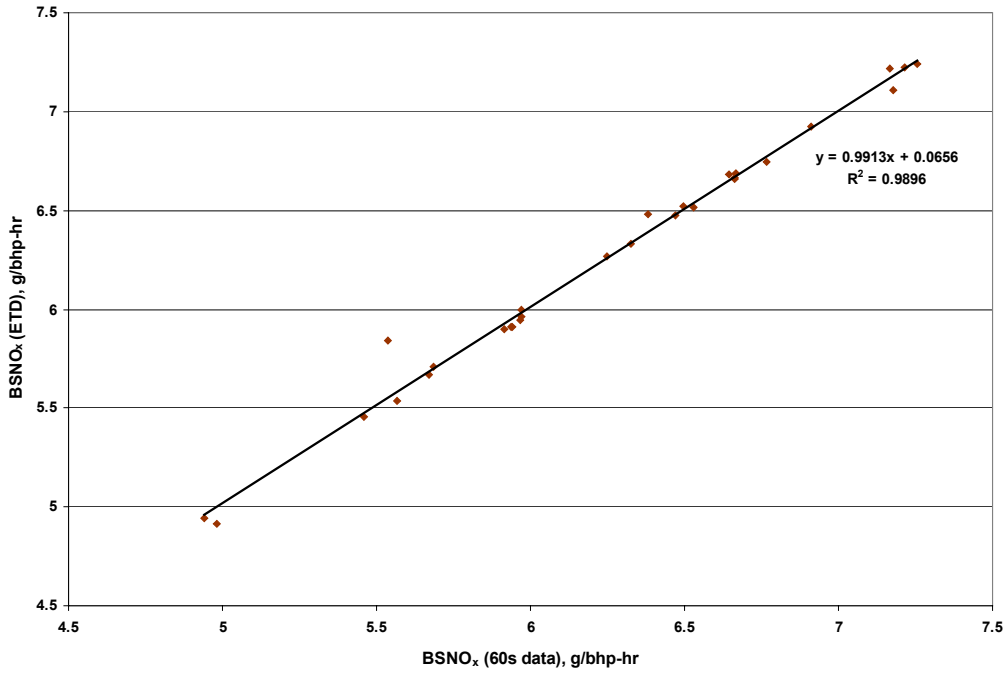


**Figure 4.15 Comparison of Brake-specific $NO_x$ Emissions**

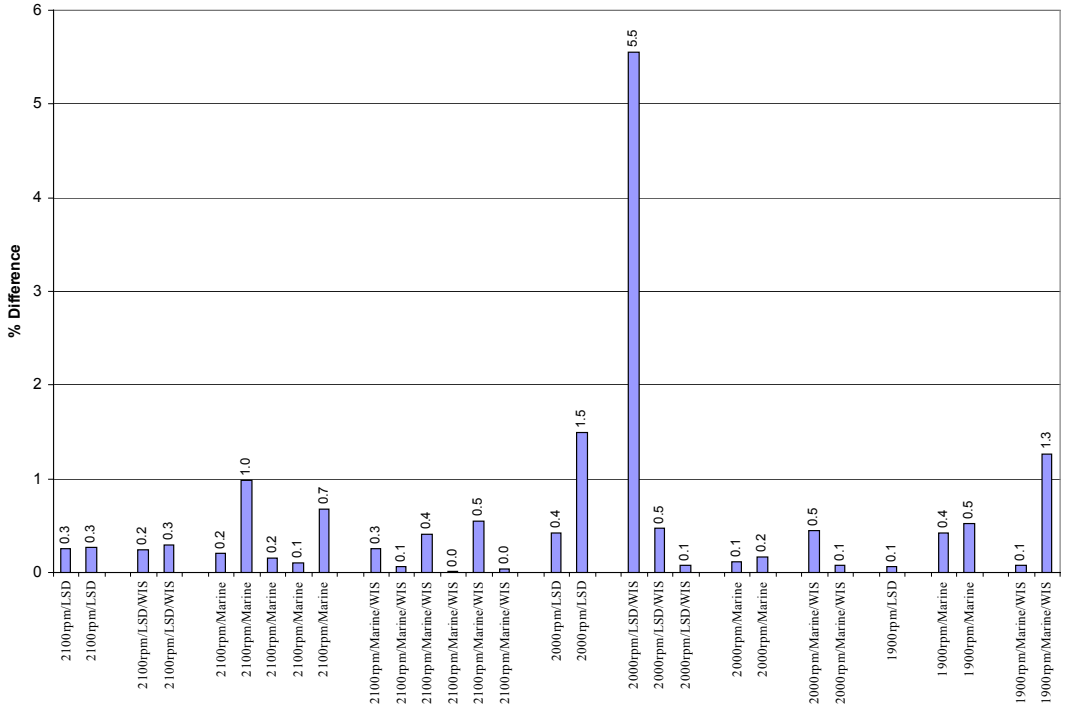


**Figure 4.16 Percentage Difference in Brake-specific $NO_x$ Emissions**

## 4.6 Comparison of Exhaust Temperatures

Exhaust temperature was logged manually during each test. Figure 4.17 shows the average exhaust temperatures at the three different engine speeds for the four different configurations. The exhaust temperatures for the modes with intake air water injection are lower than those without water injection, which result from lower in-cylinder temperatures due to water injection. The reductions in $NO_x$ emissions with intake air water injection are also resultant of the lower combustion temperatures.

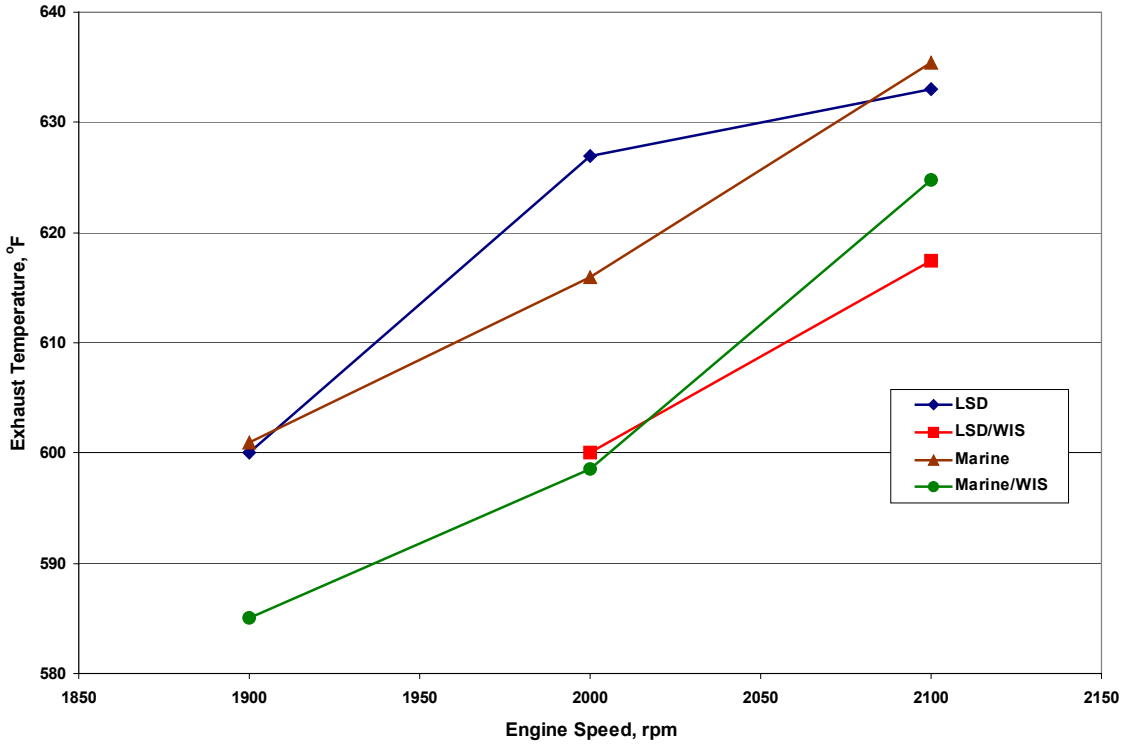


**Figure 4.17 Comparison of Exhaust Temperature vs. Engine Speed**

## 4.7 Effects of Shipping and Handling on Filter Weights

As mentioned in Chapter 3, the filters used for collecting particulate matter for the tests were not conditioned immediately prior to or following the tests as set forth in Title 40 CFR Parts 86 and 89 [7, 8]. Rather, the filters were conditioned a few days prior to the test

dates, and a few days after the in-field tests, because the filters had to be shipped back and forth to the test site. In addition to the test filters, another set of fifty-two filters was also shipped. These filters were used to determine the effects of shipping and handling on the filters, and also to determine the effects of not conditioning the filters immediately before and after the tests. Figure 4.18 shows the difference in filter weights, and the percentage difference in filter weights, for the unused filters before they were shipped out from the WVU EERL, and after they were received from the test site. The x-axis represents the filter identification numbers.

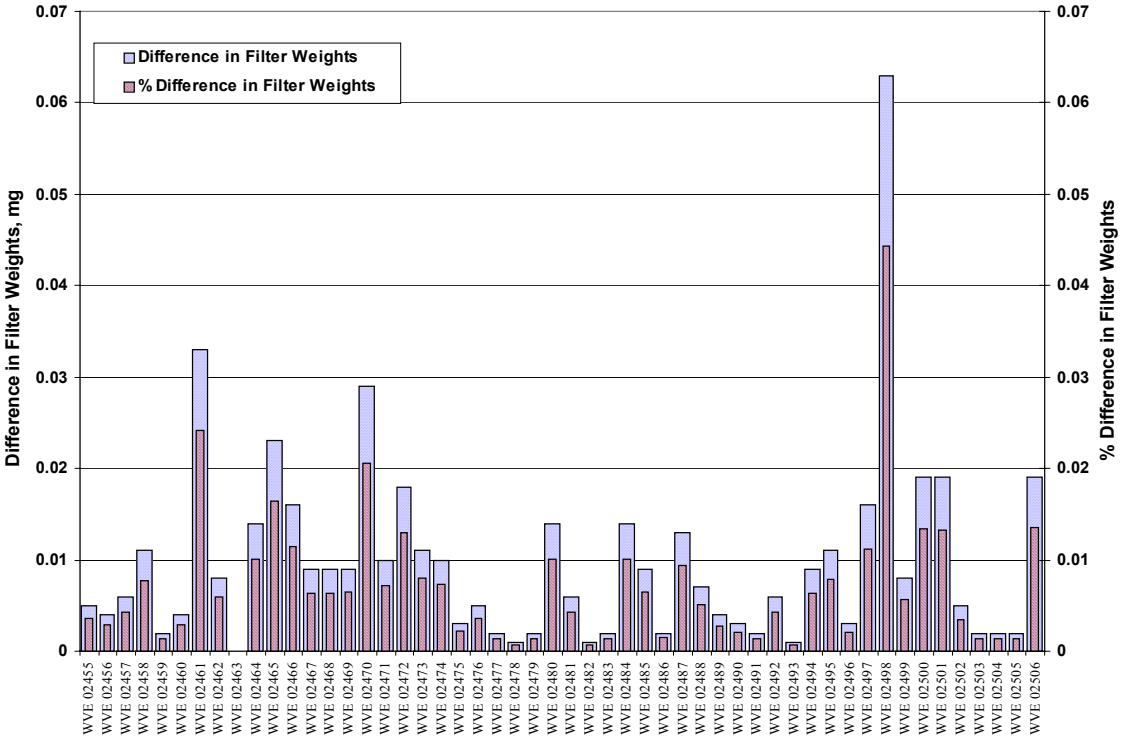


**Figure 4.18 Differences and Percentage Differences in Weights for the Unused Filters**

The set of unused filters was also conditioned, pre-weighed and shipped to and from the test site, but were kept unused. The results show that the differences in filter weights due to shipping, handling and not conditioning immediately prior to and after the tests are negligible. The maximum percentage difference in filter weight seen is below 0.05%.

## 4.8 Validation Test Results

This section discusses the results of the validation tests that were conducted for the partial flow dilution tunnel and the Mobile Emissions Measurement System (MEMS). A Detroit Diesel Corporation Series 60 engine was used for this validation. Particulate matter measurements were taken simultaneously using the partial flow dilution tunnel and the full flow double-dilution tunnel at the WVU EERL test facility. Gaseous emissions measurements for $NO_x$ and $CO_2$ were made using the MEMS, and were compared to those obtained using the laboratory-grade analyzers. The test engine used for the validation tests, as well as the WVU EERL, is discussed in Section 3.9.

### 4.8.1 Gaseous Emissions Comparison

The results for gaseous emissions measurements show that the MEMS measures within ± 10% of the laboratory grade measurement system for the tests conducted. Figure 4.19 and Figure 4.20 show the $NO_x$ and $CO_2$ emission results comparison between the two systems in g/s. The data points in the figures represent the different test configurations. Figure B-12 and Figure B-13, found in the appendix show the same in the form of bar charts. Figure 4.21 shows the percentage difference in the $NO_x$ and $CO_2$ measurements between the two systems.

### 4.8.2 Particulate Measurement Comparison

Brake-specific particulate matter (BSPM) emissions measurements were obtained by gravimetric analysis of PM samples collected on filters using the partial flow dilution tunnel, and the full-flow, double-dilution CVS system. Results obtained using the mini-tunnel had a difference of approximately ± 15% with those obtained using the full flow dilution tunnel.

Accuracy of the partial flow tunnel was inherently related to the stability of the dilution ratio control. The dilution ratio (*DR*) is expressed as,

$$DR = \frac{V_t}{V_t - V_d}$$

where, $V_t$, is the total sample volume through the mini-tunnel and, $V_d$, is the volume of dilution air. Differentiating *DR* with respect to $V_t$, considering $V_d$ to remain constant results in,

$$\frac{dDR}{DR} = (1 - DR)\frac{dV_t}{V_t}$$

The above equation shows that small changes in the total flow results in higher instabilities of the dilution ratio. These instabilities would be directly proportional to dilution ratio. A dilution ratio of 4:1, which is the minimum allowable dilution ratio as specified by ISO 8178-1:1996(E) [11], was chosen for all the tests conducted. Figure 4.22 shows the comparison of BSPM data obtained using the mini-tunnel and the CVS, while Figure 4.23 shows the percentage differences between the two.

The errors were very high in cases where the dilution ratio was unstable, which results from the changes in the total flow. These results show that attempts to correlate mini-tunnel PM results with total exhaust dilution tunnel are very much dependent on the stability and the set-point of the dilution ratio.

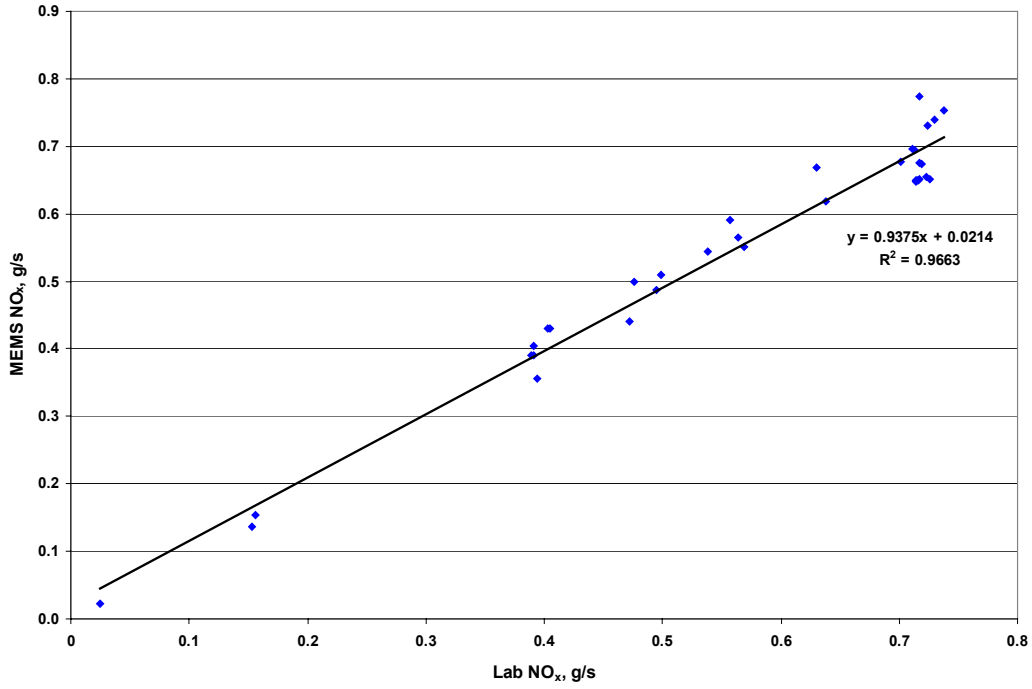


**Figure 4.19 Comparison of Laboratory-MEMS $NO_x$ Measurements**

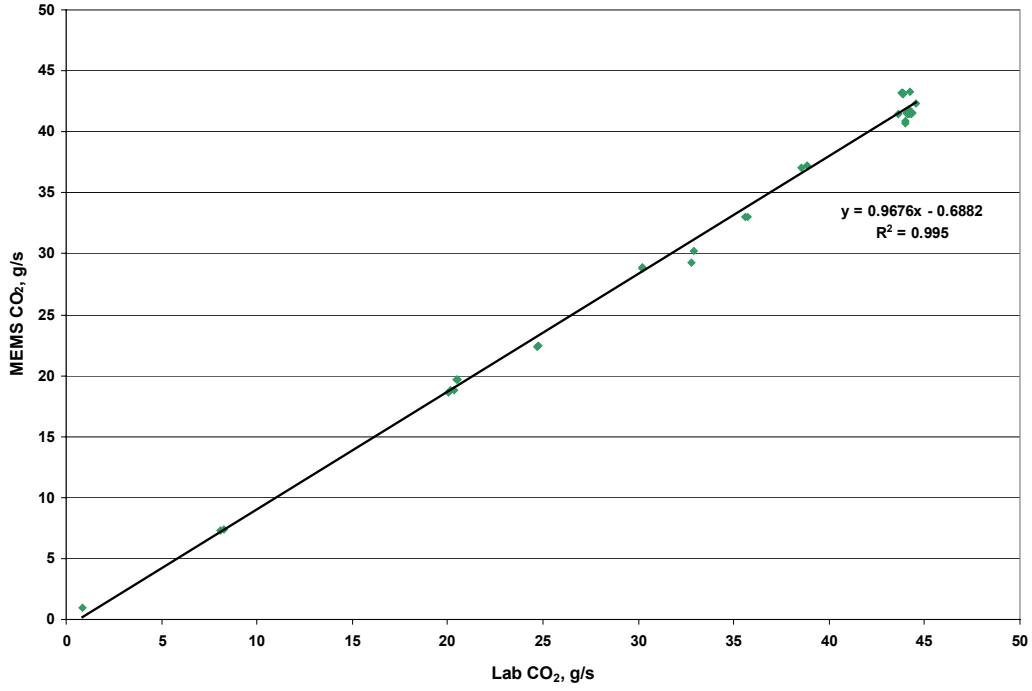


**Figure 4.20 Comparison of Laboratory-MEMS $CO_2$ Measurements**

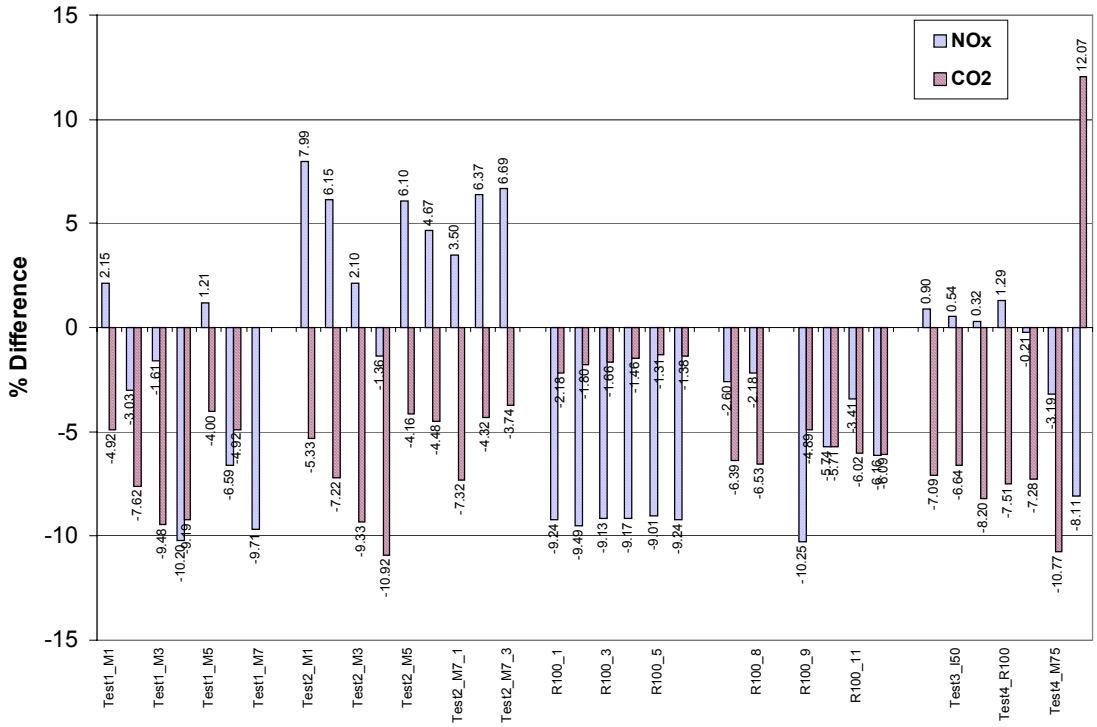


**Figure 4.21 Percentage Difference between Laboratory-MEMS $NO_x$ and $CO_2$ Measurements**

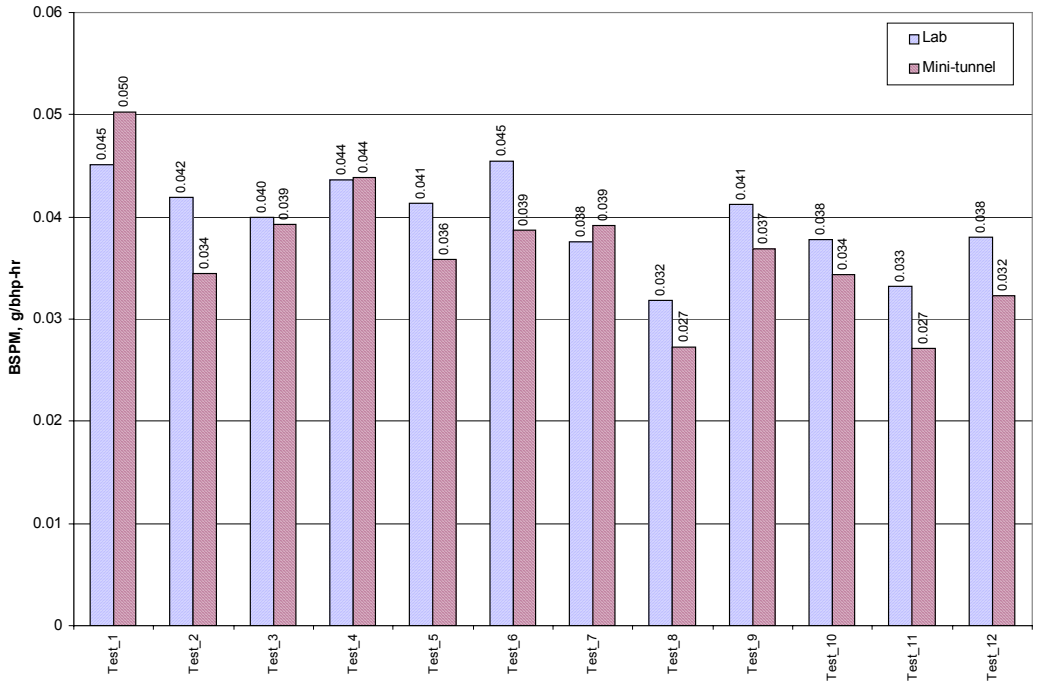


**Figure 4.22 Comparison of Laboratory-Mini-tunnel BSPM Measurements**

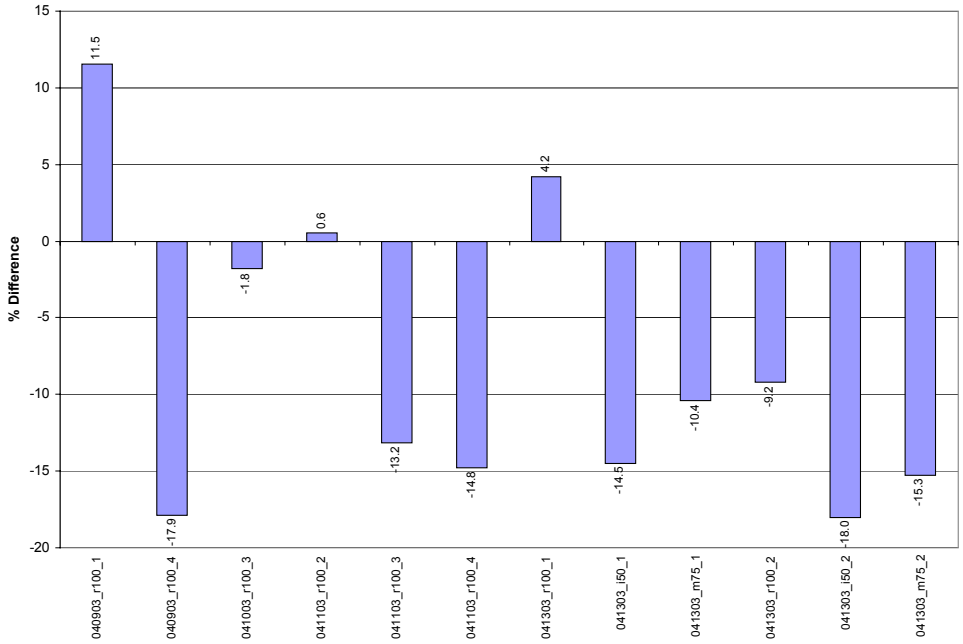


**Figure 4.23 Percentage Difference between Laboratory-Mini-tunnel BSPM Measurements**

### 4.8.3 Comparison of Brake-specific Fuel Consumption (BSFC) Data

Validation tests were also conducted at WVU EERL prior to the on-board tests for the Micro Motion CMF025 Coriolis flow meters. The Coriolis flow meter data was collected by the MEMS data acquisition system on a continuous basis. The fuel flow data was compared with the fuel flow obtained from the Max Flow Media 710 Series Fuel Measurement System at the WVU EERL. Brake-specific fuel consumption was calculated from the data obtained from the Max Flow fuel meter, Coriolis flow meter and carbon balance from the emissions data. Most of the validation tests conducted were at Rated 100 conditions as the ferry operated mostly at high load conditions.

The results for BSFC data show that the average percentage difference between the laboratory fuel flow meter and the Coriolis flow meter, laboratory fuel flow meter and the carbon balance, and the carbon balance and the Coriolis flow meter were approximately 5%,

7%, and 6% respectively for all the tests conducted. Figure 4.24 shows the BSFC results comparison between the different methods lb/bhp-hr. Figure 4.25 shows the percentage difference in the measurements between the three methods of BSFC calculation.

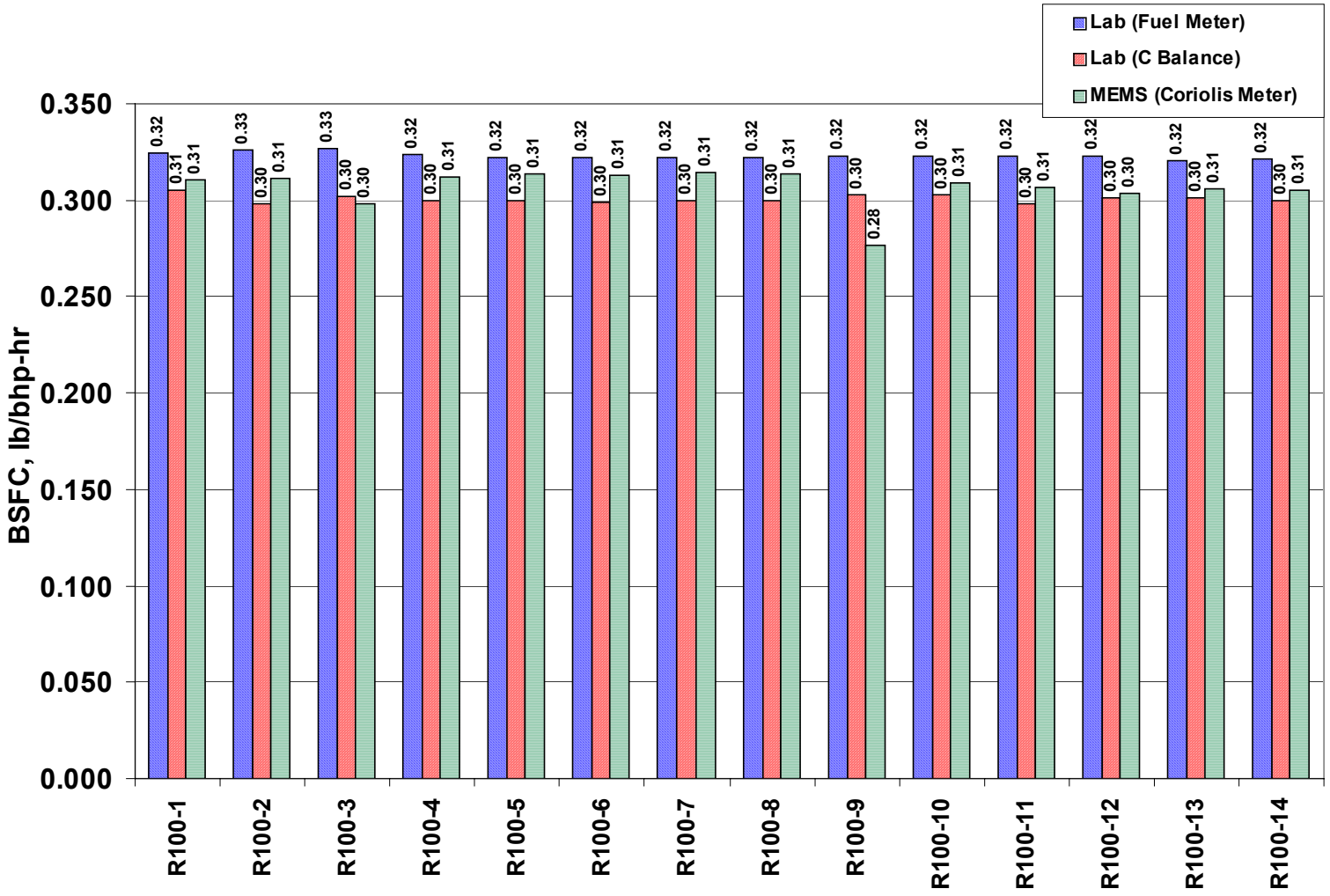


**Figure 4.24 Comparison of Brake-specific Fuel Consumption (BSFC) Data**

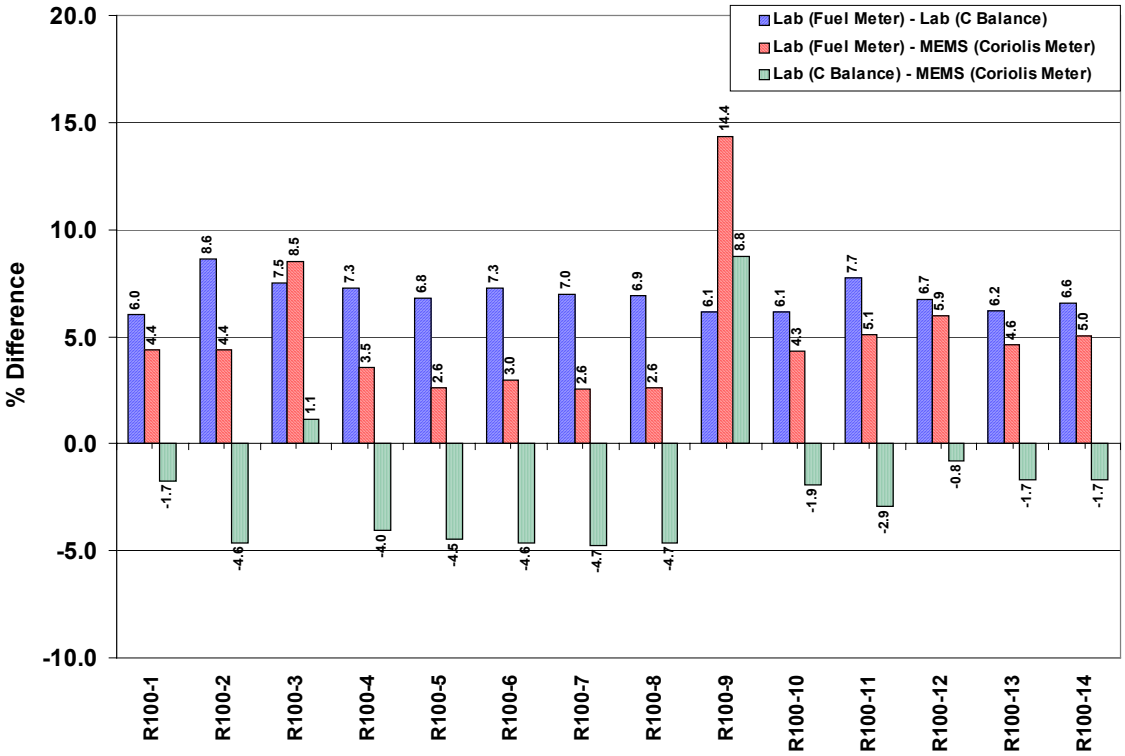


**Figure 4.25 Percentage Difference in BSFC Calculations**

# 5 CONCLUSIONS AND RECOMMENDATIONS

## 5.1 Conclusions

This study was part of the United States Maritime Administration (MARAD)'s Marine Exhaust Reduction Program. The water injection system manufactured by M.A.Turbo/Engine Ltd. [18] was successfully tested onboard the high-speed passenger ferry (hydrofoil) operated by SCX Inc. between San Diego and Oceanside, California. The benefit of operating the engine using low sulfur diesel (LSD) fuel was also determined. Gaseous emissions of $NO_x$ and CO2 were measured successfully using the Mobile Emissions Measurement System (MEMS), while PM emissions were measured using a partial flow dilution tunnel. The major conclusions of this study are summarized below:

- A reduction of approximately 11%-17% was observed in average brake-specific $NO_x$ ($BSNO_x$) emissions with the intake air water injection system for all modes and engine configurations.
- The reduction in $BSNO_x$ emissions was dependent upon the amount of water being injected. This could be concluded from the fact that the reductions in $NO_x$ emissions were higher for lower engine speeds, for a given water injection rate.
- A reduction in PM emissions of approximately 38%-45% was realized with the engine operating on low sulfur diesel (LSD) fuel, as compared to operation on conventional marine diesel fuel.
- There was not a significant effect on the PM emissions with intake air water injection.
- Fuel consumption and work output were relatively unaffected by fuel type variations or intake air water injection.

- Combined usage of the intake air water injection system (WIS) and low sulfur diesel (LSD) fuel proved to effect significant reductions in $NO_x$ and PM emissions.
- Engine oil sample analysis showed abnormal engine wear. It was not concluded whether the engine wear problem was a result of intake air water injection. One previous study [19] had also shown a similar oil analysis result.
- The calculation of brake-specific emissions from BSFC data (carbon balance method) provided similar results as those calculated through the use of direct engine-out work measurements. This method of calculation would enable measurement of brake-specific emissions without requiring speed and torque measurements.
- The partial flow dilution tunnel showed instabilities at high dilution ratios in the validation tests conducted prior to the on-board tests.
- $BSNO_x$ emissions for the test engine were below the EPA Tier 1 standards set for the engine category to which it belonged for all modes and configurations. However, the WIS and LSD combination may not be effective in meeting the EPA Tier 2 $BSNO_x$ standards for this engine.
- Operation on LSD fuel can achieve the Tier 2 and the Voluntary PM emission limits set for this engine.
- Emissions data integrated over the entire test duration can be used in brake-specific emissions calculations if the load conditions remain stable during the entire data collection period and a sufficient stabilization period is provided at each mode before the data collection period.
- Shipping of PM sample filters to and from the test site did not show any effect on the PM results. Conditioning of these filters as specified in Title 40 CFR Part 86 [7],

is required prior to shipping and after the completion of tests. Results suggest that immediate pre- and post-conditioning of filters were not necessary.

## 5.2 Recommendations

Modifications are required to the water injection system to make it effective over different engine speeds. This study did not include testing of different amounts of water injection into the intake air. Tests could be conducted to determine the optimum amount of water injection required to obtain maximum $NO_x$ reductions at different engine speeds.

The partial flow dilution tunnel needs to be modified so as to make it stable for higher dilution ratios.

Further tests need to be conducted using the tests procedures and equipments used in this study before a comprehensive test protocol could be developed.

Engine oil and fuel samples need to be taken before and after tests, as well as over extended periods of operation, so that analysis could be performed in order to determine the effects of the intake air water injection on engine wear.

# REFERENCES


1. "An Assessment of the U.S. Marine Transportation System", A Report to Congress, 1999, http://www.marad.dot.gov/publications/MTSreport/mtsfinal.pdf

2. Gautam, M., Clark, N. N., Thompson, G. J., and Lyons, D. W., "Assessment of Mobile Monitoring Technologies for Heavy-Duty Vehicle Emissions", Whitepaper Submitted to the Settling Heavy-Duty Diesel Engine Manufacturers, Department of Mechanical and Aerospace Engineering, West Virginia University, Morgantown, WV, 1999, www.epa.gov/Compliance/civil/programs/caa/diesel/test.html

3. Gautam, M., Clark, N. N., Thompson, G. J., Carder, D. K., and Lyons, D. W., "Evaluation of Mobile Monitoring Technologies for Heavy-Duty Diesel-Powered Vehicle Emissions", Phase I Final Report Submitted to the Settling Heavy-Duty Diesel Engine Manufacturers, Department of Mechanical and Aerospace Engineering, West Virginia University, Morgantown, WV, 2000, www.epa.gov/Compliance/civil/programs/caa/diesel/test.html

4. Gautam, M., Clark, N. N., Thompson, G. J., Carder, D. K., and Lyons, D. W., "Development of Inuse Testing Procedures for Heavy-Duty Diesel-Powered Vehicle Emissions", Phase II Final Report Submitted to the Settling Heavy-Duty Diesel Engine Manufacturers, Department of Mechanical and Aerospace Engineering, West Virginia University, Morgantown, WV, 2000, www.epa.gov/Compliance/civil/programs/caa/diesel/test.html

5. Gautam, M., Thompson, G. J., Carder, D. K., Clark, N. N., Shade, B. C., Riddle, W. C., and Lyons, D. W., "Measurement of In-Use, On-Board Emissions from Heavy-Duty Diesel Vehicles: Mobile Emissions Measurement System", SAE Technical Paper No. 2001-01-3643, 2001.

6. Gautam, M., Thompson, G.J., Clark, N.N., Riddle, W.C., and Carder, D.K., "Development of a Test Method to Measure Stationary and Portable Engine Emissions", Task I Report Submitted to California Air Resources Board, Department of Mechanical and Aerospace Engineering, West Virginia University, Morgantown, West Virginia, January 3, 2002.

7. Code of Federal Regulations, Title 40 Part 86, U.S. Government Printing Office, Washington DC, 2000.

8. Code of Federal Regulations, Title 40 Part 89, U.S. Government Printing Office, Washington DC, 2000.

9. Code of Federal Regulations, Title 40 Part 92, U.S. Government Printing Office, Washington DC, 2000.

10. Code of Federal Regulations, Title 40 Part 94, U.S. Government Printing Office, Washington DC, 2000.

11. “Reciprocating Internal Combustion Engines – Exhaust Emissions Measurement”, International Organization for Standardization, ISO/DIS 8178, Geneva, Switzerland, 1993.

12. "Measurement of Carbon Dioxide, Carbon Monoxide, and Oxides of Nitrogen in Diesel Exhaust," SAE Standard, SAE J177, Warrendale, PA 1995.

13. “Emission Standards: U.S.A. - Marine Diesel Engines”, 2002, http://www.dieselnet.com/standards/us/marine.html

14. “International Convention for the Prevention of Pollution from Ships (MARPOL 73/78)”, International Maritime Organization (IMO).

15. “Emission Standards Adopted for New Marine Diesel Engines”, Regulatory Announcement, Office of Transportation and Air Quality, U.S. EPA, 2003, http://www.epa.gov/otaq/regs/nonroad/marine/ci/f03001.pdf

16. Bentz, A.P., and Weaver, E., “Marine Diesel Exhaust Emissions Measured by Portable Instruments”, SAE Paper No. 941784, 1994.

17. “Marine Vehicles Exhaust Emissions Program: A Study of the Effects of Multiple Emissions Reduction Technologies on the Exhaust Emissions of Marine Diesel Engines”, Emissions Research and Measurement Division, Environment Canada, April 2003, http://www.tc.gc.ca/tdc/publication/pdf/14000/14099e.pdf

18. M.A. Turbo/Engine, Ltd., Vancouver, BC.

19. “M/V Oski Emissions Tests: Bio-diesel and Inlet Air Water Injection”, Final Report to MARAD, Walther Engineering Services, Inc., June 26, 2002, http://www.marad.dot.gov/nmrec/energy_technologies/images/Final%20Report%201.pdf

20. Thompson, G.J., Carder, D.K., Riddle, W.C., Gautam, M., and Lyons ,D.W., “Evaluation of Exhaust Emissions from Elizabeth River Ferries”, Final Report to MARAD, Department of Mechanical and Aerospace Engineering, West Virginia University, Morgantown, West Virginia, July, 2002.

21. Weaver, C.S., Chan, L., and Peety, L., “Measurement of Air Pollutant Emissions from In-service Passenger Ferries”, Engine, Fuel and Emissions Engineering, Inc., Emissions Data Report Submitted to San Francisco Bay Area Water Transit Authority, 2002.

22. Weaver, C.S., and Balam-Almanza, M.V., “Development of the “RAVEM” Ride-Along Vehicle Emission Measurement System for Gaseous and Particulate Emissions”, SAE Paper No. 2001-01-3644, 2001.

23. "Water in Diesel Combustion", http://www.dieselnet.com/tech/engine_water.html

24. Sawa, N., and Kajitani, S., "Physical Properties of Emulsion Fuel (Water/Oil-Type) and Its Effects on Engine Performance under Transient Operation", SAE Paper No. 920198, 1992.

25. Miyamoto, N., "Significant $NO_x$ Reductions with Direct Water Injection into the Sub-Chamber of an IDI Diesel Engine", SAE Paper No. 950609, 1995.

26. Mollenhauer, K., and Zelenka, P., "Combustion of Water-in-Fuel Emulsions in Stationary Operating Diesel Engines", Motortechnische Zeitschrift, No.47, Heft 1, pp. 3-7, 1986.

27. Holtbecker, R., and Geist, M., "Exhaust Emissions Reduction Technology for Sulzer Marine Diesel Engines: General Aspects", Wartsila NSD Switzerland Ltd., Winterthur, 1998, www.wartsila.com/english/pdf/emissions_tech_review.pdf

28. Henningsen, S., "Influence of the Fuel Injection Equipment on $NO_x$ Emissions and Particulates on a Large Heavy-Duty Two-Stroke Diesel Engine Operating on Water-in-Fuel Emulsion", 1994.

29. Wirbeleit, F., Enderle, C., Lehner, W., Raab, A., and Binder, K., "Stratified Diesel Fuel-Water-Diesel Fuel Injection Combined with EGR- The Most Efficient In-Cylinder $NO_x$ and PM Reduction Technology", SAE Paper No. 972962, 1997.

30. "Emission Control: Direct Water Injection", Wartsila, Product brochure, Wartsila Finland Oy, 2000, www.wartsila.com/english/pdf/en_direct_water_inj.pdf

31. "Cost-benefit Analysis of Marine Emission Control Technologies", Environmental Technology Center, Environment Canada, Ottawa, Ontario, 2001, http://www.tc.gc.ca/tdc/projects/marine/g/9904.htm

32. Odaka, M., Koike, N., Tsukamoto, Y., Narusawa, K., and Yoshida, K., "Effects of EGR with a Supplemental Water Injection to Control Exhaust Emissions from Heavy-Duty Diesel Powered Vehicles", SAE Paper No. 910739, 1991.

33. Ishida, M., and Chen, Z., "An Analysis of the Added Water Effect on NO Formation in D.I. Diesel Engines", SAE Paper No. 941691, 1994.

34. Mellor, A.M., and Mello, J.P., "$NO_x$ Emissions from Direct Injection Diesel Engines with Water/Steam Dilution", SAE Paper No. 1999-01-0836.

35. http://www.ctts.nrel.gov/heavy_vehicle/what/ec_diesel.html

36. Gekas, I., Gabrielson, P., Johansen, K., Nvengaard, L., and Lund, T., "Urea-SCR Catalyst System Selection for Fuel and PM Optimized Engines and a Demonstration of a Novel Urea Injection System", SAE Paper No. 2002-01-0289.

37. Miller, W.R., Klein, J.T., Mueller, R., and Doelling, W., "The Development of Urea-SCR Technology for US Heavy-duty Trucks", SAE Paper No. 2001-01-0190.

38. Scarnegie, B., Miller, W.R., and Ballmert, B., "Recent DPF/SCR Results Targeting US2007 and Euro 4/5 HD Emissions", SAE Paper No. 2003-03FL-133.

39. "Diesel Particulate Filters", http://www.dieselnet.com/tech/dpf_top.html

40. Zhou, P.L., Thorp, I., "Marine Diesel Emissions and Their Control", Department of Marine Technology, University of New Castle upon Tyne, United Kingdom, 1997.

41. Khair, M., Lemaire, J., Fischer, S., "Integration of Exhaust Gas Recirculation, Selective Catalytic Reduction, Diesel Particulate Filters, and Fuel-borne Catalyst for $NO_x$/PM Reduction", SAE Paper No. 2000-01-1933.

42. Thompson, G.J., "SCX Inc. Ferry Emissions Tests", Final Data Report Submitted to National Renewable Energy Laboratory, Department of Mechanical and Aerospace Engineering, West Virginia University, Morgantown, West Virginia, September 5, 2003.

43. Krishnamurthy, M., "Characterization of In-use Emissions from On-highway Heavy-duty Diesel Engines", M.S. Thesis, Department of Mechanical and Aerospace Engineering, West Virginia University, Morgantown, WV, 2003.

44. Wall, J.C. and Hoekman, S.K., "Fuel Composition Effects of Heavy-duty Diesel Particulate Emissions", SAE Paper 841364, 1984.

45. Ferguson, D.H., "Design, Fabrication, and Testing of an Emissions Measurement System for a Transportable Heavy Duty Vehicle Emissions Testing Laboratory", M.S. Thesis, Department of Mechanical and Aerospace Engineering, West Virginia University, Morgantown, WV, 1993.

46. Kittelson, D.B. and Johnson, J.H., "Variability in Particle Emission Measurements in the Heavy Duty Transient Test", SAE 910738, 1991.

47. Smith, R.E. Jr., and Matz, R.J., "A Theoretical Method of Determining Discharge Coefficients for Venturis Operating at Critical Flow Conditions", Journal of Basic Science, 1962, pp. 434-446.

48. Smith II, R.C., "Comparison of Heavy-Duty Diesel Engine Transient Emissions Measurements Using a Mini- and a Full-flow Dilution Tunnel", M.S. Thesis, Department of Mechanical and Aerospace Engineering, West Virginia University, Morgantown, WV, 1993.

49. Abbass, M.K., Andrews, G.E., Williams, P.T. and Bartle, K.D., "Diesel Particulate Composition Changes Along an Air Cooled Exhaust Pipe and Dilution Tunnel", SAE 890789, 1989.

50. Heinein, N.A. and Patterson, D.J., "Emissions from Combustion Engines", Ann Arbor Science Publishers, Inc., Ann Arbor, 1972.

51. Reschke, G.D., "Optimization of a Flame Ionization Detector for Determination of Hydrocarbon in Diluted Automotive Exhausts", SAE 770141, 1977.

52. Chasey, T.D., "Design and Data Acquisition and Control System Hardware and Software for Transportable Emissions Testing Laboratory", M.S. Thesis, Department of Mechanical and Aerospace Engineering, West Virginia University, Morgantown, WV, 1992.

53. Pei, Y., "Development of Software for the Heavy-Duty Engine Testing at Engine Research Center", M.S. Thesis, Department of Mechanical and Aerospace Engineering, West Virginia University, Morgantown, WV, 1993.

54. McMillian, M.H., Gautam, M., "Consideration for Fischer-Tropsch Derived Liquid Fuels as a Fuel Injection Emission Control Parameter", SAE Paper 982489, 1998.

55. Nagendran, V., "Characterization of Exhaust Emissions from Catalyzed Trap-Equipped Non-Road Heavy-duty Diesel Engines", M.S. Thesis, Department of Mechanical and Aerospace Engineering, West Virginia University, Morgantown, WV, 2003.

# APPENDIX A
# Fuel and Oil Sample Analysis Reports

**Table A-1 Fuel Analysis Reports for Low Sulfur Diesel (LSD) and Marine Diesel**
*(Note: The sulfur content for LSD fuel (**BP ECD®**) is highlighted because of suspected contamination of the fuel; hence may not be the correct value.)*

| Test | Units | Method | Fuel | |
|---|---|---|---|---|
| | | | LSD | Marine |
| API Gravity @ 60 Deg. F | deg.API | ASTM D-1298 | 39.2 | 34.7 |
| Carbon | wt% | ASTM D-5291M | 86.36 | 86.49 |
| Cetane Index, Calculated | - | ASTM D-976 | 51.8 | 47 |
| Cetane Number | - | ASTM D-613 | 53.1 | 46.1 |
| Hydrogen Content | wt% | ASTM D-5291M | 13.56 | 13.42 |
| Kinematic Viscosity @ 40 deg. F | cSt | ASTM D-445 | 3.33 | 2.7 |
| Specific Gravity | @ 60 deg.F | ASTM D-1298 | 0.8289 | 0.8514 |
| Total Sulfur | wt% | ASTM D-4294 | 0.032 | 0.394 |
| **Distillation** | | | | |
| IBP | deg.F | ASTM D-86 | 365.6 | 347.9 |
| 5% Rec | deg.F | | 389.4 | 390.4 |
| 10% Rec | deg.F | | 401.2 | 413.4 |
| 20% Rec | deg.F | | 424.8 | 444.5 |
| 30% Rec | deg.F | | 447.3 | 469 |
| 40% Rec | deg.F | | 467.8 | 492 |
| 50% Rec | deg.F | | 492.1 | 514.1 |
| 60% Rec | deg.F | | 517.1 | 536.6 |
| 70% Rec | deg.F | | 542.8 | 559.7 |
| 80% Rec | deg.F | | 574.3 | 54.3 |
| 90% Rec | deg.F | | 612.5 | 623.3 |
| 95% Rec | deg.F | | 644.9 | 664.4 |
| FBP | deg.F | | 667.2 | 676.4 |
| Recovery | % | | 98.2 | 97.6 |
| Residue | % | | 1.5 | 1.2 |
| Loss | % | | 0.3 | 1.3 |
| Flash Point, PMCC | deg.F | ASTM D-93(A) | 140 | 136 |
| **Hydrocarbon Type - FIA** | | ASTM D-1319 | | |
| Aromatics | lv% | | 21.8 | 27 |
| Olefins | lv% | | 0.8 | 0.7 |
| Saturates | lv% | | 77.4 | 72.3 |

**Table A- 2 Fuel Analysis Report for a Typical Emissions Control (EC) Diesel Fuel [55]**

| Test | Units | Method | ECD1 |
|---|---|---|---|
| API Gravity @ 60°F | deg.API | ASTM D-1298 | 39.2 |
| Cetane Number | - | ASTM D-613 | 52.8 |
| Kinematic Viscosity @ 40° F | cSt | ASTM D-445 | 2.115 |
| Total Sulfur | wt% | ASTM D-4294 | 0.0014 |
| Distillation | | | |
| IBP | deg.F | ASTM D-86 | 341.1 |
| 5% Rec | deg.F | | 377.1 |
| 10% Rec | deg.F | | 388.2 |
| 20% Rec | deg.F | | 410.9 |
| 30% Rec | deg.F | | 430.7 |
| 40% Rec | deg.F | | 453.3 |
| 50% Rec | deg.F | | 476.9 |
| 60% Rec | deg.F | | 502.3 |
| 70% Rec | deg.F | | 530.2 |
| 80% Rec | deg.F | | 563.3 |
| 90% Rec | deg.F | | 608.9 |
| 95% Rec | deg.F | | 647.8 |
| FBP | deg.F | | 665.4 |
| Recovery | % | | 97.4 |
| Residue | % | | 1.4 |
| Loss | % | | 1.2 |
| Flash Point, PMCC | deg.F | ASTM D-93(A) | 141 |
| Hydrocarbon Type - FIA | | ASTM D-1319 | |
| Aromatics | lv% | | 16.2 |
| Olefins | lv% | | 3.2 |
| Saturates | lv% | | 80.6 |

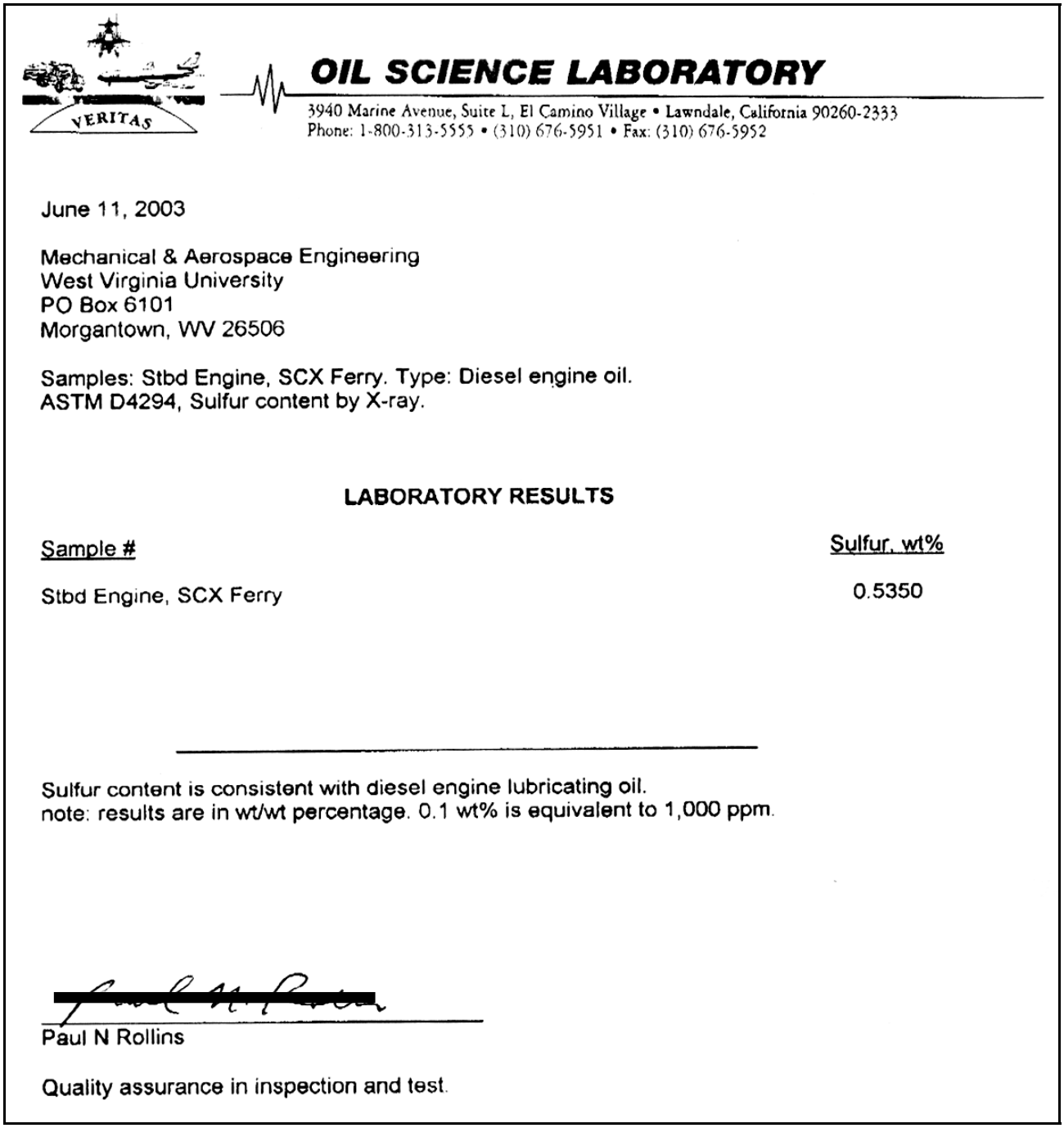

**OIL SCIENCE LABORATORY**

3940 Marine Avenue, Suite L, El Camino Village • Lawndale, California 90260-2333
Phone: 1-800-313-5555 • (310) 676-5951 • Fax: (310) 676-5952

June 11, 2003

Mechanical & Aerospace Engineering
West Virginia University
PO Box 6101
Morgantown, WV 26506

Samples: Stbd Engine, SCX Ferry. Type: Diesel engine oil.
ASTM D4294, Sulfur content by X-ray.

**LABORATORY RESULTS**

| Sample # | Sulfur, wt% |
|---|---|
| Stbd Engine, SCX Ferry | 0.5350 |

Sulfur content is consistent with diesel engine lubricating oil.
note: results are in wt/wt percentage. 0.1 wt% is equivalent to 1,000 ppm.

Paul N Rollins

Quality assurance in inspection and test.

**Figure A-1 Ferry Starboard Engine Oil Analysis Report**

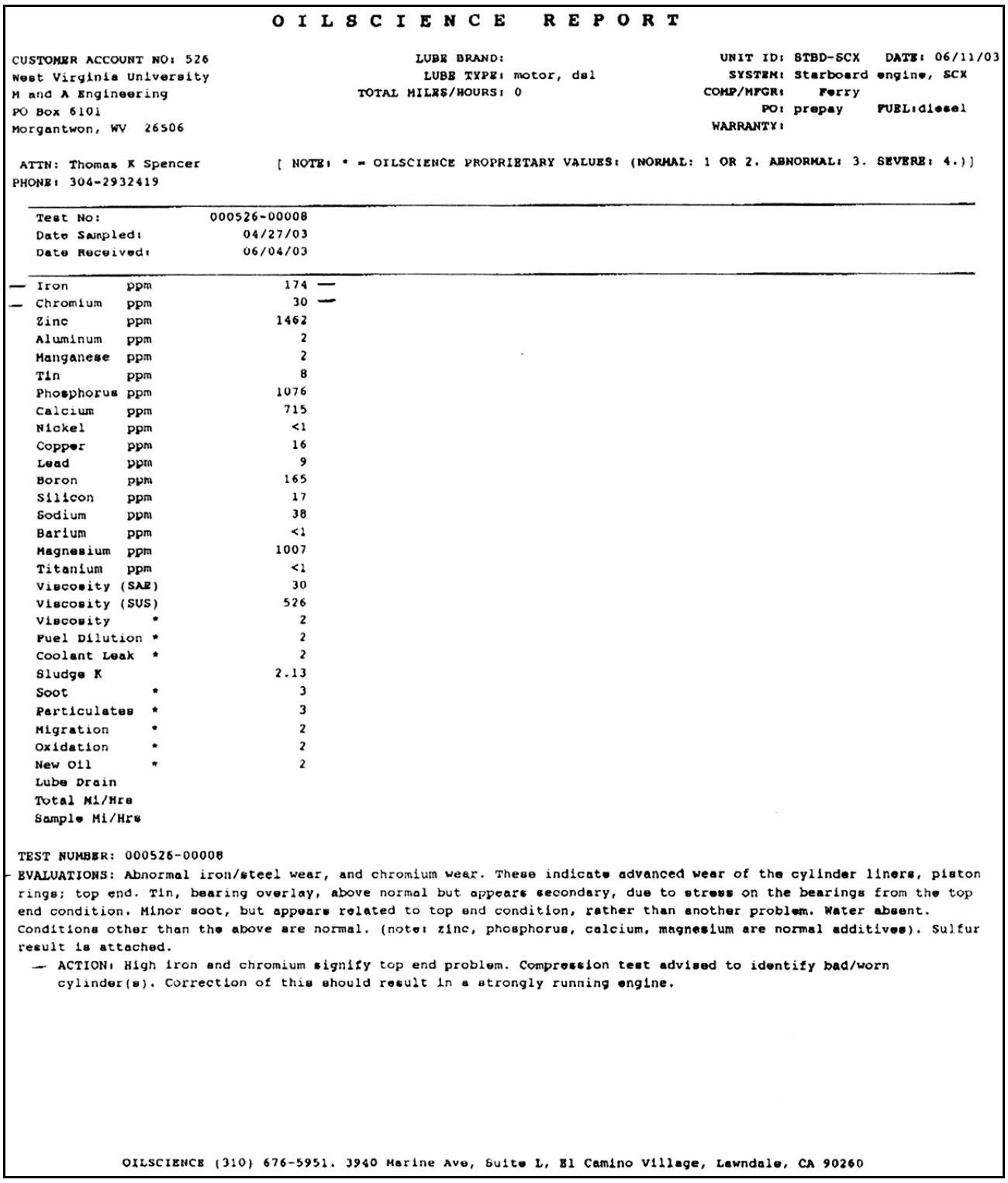

# OILSCIENCE REPORT

CUSTOMER ACCOUNT NO: 526
West Virginia University
M and A Engineering
PO Box 6101
Morgantwon, WV 26506

LUBE BRAND:
LUBE TYPE: motor, dsl
TOTAL MILES/HOURS: 0

UNIT ID: STBD-SCX DATE: 06/11/03
SYSTEM: Starboard engine, SCX
COMP/MFGR: Ferry
PO: prepay FUEL:diesel
WARRANTY:

ATTN: Thomas K Spencer
PHONE: 304-2932419

[ NOTE: * = OILSCIENCE PROPRIETARY VALUES: (NORMAL: 1 OR 2. ABNORMAL: 3. SEVERE: 4.)]

| | | | |
|---|---|---|---|
| Test No: | | | 000526-00008 |
| Date Sampled: | | | 04/27/03 |
| Date Received: | | | 06/04/03 |
| Iron | ppm | | 174 |
| Chromium | ppm | | 30 |
| Zinc | ppm | | 1462 |
| Aluminum | ppm | | 2 |
| Manganese | ppm | | 2 |
| Tin | ppm | | 8 |
| Phosphorus | ppm | | 1076 |
| Calcium | ppm | | 715 |
| Nickel | ppm | | <1 |
| Copper | ppm | | 16 |
| Lead | ppm | | 9 |
| Boron | ppm | | 165 |
| Silicon | ppm | | 17 |
| Sodium | ppm | | 38 |
| Barium | ppm | | <1 |
| Magnesium | ppm | | 1007 |
| Titanium | ppm | | <1 |
| Viscosity (SAE) | | | 30 |
| Viscosity (SUS) | | | 526 |
| Viscosity | * | | 2 |
| Fuel Dilution | * | | 2 |
| Coolant Leak | * | | 2 |
| Sludge K | | | 2.13 |
| Soot | * | | 3 |
| Particulates | * | | 3 |
| Migration | * | | 2 |
| Oxidation | * | | 2 |
| New Oil | * | | 2 |
| Lube Drain | | | |
| Total Mi/Hrs | | | |
| Sample Mi/Hrs | | | |

TEST NUMBER: 000526-00008
EVALUATIONS: Abnormal iron/steel wear, and chromium wear. These indicate advanced wear of the cylinder liners, piston rings; top end. Tin, bearing overlay, above normal but appears secondary, due to stress on the bearings from the top end condition. Minor soot, but appears related to top end condition, rather than another problem. Water absent. Conditions other than the above are normal. (note: zinc, phosphorus, calcium, magnesium are normal additives). Sulfur result is attached.
ACTION: High iron and chromium signify top end problem. Compression test advised to identify bad/worn cylinder(s). Correction of this should result in a strongly running engine.

OILSCIENCE (310) 676-5951. 3940 Marine Ave, Suite L, El Camino Village, Lawndale, CA 90260

**Figure A-2 Ferry Starboard Engine Oil Analysis Report (Contd…)**

# APPENDIX B
# Results of Individual Runs of Tests Performed Onboard the Ferry

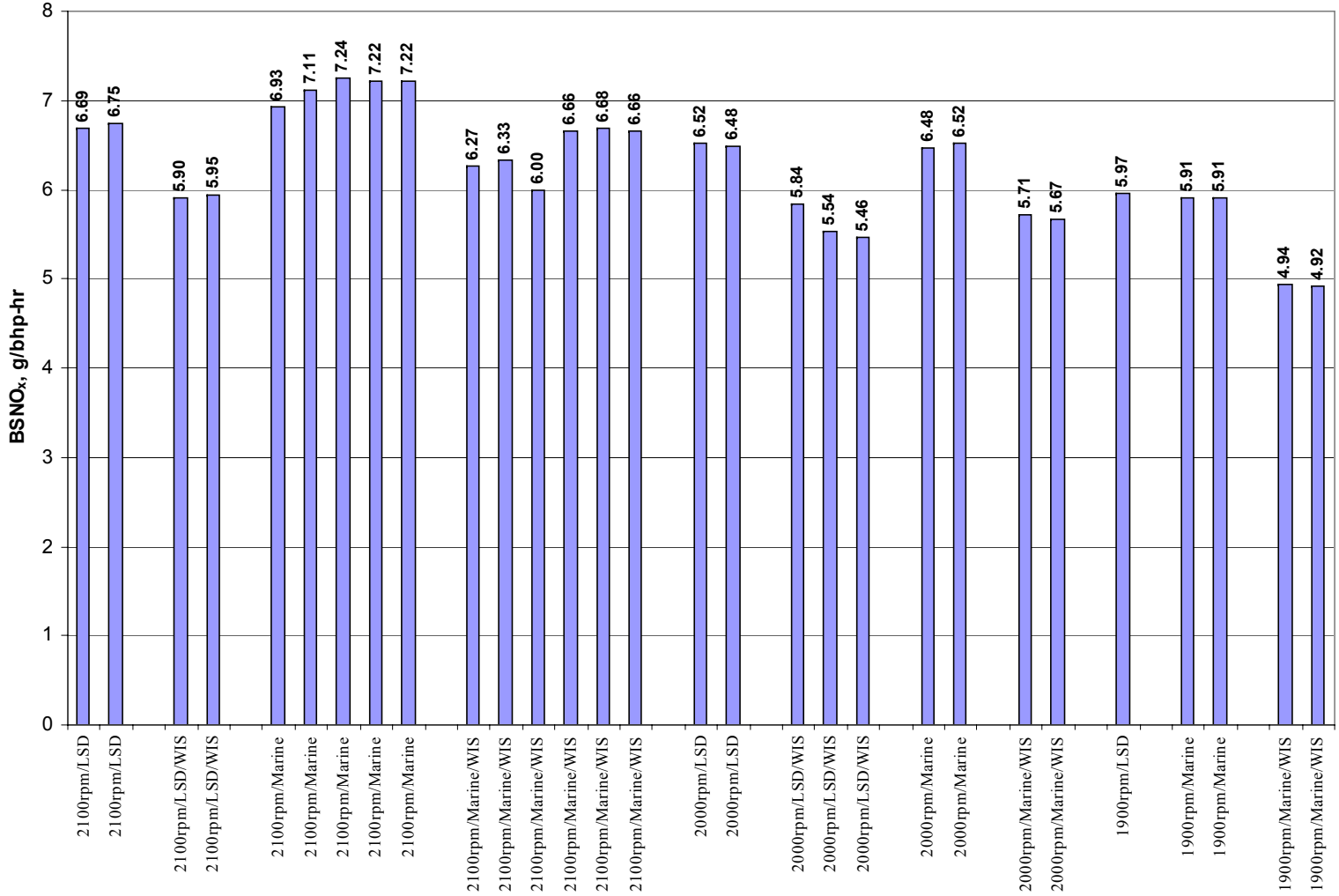


**Figure B-1 Individual Run Data of Brake Specific $NO_x$ ($BSNO_x$) Emissions for Various Modes and Configurations**

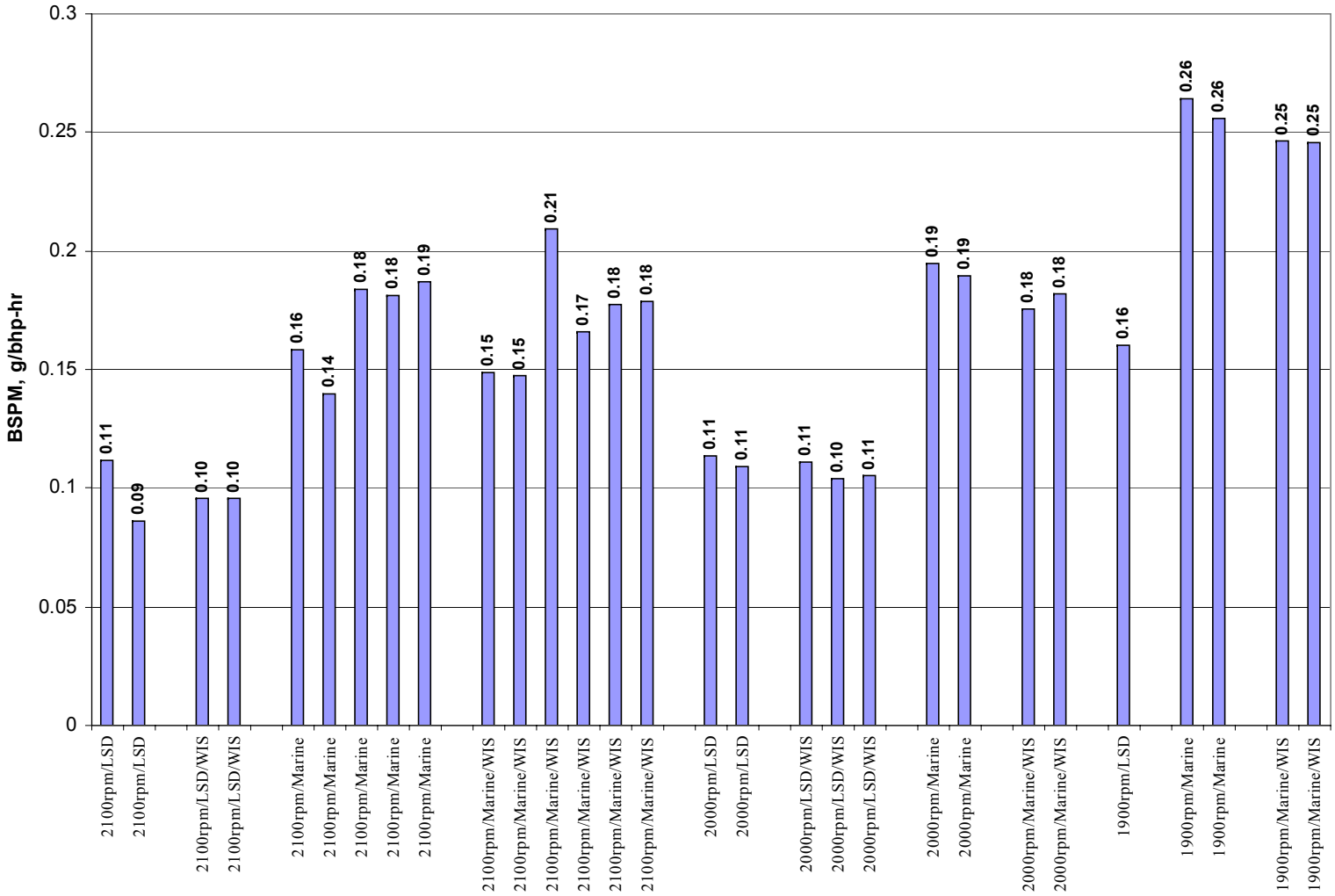


**Figure B-2 Individual Run Data of Brake Specific PM (BSPM) Emissions for Various Modes and Configurations**

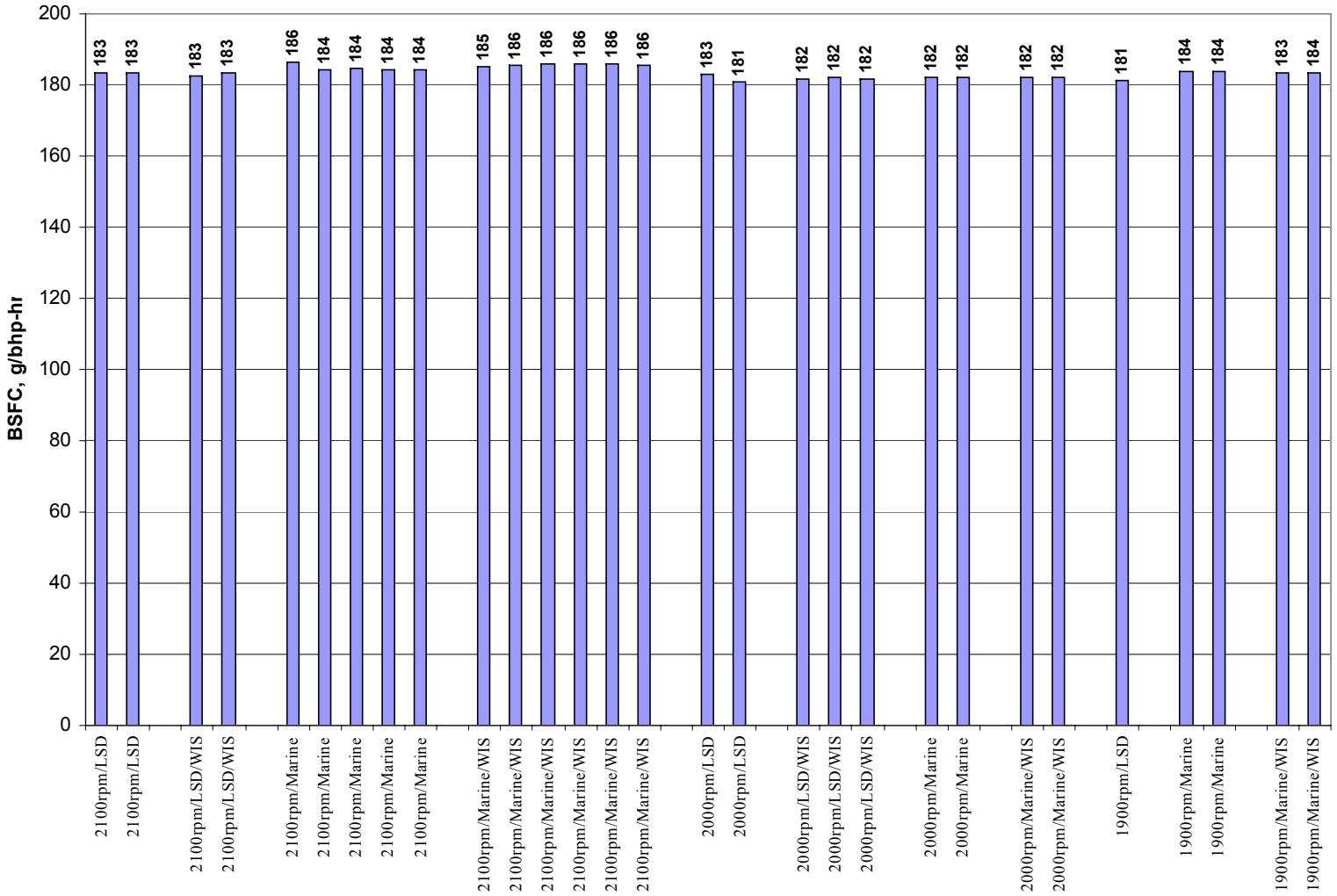


**Figure B-3 Individual Run Data of Brake Specific Fuel Consumption (BSFC) Emissions for Various Modes and Configurations**

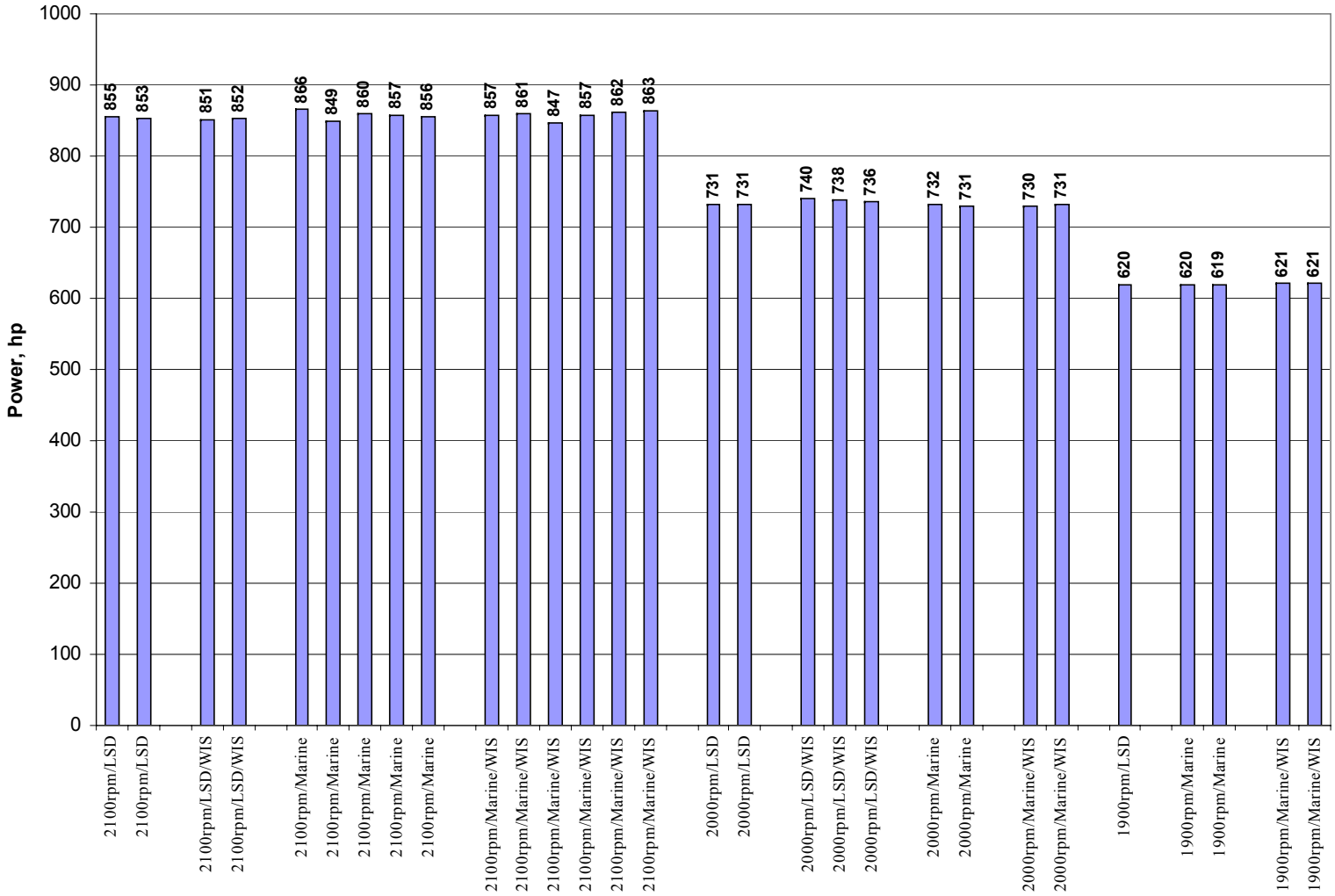


**Figure B-4 Individual Run Data of Power Output for Various Modes and Configurations**

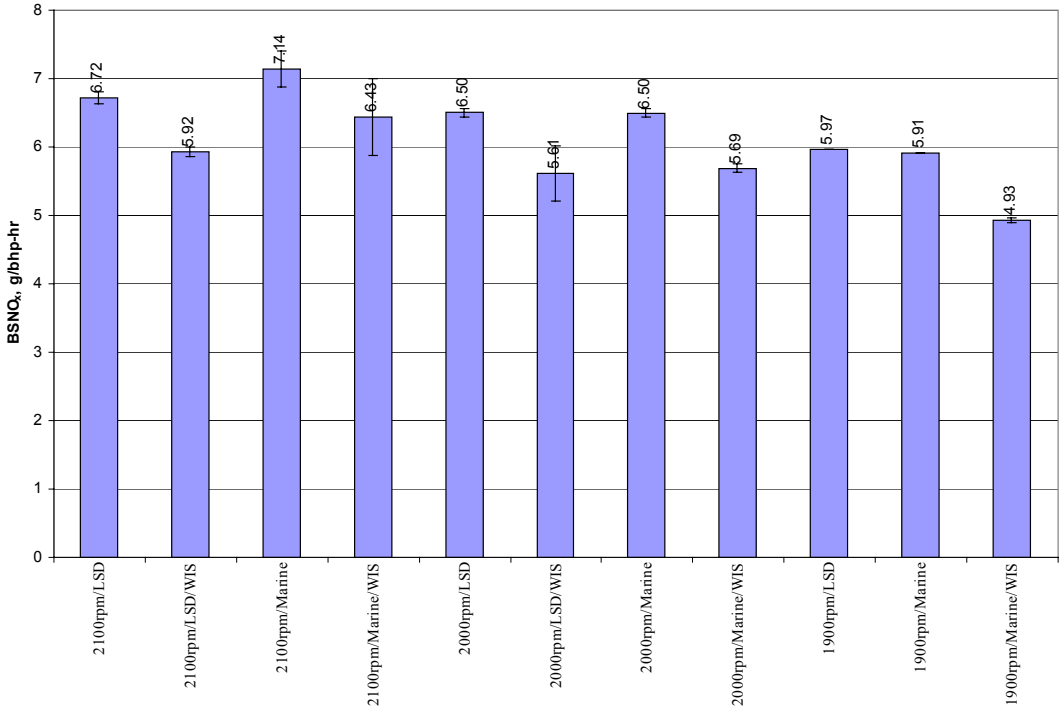


**Figure B-5 Average Brake-specific $NO_x$ ($BSNO_x$) Emissions for Various Modes and Configurations (Error Bars Denote $\pm 2\sigma$)**

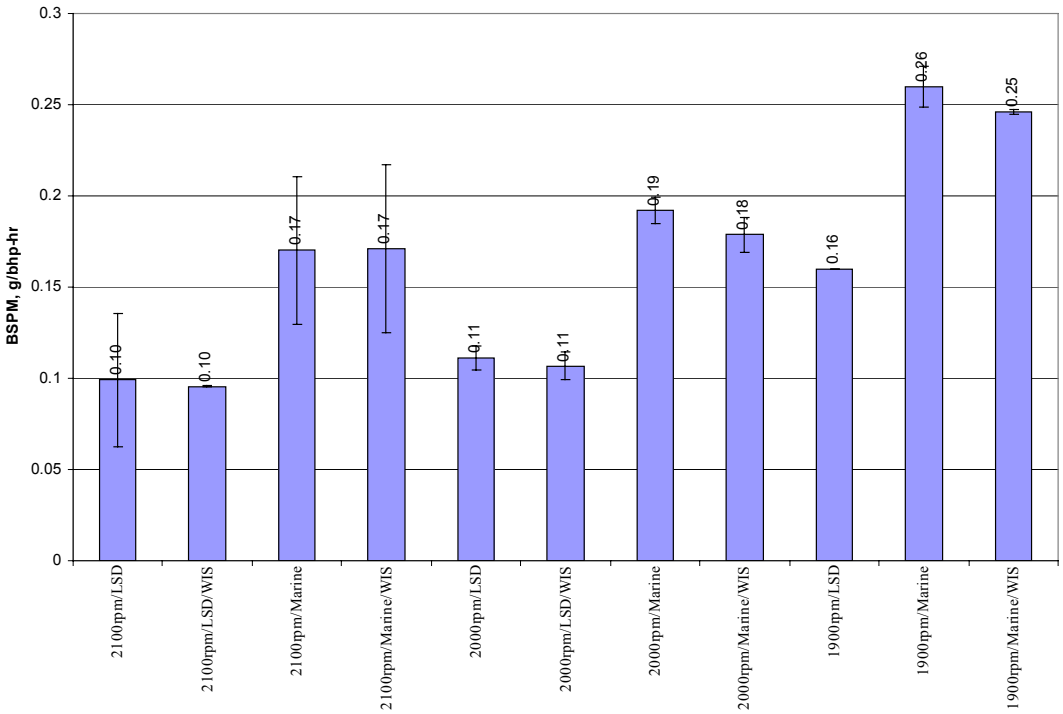


**Figure B-6 Average Brake-specific PM (BSPM) Emissions for Various Modes and Configurations (Error Bars Denote $\pm 2\sigma$)**

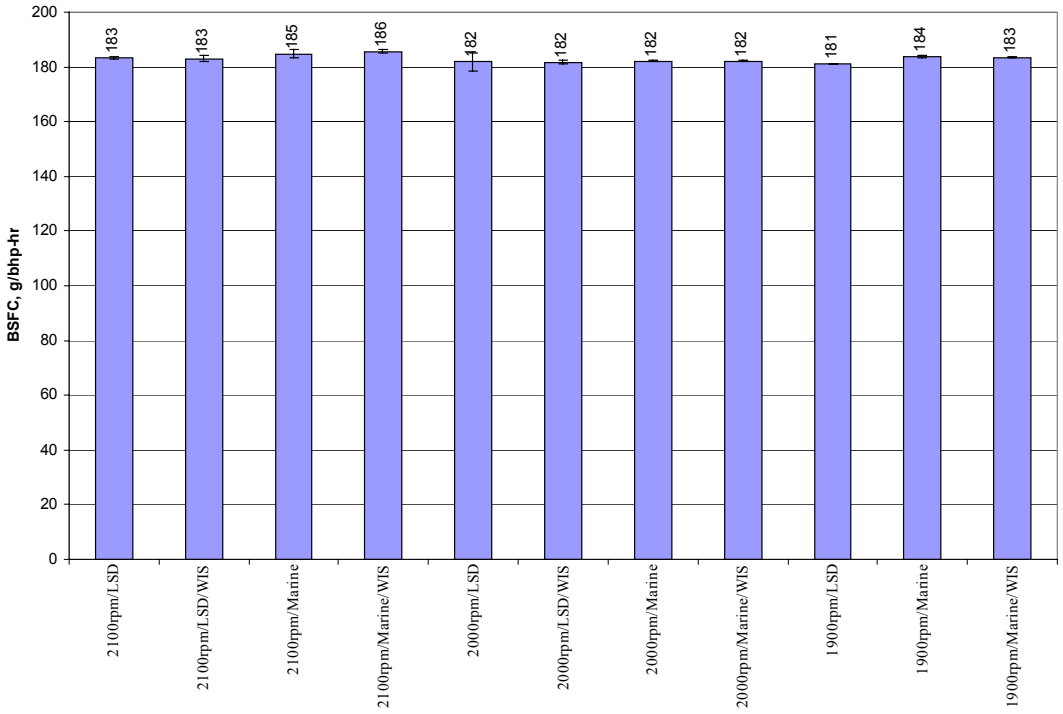


**Figure B-7 Average Brake-specific Fuel Consumption (BSFC) Emissions for Various Modes and Configurations (Error Bars Denote $\pm 2\sigma$)**

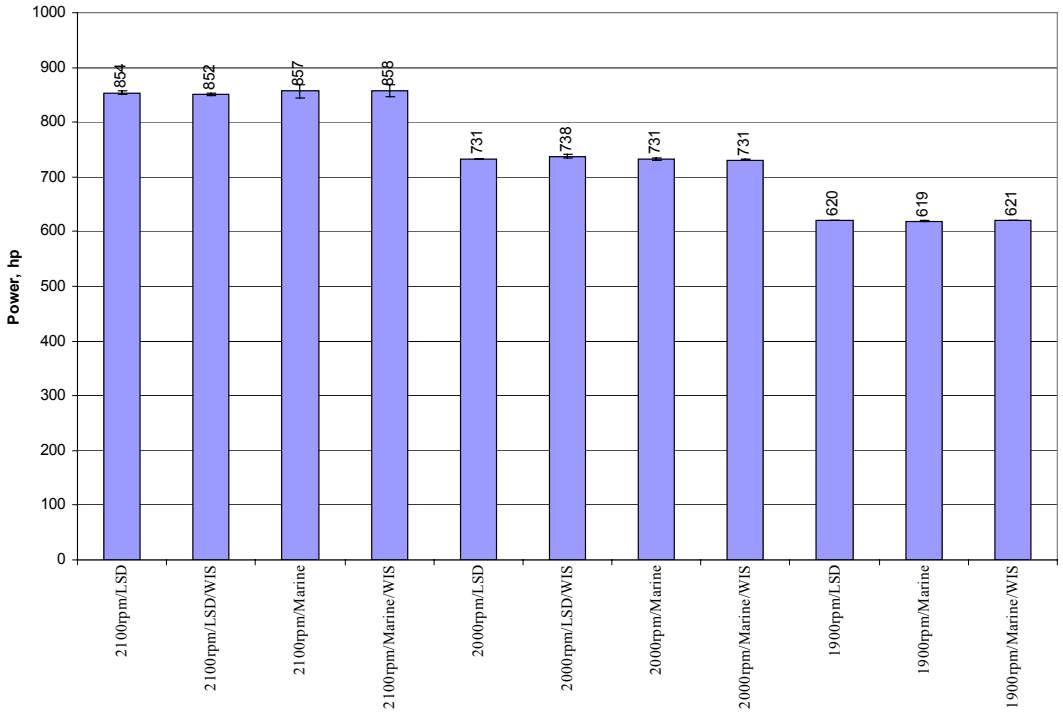


**Figure B-8 Average Power Output for Various Modes and Configurations (Error Bars Denote $\pm 2\sigma$)**

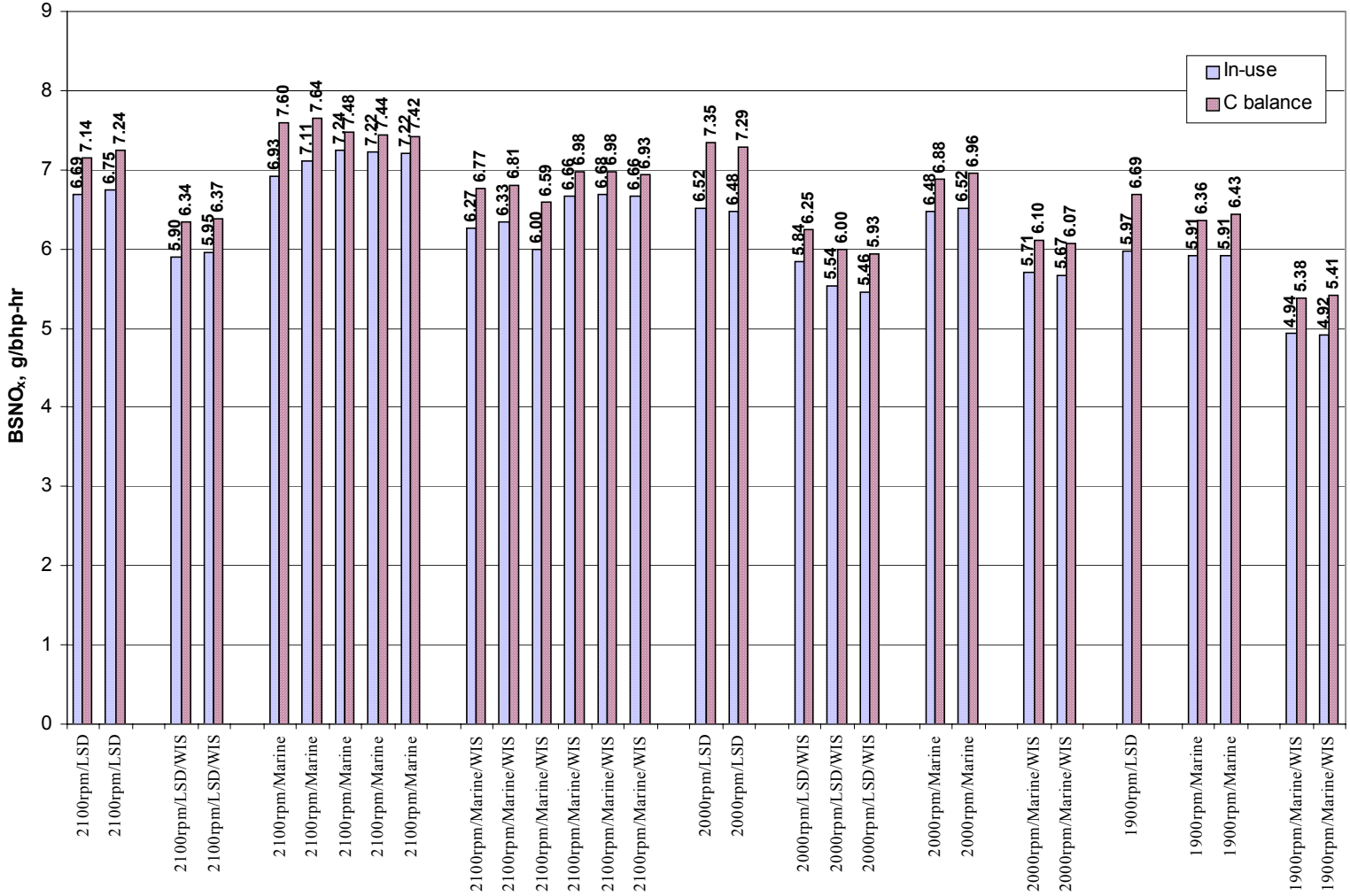


**Figure B-9 Comparison of $BSNO_x$ emissions Obtained from Carbon (C) Balance Method with that Obtained from In-use Calculations**

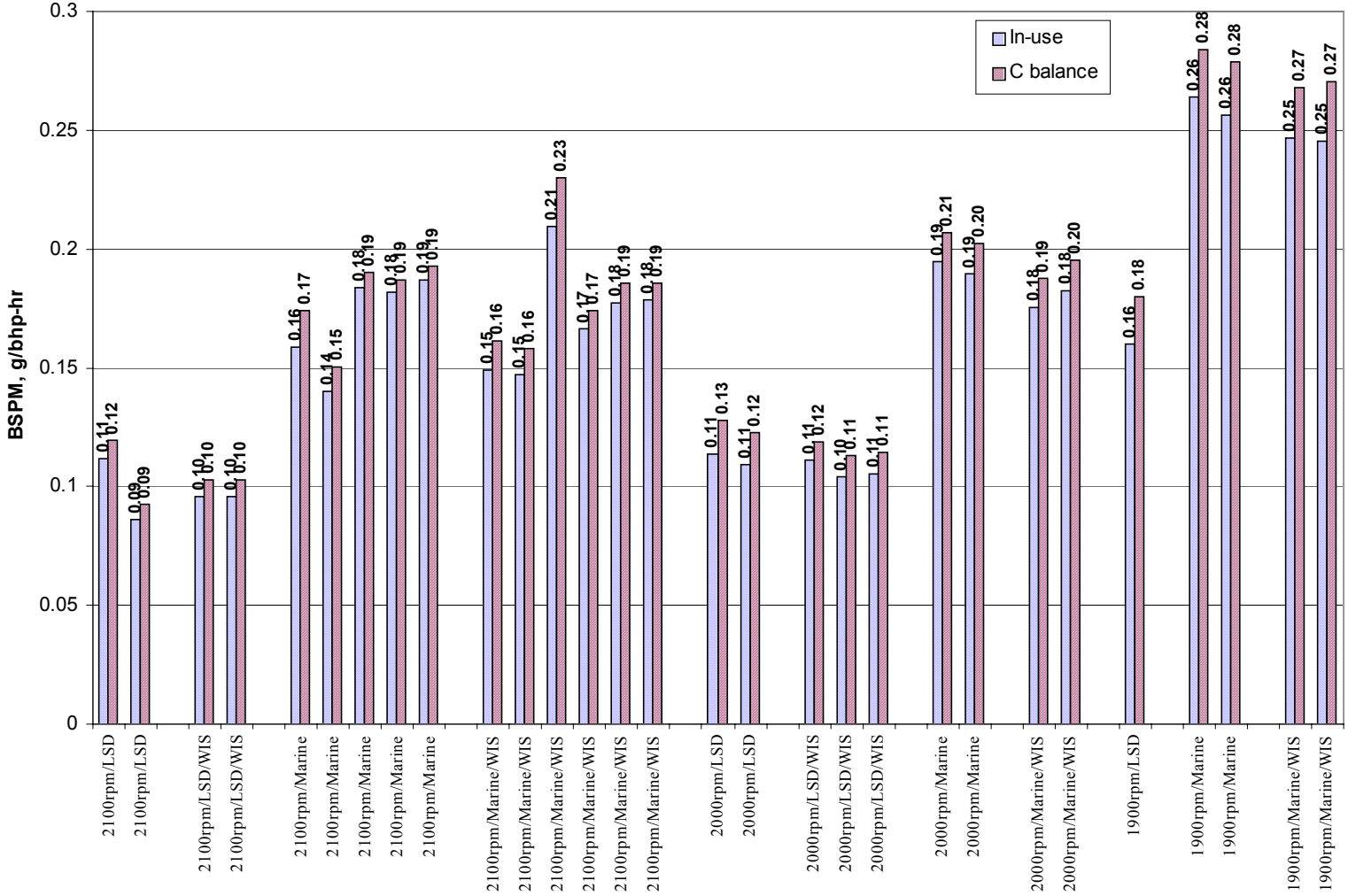


**Figure B-10 Comparison of BSPM Emissions Obtained from Carbon (C) Balance Method With that Obtained from In-use Calculations**

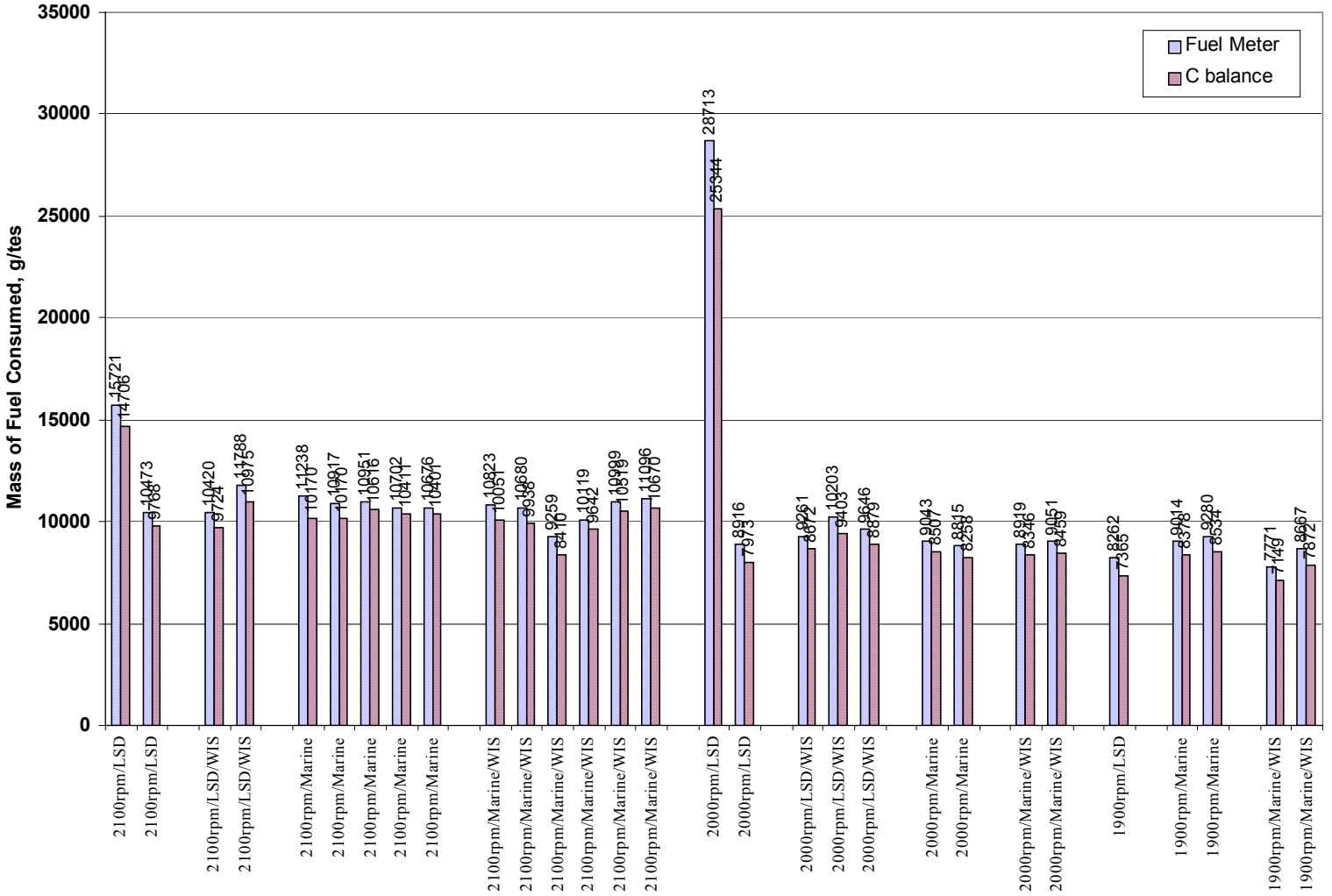


**Figure B-11 Comparison of Fuel Consumptions During Each Test (Fuel Meter vs. Carbon Balance)**

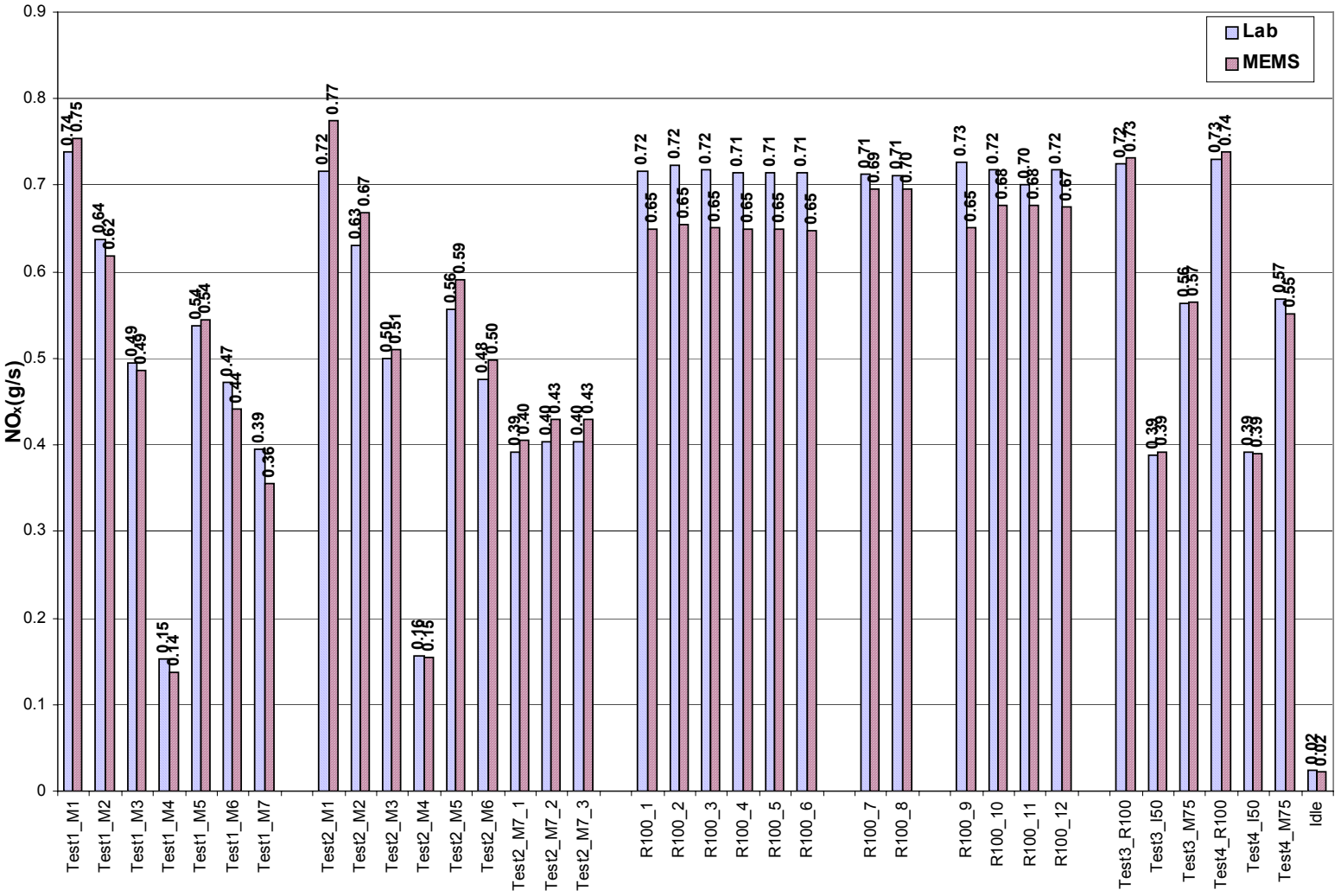


**Figure B-12 Comparison of Laboratory-MEMS $NO_x$ Measurements**

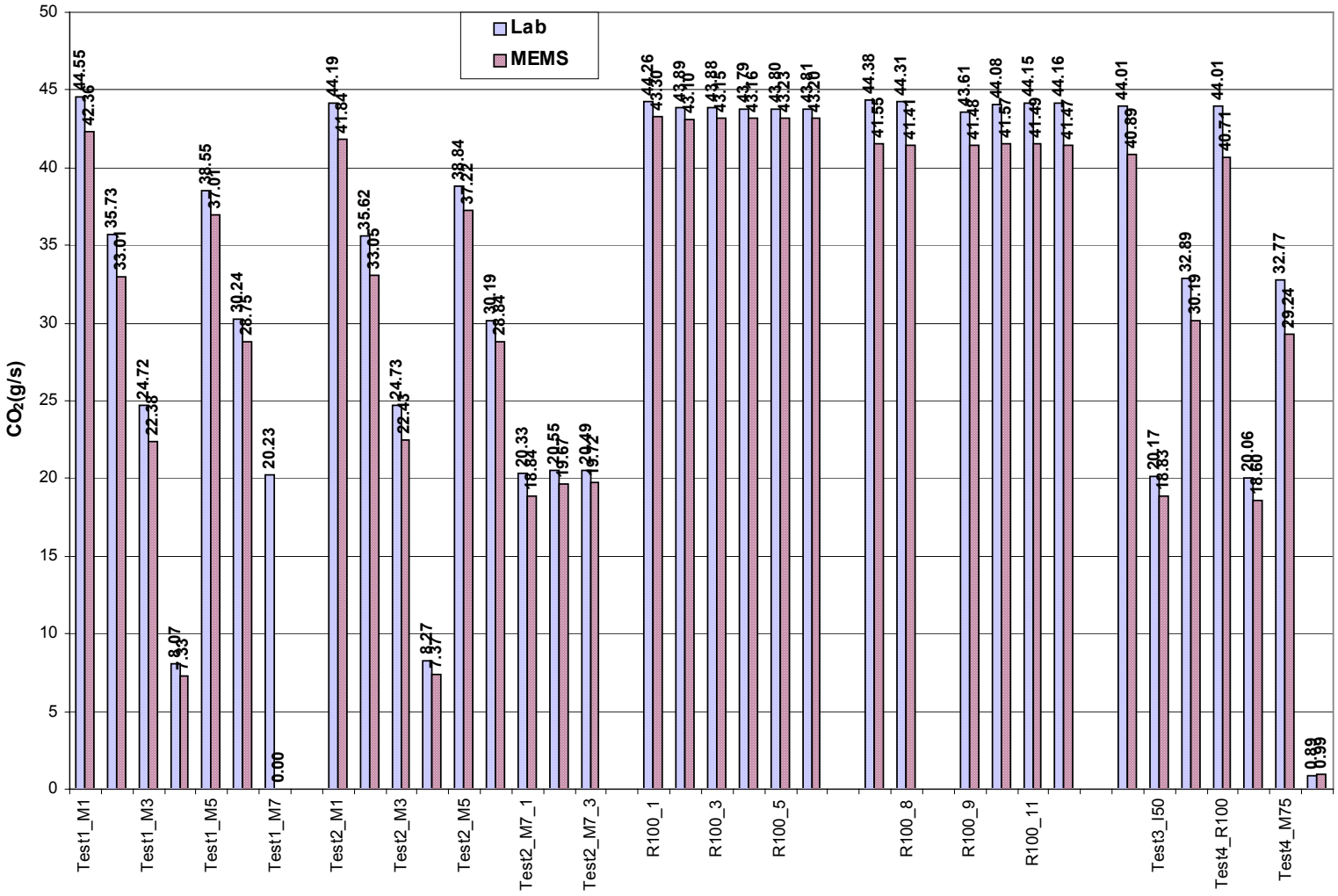


**Figure B-13 Comparison of Laboratory-MEMS $CO_2$ Measurements**

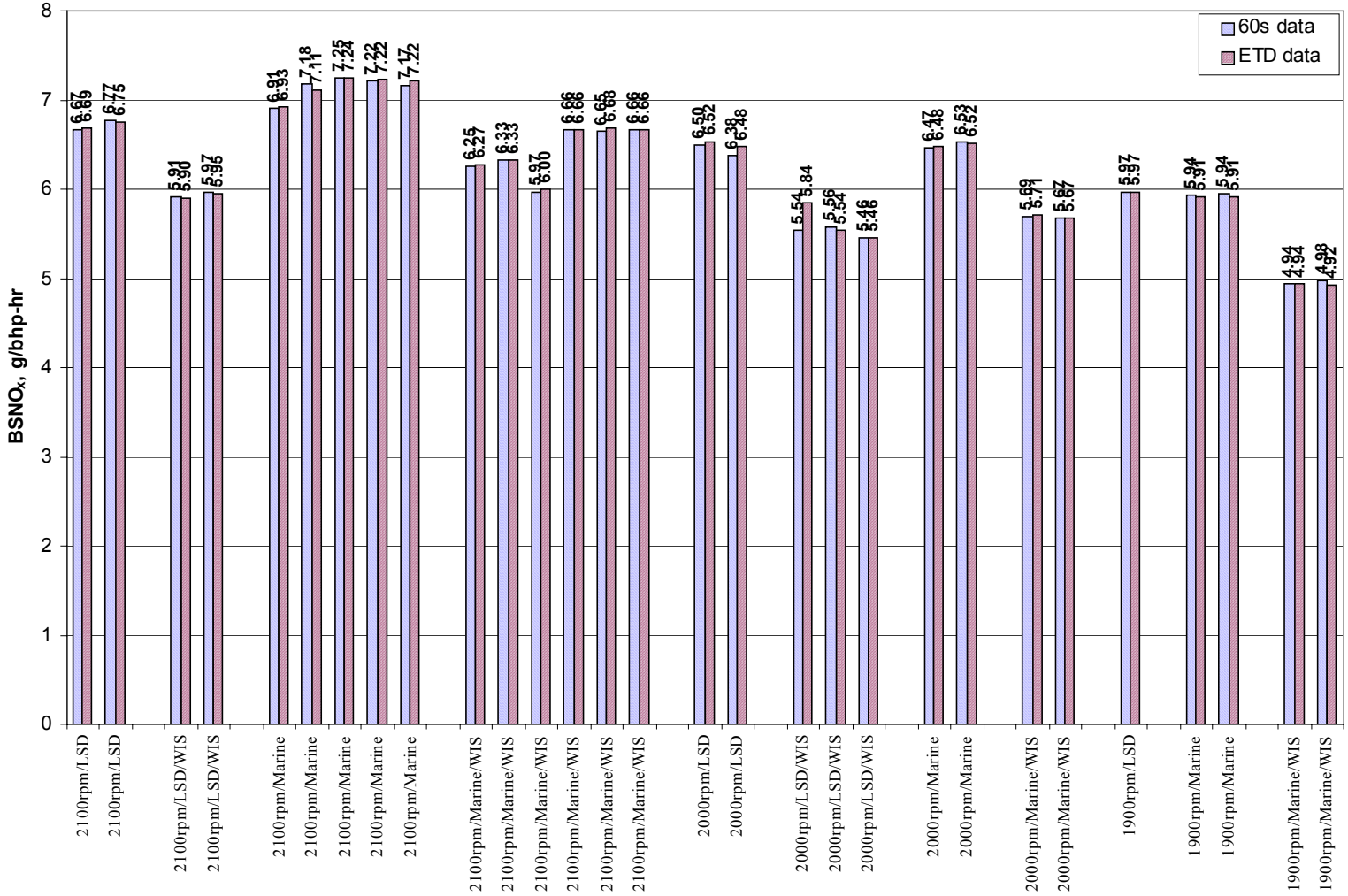


**Figure B-14 Comparison of 60s Data and Entire Test Time Duration Data (ETD) of Brake-specific $NO_x$ Emissions**

**Table B-1 Individual Run Data for Various Modes and Engine Configurations**

*(Note: The1900rpm/LSD/WIS data was not collected)*

| Test No. | Test Description | Speed (rpm) | Torque (lb-ft) | Power (hp) | Time (s) | $BSNO_x$ (g/bhp-hr) | BSPM (g/bhp-hr) | BSFC (g/bhp-hr) |
|---|---|---|---|---|---|---|---|---|
| M010113-02 | 2100rpm/LSD | 2100 | 2138 | 855 | 361 | 6.69 | 0.11 | 183 |
| M010113-03 | 2100rpm/LSD | 2100 | 2133 | 853 | 241 | 6.75 | 0.09 | 183 |
| | | | | | | | | |
| M010114-01 | 2100rpm/LSD/WIS | 2100 | 2128 | 851 | 241 | 5.90 | 0.10 | 183 |
| M010114-02 | 2100rpm/LSD/WIS | 2100 | 2132 | 852 | 271 | 5.95 | 0.10 | 183 |
| | | | | | | | | |
| M010119-01 | 2100rpm/Marine | 2100 | 2165 | 866 | 251 | 6.93 | 0.16 | 186 |
| M010119-02 | 2100rpm/Marine | 2100 | 2123 | 849 | 251 | 7.11 | 0.14 | 184 |
| M010129-01 | 2100rpm/Marine | 2100 | 2150 | 860 | 249 | 7.24 | 0.18 | 184 |
| M010129-02 | 2100rpm/Marine | 2100 | 2143 | 857 | 244 | 7.22 | 0.18 | 184 |
| M010129-03 | 2100rpm/Marine | 2100 | 2140 | 856 | 244 | 7.22 | 0.19 | 184 |
| | | | | | | | | |
| M010120-01 | 2100rpm/Marine/WIS | 2100 | 2143 | 857 | 246 | 6.27 | 0.15 | 185 |
| M010120-02 | 2100rpm/Marine/WIS | 2100 | 2152 | 861 | 241 | 6.33 | 0.15 | 186 |
| M010125-01 | 2100rpm/Marine/WIS | 2100 | 2119 | 847 | 212 | 6.00 | 0.21 | 186 |
| M010128-01 | 2100rpm/Marine/WIS | 2100 | 2144 | 857 | 229 | 6.66 | 0.17 | 186 |
| M010128-02 | 2100rpm/Marine/WIS | 2100 | 2155 | 862 | 247 | 6.68 | 0.18 | 186 |
| M010128-03 | 2100rpm/Marine/WIS | 2100 | 2159 | 863 | 249 | 6.66 | 0.18 | 186 |
| | | | | | | | | |
| M010116-01 | 2000rpm/LSD | 2000 | 1921 | 731 | 772 | 6.52 | 0.11 | 183 |
| M010116-02 | 2000rpm/LSD | 2000 | 1921 | 731 | 243 | 6.48 | 0.11 | 181 |
| | | | | | | | | |
| M010115-01 | 2000rpm/LSD/WIS | 2000 | 1942 | 740 | 248 | 5.84 | 0.11 | 182 |
| M010115-02 | 2000rpm/LSD/WIS | 2000 | 1937 | 738 | 273 | 5.54 | 0.10 | 182 |
| M010115-03 | 2000rpm/LSD/WIS | 2000 | 1932 | 736 | 260 | 5.46 | 0.11 | 182 |
| | | | | | | | | |
| M010122-01 | 2000rpm/Marine | 2000 | 1923 | 732 | 244 | 6.48 | 0.19 | 182 |
| M010122-02 | 2000rpm/Marine | 2000 | 1919 | 731 | 238 | 6.52 | 0.19 | 182 |
| | | | | | | | | |
| M010121-01 | 2000rpm/Marine/WIS | 2000 | 1918 | 730 | 241 | 5.71 | 0.18 | 182 |
| M010121-02 | 2000rpm/Marine/WIS | 2000 | 1920 | 731 | 245 | 5.67 | 0.18 | 182 |
| | | | | | | | | |
| M010117-01 | 1900rpm/LSD | 1900 | 1714 | 620 | 265 | 5.97 | 0.16 | 181 |
| | | | | | | | | |
| M010123-01 | 1900rpm/Marine | 1900 | 1713 | 620 | 285 | 5.91 | 0.26 | 184 |
| M010123-02 | 1900rpm/Marine | 1900 | 1710 | 619 | 294 | 5.91 | 0.26 | 184 |
| | | | | | | | | |
| M010124-01 | 1900rpm/Marine/WIS | 1900 | 1716 | 621 | 246 | 4.94 | 0.25 | 183 |
| M010124-02 | 1900rpm/Marine/WIS | 1900 | 1716 | 621 | 274 | 4.92 | 0.25 | 184 |
| | | | | | | | | |
| M010126-01 | Harbor(In)/Marine | 650 | 171 | 21 | 311 | 16.68 | 0.17 | 388 |
| M010127-01 | Harbor(Out)/Marine | 650 | 164 | 20 | 361 | 20.71 | 0.16 | 441 |
| M010130-01 | Harbor(In)/Marine | 650 | 179 | 22 | 245 | 17.55 | 0.15 | 377 |

**Table B-2 Manual Data Collected from Starboard Forward and Aft Engines.**

*(Note: The1900rpm/LSD/WIS data was not collected)*

| | | | | Forward Starboard Engine | | | | | | | Aft Starboard Engine | | | | |
|---|---|---|---|---|---|---|---|---|---|---|---|---|---|---|---|
| | | | | | | | Exh Temp | | Turbo Pres | | | | | Turbo Pres | |
| Description | Seq No | Run No | GPS Spd | Eng Spd | Oil Pres | Water Temp | T1 | T2 | P1 | P2 | Eng Spd | Oil Pres | Water Temp | P3 | P4 |
| | | | knts | RPM | psig | F | F | F | psig | psig | RPM | psig | F | psig | psig |
| 2100 rpm, LSD | M010113 | 2 | | 2100 | 60 | 180 | 635 | | 18.7 | 19.2 | 2100 | 60 | 180 | 19.2 | 19.9 |
| 2100 rpm, LSD | M010113 | 3 | 37.0 | 2100 | 60 | 180 | 631 | | 18.8 | 19.3 | 2100 | 60 | 180 | 19.0 | 19.4 |
| 2100 rpm, LSD, WIS | M010114 | 1 | 36.0 | 2100 | 60 | 180 | 617 | | 18.9 | 19.3 | 2100 | 60 | 180 | 19.3 | 19.6 |
| 2100 rpm, LSD, WIS | M010114 | 2 | 33.6 | 2100 | 60 | 180 | 618 | | 18.9 | 19.4 | 2100 | 60 | 180 | 19.1 | 19.6 |
| 2000 rpm, LSD, WIS | M010115 | 2 | 30.3 | 2000 | 60 | 180 | 600 | | 15.8 | 16.2 | 2000 | 60 | 180 | 15.4 | 16.0 |
| 2000 rpm, LSD, WIS | M010115 | 3 | 32.6 | 2000 | 60 | 180 | 600 | | 15.6 | 16.1 | 2000 | 60 | 180 | 15.2 | 15.8 |
| 2000 rpm, LSD | M010116 | 1 | 30.3 | 2000 | 60 | 180 | - | | 15.3 | 15.6 | 2000 | 60 | 180 | 15.2 | 15.9 |
| 2000 rpm, LSD | M010116 | 2 | 28.8 | 2000 | 60 | 180 | 627 | | 15.5 | 15.7 | 2000 | 60 | 180 | 15.1 | 15.6 |
| 1900 rpm, LSD | M010117 | 1 | 24.4 | 1900 | 60 | 170 | 600 | | 12.3 | 12.6 | 2000 | 60 | 170 | 12.0 | 12.5 |
| Idle, 650 rpm, LSD | M010118 | 1 | 0.0 | 670 | 25 | 120 | 137 | | 0.1 | 0.1 | 670 | 25 | 120 | 0.2 | 0.2 |
| Idle, 650 rpm, LSD | M010118 | 2 | 0.0 | 670 | 25 | 115 | 137 | | 0.1 | 0.1 | 670 | 25 | 115 | 0.2 | 0.2 |
| | | | | | | | | | | | | | | | |
| 2100 rpm, Marine | M010119 | 1 | 35.6 | 2100 | 60 | 180 | 636 | | 19.5 | 19.9 | 2100 | 60 | 180 | 19.8 | 20.2 |
| 2100 rpm, Marine | M010119 | 2 | 34.0 | 2100 | 60 | 180 | 632 | | 18.7 | 19.2 | 2100 | 60 | 180 | 19.0 | 19.7 |
| 2100 rpm, Marine, WIS | M010120 | 1 | 33.0 | 2100 | 60 | 180 | 625 | | 19.2 | 19.7 | 2100 | 60 | 180 | 19.7 | 20.3 |
| 2100 rpm, Marine, WIS | M010120 | 2 | 33.8 | 2100 | 60 | 180 | 621 | | 19.4 | 19.8 | 2100 | 60 | 180 | 19.7 | 20.2 |
| 2000 rpm, Marine, WIS | M010121 | 1 | 28.6 | 2000 | 60 | 180 | 600 | | 15.7 | 16.1 | 2000 | 60 | 180 | 15.1 | 15.9 |
| 2000 rpm, Marine, WIS | M010121 | 2 | 30.0 | 2000 | 60 | 180 | 597 | | 15.7 | 16.2 | 2000 | 60 | 180 | 15.2 | 15.8 |
| 2000 rpm, Marine | M010122 | 1 | 29.2 | 2000 | 60 | 180 | 615 | | 15.6 | 15.9 | 2000 | 60 | 180 | 15.3 | 15.9 |
| 2000 rpm, Marine | M010122 | 2 | 30.0 | 2000 | 60 | 180 | 617 | | 15.5 | 15.9 | 2000 | 60 | 180 | 15.2 | 15.9 |
| 1900 rpm, Marine | M010123 | 1 | 25.5 | 1900 | 60 | 180 | 600 | | 12.5 | 12.8 | 1900 | 60 | 180 | 12.5 | 12.5 |
| 1900 rpm, Marine | M010123 | 2 | 24.7 | 1900 | 60 | 180 | 602 | | 12.5 | 12.8 | 1900 | 60 | 180 | 12.4 | 12.4 |
| 1900 rpm, Marine, WIS | M010124 | 1 | 25.0 | 1900 | 60 | 180 | 585 | | 12.8 | 13.1 | 1900 | 60 | 180 | 12.3 | 12.3 |
| 1900 rpm, Marine, WIS | M010124 | 2 | 27.8 | 1900 | 60 | 180 | 585 | | 12.8 | 13.1 | 1900 | 60 | 180 | 12.3 | 12.3 |
| 2100 rpm, Marine, WIS | M010125 | 1 | 32.2 | 2100 | 60 | 180 | 625 | | 19.1 | 19.5 | 2100 | 60 | 180 | 19.1 | 19.1 |
| 650, Marine, Harbor, Temperature dropped through test | M010126 | 1 | 5.5 | 650 | 25 | 170 | 275-235 | | 0.2 | 0.2 | 650 | 25 | 175 | 0.1 | 0.1 |
| 650, Marine, Harbor | M010127 | 1 | 3.2 | 650 | 25 | 125 | 190 | | 0.2 | 0.1 | 650 | 25 | 125 | 0.3 | 0.3 |
| 2100 rpm, Marine, WIS | M010128 | 1 | 37.0 | 2100 | 60 | 180 | 620 | | 19.2 | 19.5 | 2100 | 60 | 180 | 19.5 | 20.0 |
| 2100 rpm, Marine, WIS | M010128 | 2 | 35.5 | 2100 | 60 | 180 | 630 | | 19.2 | 19.9 | 2100 | 60 | 180 | 19.7 | 20.1 |
| 2100 rpm, Marine, WIS | M010128 | 3 | 36.0 | 2100 | 60 | 180 | 628 | | 19.3 | 20.0 | 2100 | 60 | 180 | 19.7 | 20.0 |
| 2100 rpm, Marine | M010129 | 1 | 31.5 | 2100 | 60 | 180 | 636 | | 18.9 | 19.5 | 2100 | 60 | 180 | 19.2 | 19.7 |
| 2100 rpm, Marine | M010129 | 2 | 31.3 | 2100 | 60 | 180 | 636 | | 19.0 | 19.5 | 2100 | 60 | 180 | 19.0 | 19.6 |
| 2100 rpm, Marine | M010129 | 3 | 31.8 | 2100 | 60 | 180 | 637 | | 19.1 | 19.5 | 2100 | 60 | 180 | 19.0 | 19.7 |
| 650, Marine, Harbor, Temperature dropped through test | M010130 | 1 | 4.3 | 650 | 15 | 170 | 282-240 | | 0.2 | 0.2 | 650 | 15 | 170 | 0.3 | 0.3 |
| Idle, 650, Marine | M010131 | 1 | 0.0 | 650 | 12 | 120 | 143 | | 0.5 | 0.5 | 650 | 0 | 0 | 0.0 | 0.0 |
| Idle, 650, Marine | M010131 | 2 | 0.0 | 650 | 12 | 120 | 140 | | - | - | 650 | 0 | 0 | 0.0 | 0.0 |